

Characterisation of the UVA-induced DNA damage response in directly irradiated and bystander cells



This thesis is submitted for the degree of Master of Science by Research

by

Kendal Wilson

Division of Biomedical and Life Sciences

Faculty of Health and Medicine

Lancaster university

July 2022

Declaration

I declare that this thesis is my own work and has not been submitted in part, or as a whole, for the award of a higher degree of qualification at this university or elsewhere.

Kendal Wilson

Acknowledgements

I would like to thank my supervisor Dr. Sarah Allinson for helping me during my project and guiding me through some difficult times during the pandemic which provided some unusual challenges. I would also like to thank all members of A27 for creating a positive and supportive work environment in a very stressful time and providing advice and assistance when things went wrong or when learning new techniques. Thank you to friends in the department who provided some much-needed mental health support during my research and sharing our experiences to keep me going. Finally, I would like to thank my family for their continued support from home to keep me motivated and patience during the writing phase.

Table of Contents

| | |
|--|-----------|
| I: Abbreviations | 8 |
| II: Abstract..... | 10 |
| Chapter 1: Introduction..... | 11 |
| 1.1. UV radiation | 12 |
| 1.2. Skin cancer | 14 |
| 1.2.1. Structure of the skin..... | 14 |
| 1.2.2. What is skin cancer?..... | 15 |
| 1.2.3. Risk factors for skin cancer..... | 16 |
| 1.2.4 Association between skin cancer and UV exposure | 16 |
| 1.3. UV-induced DNA damage..... | 18 |
| 1.3.1. Pyrimidine dimers | 18 |
| 1.3.2. Oxidative stress | 22 |
| 1.4. The cell cycle | 26 |
| 1.4.1. The cell cycle | 26 |
| 1.4.2. Impact of UV on the cell cycle..... | 28 |
| 1.5. DNA damage response..... | 31 |
| 1.5.1. DNA damage response pathway..... | 31 |
| 1.5.2. Repair of DSBs | 36 |
| 1.6. The bystander effect | 39 |
| 1.6.1. What is the bystander effect?..... | 39 |
| 1.6.2. Methods for studying bystander effect | 39 |
| 1.6.3. Bystander communication | 40 |
| 1.6.4. Apoptosis..... | 43 |
| 1.6.5. Impact on the cell cycle and DNA damage response..... | 44 |
| 1.6.6. Differences between bystander responses..... | 45 |
| 1.6.7. Protective function of the bystander effect..... | 47 |
| 1.7. Aims..... | 47 |
| 1.7.1. The UVA induced DDR in directly irradiated cells | 47 |
| 1.7.2. The activation of the DDR in UVA-induced bystander cells..... | 47 |
| Chapter 2: Methods | 49 |
| 2.1. Buffers and solutions | 50 |
| 2.2. Cell culture | 50 |
| 2.2.1. Cell culture conditions | 50 |
| 2.2.2. Trypsinisation and cell counting..... | 51 |

| | |
|--|-----------|
| 2.3. Experimental culture conditions | 51 |
| 2.3.1. Direct irradiation cell culture conditions | 51 |
| 2.3.2. Bystander cell culture conditions..... | 51 |
| 2.4. UV irradiation | 52 |
| 2.5. Western blots..... | 52 |
| 2.5.1. Sample collection | 52 |
| 2.5.2. Protein concentration quantification via Bradford assay | 52 |
| 2.5.3. SDS-PAGE | 53 |
| 2.5.4. Gel transfer | 53 |
| 2.5.5. Protein detection | 53 |
| 2.6. Immunofluorescence | 55 |
| 2.7. Statistics | 56 |
| Chapter 3: Characterisation of the DNA damage response in directly UVA-irradiated HaCaT cells | 57 |
| 3.1. Introduction | 58 |
| 3.2. Aims..... | 59 |
| 3.3. Results | 60 |
| 3.3.1. Western blot analysis of DDR protein activation | 61 |
| 3.3.2. Immunofluorescence analysis of γ H2AX..... | 68 |
| 3.3.3. Comparison of doses..... | 75 |
| 3.4. Discussion..... | 77 |
| 3.4.1. Activation of the DDR branches could be dose dependent | 77 |
| 3.4.2. Timings of DNA damage generation and repair..... | 79 |
| 3.4.3. Possible late generation of DNA damage | 81 |
| 3.4.4. UVA may be more mutagenic than first thought..... | 82 |
| 3.4.5. Future research | 84 |
| Chapter 4: Characterisation of the DNA damage response induced by the UVA bystander effect..... | 85 |
| 4.1. Introduction | 86 |
| 4.2. Aims..... | 87 |
| 4.3. Results | 88 |
| 4.3.1. Activation of the DDR..... | 90 |
| 4.3.2. IF analysis of γ H2AX generation..... | 95 |
| 4.3.3. Comparison across all doses | 101 |
| 4.3.4. Anomalies in γ H2AX activation | 101 |
| 4.4. Discussion..... | 104 |

| | |
|--|------------|
| 4.4.1. Dose dependent changes in protein activation | 105 |
| 4.4.2. γ H2AX is possibly activated via ATM and prior to ATR activation | 105 |
| 4.4.3. Bystander effect observed at 24 hours post irradiation | 107 |
| 4.4.4. Unexpected γ H2AX findings | 107 |
| 4.4.5. Future research | 108 |
| Chapter 5: General discussion | 110 |
| 5.1. Introduction | 111 |
| 5.2. Characterising the DDR in directly UVA irradiated cells | 112 |
| 5.3. DDR activation in the UVA-induced bystander effect..... | 114 |
| 5.4. Dose dependent changes in direct and indirectly irradiated cells..... | 114 |
| 5.5. Final conclusions | 115 |
| References..... | 118 |

List of Figures

| | |
|--|-----------|
| Figure 1.1: UVA spectrum | 13 |
| Figure 1.2: Skin anatomy..... | 15 |
| Figure 1.3: Formation of pyrimidine dimers | 21 |
| Figure 1.4: Type 1 and type 2 photosensitisation reactions | 24 |
| Figure 1.5: Oxidation of guanine..... | 26 |
| Figure 1.6: The cell cycle | 27 |
| Figure 1.7: DNA damage response..... | 36 |
| Figure 1.8: Non-homologous end joining..... | 37 |
| Figure 1.9: Homologous recombination | 38 |
| <i>Figure 3.1: DDR protein activation in response to 72 kJ/m² of direct UVA irradiation.....</i> | <i>63</i> |
| <i>Figure 3.2: DDR protein activation in response to 108 kJ/m² of direct UVA irradiation.....</i> | <i>65</i> |
| <i>Figure 3.3: DDR protein activation in response to 144 kJ/m² of direct UVA irradiation.....</i> | <i>67</i> |
| <i>Figure 3.4: γH2AX protein activation in response to 72 kJ/m² of direct UVA irradiation.....</i> | <i>69</i> |
| <i>Figure 3.5: γH2AX protein activation in response to 108 kJ/m² of direct UVA irradiation.....</i> | <i>71</i> |
| <i>Figure 3.6: γH2AX protein activation in response to 144 kJ/m² of direct UVA irradiation.....</i> | <i>74</i> |
| <i>Figure 4.1: Modelling of the bystander effect.....</i> | <i>89</i> |
| <i>Figure 4.2: Activation of DDR proteins in bystander cells co-incubated with UVA irradiated cells at 72 kJ/m²</i> | <i>91</i> |
| Figure 4.3: Activation of DDR proteins in bystander cells co-incubated with UVA irradiated cells at 108 kJ/m ² | 93 |

| | |
|---|-----|
| <i>Figure 4.4: Activation of DDR proteins in bystander cells co-incubated with UVA irradiated cells at 144 kJ/m².</i> | 94 |
| <i>Figure 4.5: Activation of γH2AX in bystander cells co-incubated with UVA irradiated cells at 72 kJ/m².</i> | 96 |
| <i>Figure 4.6: Activation of γH2AX in bystander cells co-incubated with UVA irradiated cells at 108 kJ/m².</i> | 98 |
| <i>Figure 4.7: Activation of γH2AX in bystander cells co-incubated with UVA irradiated cells at 144 kJ/m².</i> | 100 |
| <i>Figure 4.8: γH2AX troubleshooting with 72 kJ/m² direct UVA irradiation.</i> | 102 |
| <i>Figure 4.9: γH2AX troubleshooting with 72 kJ/m² UVA irradiation in bystander cells</i> | 102 |
| <i>Figure 4.10: γH2AX troubleshooting with new cells.</i> | 103 |

List of Tables

| | |
|---|----|
| Table 2.1: Irradiation dose | 52 |
| Table 2.2: Antibodies for Western blot..... | 54 |
| Table 2.3: Antibodies for immunofluorescence..... | 56 |
| Table 2.4: Confocal microscope settings | 56 |

I: Abbreviations

| | |
|--------|------------------------------------|
| 6-4PP | 6-4 photoproduct |
| 6-GT | 6-thioguanine |
| 8-oxoG | 8-oxoguanine |
| 9-1-1 | Rad9-Hus1-Rad1 |
| ATM | Ataxia Telangiectasia mutated |
| ATR | ATM and Rad3 related |
| ATRIP | ATR interacting protein |
| BCC | Basal cell carcinoma |
| BER | Base excision repair |
| Cdk | Cyclin dependent kinase |
| CMM | Cutaneous malignant melanoma |
| Chk1 | Checkpoint kinase 1 |
| Chk2 | Checkpoint kinase 2 |
| CPD | Cyclobutane pyrimidine dimer |
| DDR | DNA damage response |
| DMEM | Dulbecco's modified eagles' medium |
| DNA | Deoxyribonucleic acid |
| DNA-PK | DNA-dependent protein kinase |
| DPI | Diphenyleneiodonium |
| DSB | Double strand break |
| dsDNA | Double stranded DNA |
| DTT | Dithiothreitol |
| EDTA | Ethylenediamine tetraacetic acid |
| EdU | 5'ethynyl-2'-deoxyuridine |
| FBS | Foetal bovine serum |
| H2AX | histone 2AX |
| HR | Homologous recombination |
| IF | Immunofluorescence |
| IL | Interleukin |

| | |
|-------------------|--|
| IR | Irradiated condition |
| IQR | Interquartile range |
| LPB | Lipid peroxidation by-products |
| NHEJ | Non-homologous end joining |
| NMSC | Non-melanoma skin cancer |
| MRN | Mre11-Rad50-Nbs1 |
| NER | Nucleotide excision repair |
| NT | No transwell |
| PBS | Phosphate buffered saline |
| PFA | Paraformaldehyde |
| PS | Photosensitiser |
| ROS | Reactive oxygen species |
| RFC | Replication factor C |
| RPA | Replication protein A |
| SCC | Squamous cell carcinoma |
| SDS | Sodium dodecyl sulphate |
| SDS-PAGE | SDS-polyacrylamide gel electrophoresis |
| SOD | superoxide dismutase |
| SSB | Single strand break |
| ssDNA | Single stranded DNA |
| TLS | Translesion synthesis |
| TT | Thymine thymine |
| Ub- γ H2AX | Ubiquitylated γ H2AX |
| UI | Unirradiated |
| UV | Ultraviolet |

II: Abstract

Ultraviolet (UV) radiation is a carcinogen responsible for causing skin cancer, one of the most common forms of cancer globally. UV irradiation leads to DNA damage including oxidised bases, cyclobutane pyrimidine dimer (CPD) formation and double strand breaks (DSB) activating the DNA damage response (DDR). Whilst UVB is directly more damaging to cellular DNA, it is becoming increasingly clear that UVA plays a large role in DNA damage induction and carcinogenesis. The DDR pathway is well understood, but the kinetics of protein activation need to be studied in more detail to develop our understanding of DNA damage induction, persistence and repair induced by UVA irradiation. Using dose dependent studies, human immortalised keratinocytes (HaCaTs) were exposed to UVA irradiation looking at DDR proteins, studying their activation and downregulation. A dose dependent change in activation of the DDR pathways was identified. Lower UVA doses demonstrated earlier activation of the ATR response whilst medium and higher doses indicated earlier activation of the ATM response. Furthermore, as the dose increased, peak activation of total γ H2AX was observed later, as did possible repair of DNA damage. Finally, the late activation of sensor protein RPA could indicate the late generation of DNA damage resulting from oxidative stress.

It is becoming increasingly apparent that direct irradiation is not the only cause of DNA damage and carcinogenesis. Indirect damage of neighbouring cells via factors released by the irradiated population is causing cellular stress and DNA damage. The resulting damage in bystander cells has been previously studied, but the DDR is less well understood. This research aimed to develop understanding of DDR protein activation and downregulation using a co-incubation technique. It was indicated there was a dose dependent change in DDR pathway activation where the ATM response occurred later at a higher dose whilst the reverse was observed for direct irradiations. The data implied that γ H2AX was the result of ATM activation arguing against others which suggested it becomes activated by the ATR response.

Chapter 1: Introduction

1.1. UV radiation

The ultraviolet (UV) spectrum ranges from 100-400 nm in the electromagnetic spectrum. As seen in figure 1.1, it is composed of three main regions: UVC, UVB and UVA. UVC is short wavelength UV ranging from 200-280 nm. This region of UV radiation is the most damaging to humans because it falls within the absorbance spectra of nucleic acids (230-300 nm) (figure 1.1) meaning it can be absorbed by DNA leading to DNA damage. Although it is the most dangerous, it is blocked by oxygen in the atmosphere preventing humans from being exposed to it. UVB only accounts for 5-10% of UV reaching the Earth's surface as most is unable to penetrate through the ozone layer. However, its wavelength ranges from 280-315 nm and is able to penetrate into the epidermis of the skin so it can also be absorbed by DNA causing damage such as cyclobutane pyrimidine dimers (CPD) which have the potential to cause skin cancer. Long wavelength UVA has the greatest penetrative ability as all UVA is able to pass through the ozone accounting for 90-95% of UV reaching the Earth's surface and can reach deep into the dermis of the skin. Its range of 315-400 nm falls outside of the absorbance spectra of nucleic acids and therefore cannot cause any direct DNA damage to cells. On the other hand, it can cause indirect DNA damage via photosensitisation reactions which lead to the production of reactive oxygen species (ROS). The damaging consequences of this can lead to cancer and are also involved in skin ageing (D'Orazio et al, 2013; Laikova et al, 2019; Schuch and Menck, 2010).

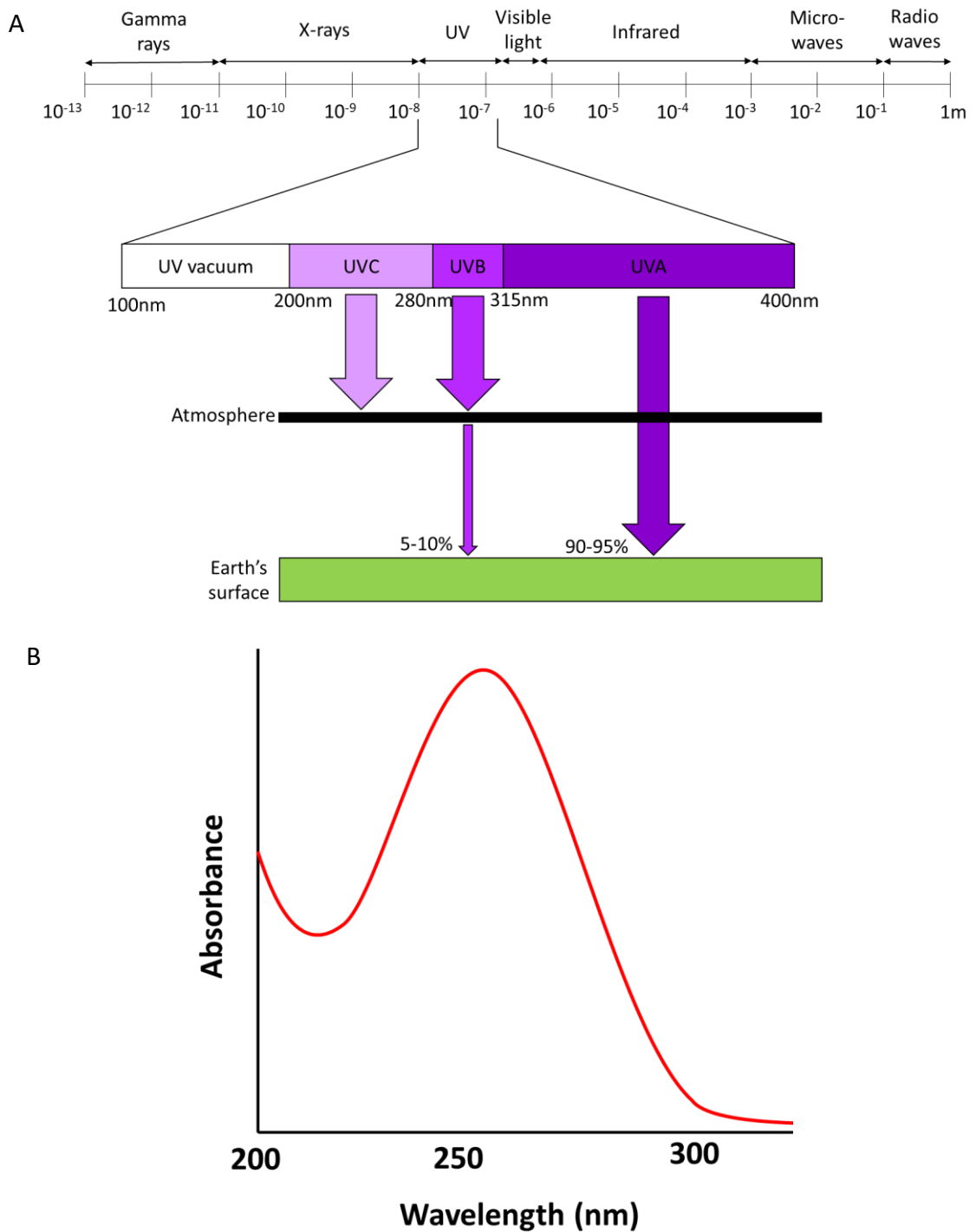


Figure 1.1: UV spectrum.

(A) The UV spectrum ranges from 100-400 nm and is formed of three main regions: UVC, UVB and UVA. The ozone layer is able to filter out most UV radiation reaching the earth's surface with 90-95% of solar UV being UVA and only 5-10% UVB. UVC is unable to penetrate through the atmosphere. (B) Absorbance spectra of DNA.

1.2. Skin cancer

1.2.1. Structure of the skin

Skin architecture is complex, made up of many different structures as depicted in figure 1.2. The epidermis is on the surface of the skin with the dermis sitting below it separated by the basement membrane. It is formed of 4-5 layers of keratinocytes joined by desmosomes and tight junctions creating a strong and protective barrier against external physiological barriers such pathogens and importantly UV. Fibroblasts are the cells located in the dermis (D’Orazio et al, 2013), meanwhile melanocytes are located in both the basal layer of the epidermis and the dermis and are in contact with 9-36 keratinocytes supplying them melanin. The melanin produced by melanocytes is transported to the keratinocytes via melanosomes and accumulate in cells forming a cap over the nuclei. As a result of its broad absorption spectrum, it protects from solar UV radiation reducing DNA damage and therefore the risk of skin cancer. It is most effective at absorbing shorter wavelengths of UV giving it a lower level of protection against UVA compared to UVB (Hennessy et al, 2005; Nishiura et al, 2012; Premi et al, 2015). It has also been suggested that melanin may act as a scavenger of free radicals to protect against oxidative stress (Premi et al, 2015). There are two types of melanin: eumelanin which is a brown/black pigment and the most effective at blocking UV radiation and pheomelanin which is a lighter pigment of a yellow/red colouration and more sensitive to UV (Hennessy et al, 2005; Premi et al, 2015). Pheomelanin is found in similar abundances between individuals of different skin tones whereas eumelanin varies and ultimately determines skin colour and UV sensitivity (D’Orazio et al, 2013). The control of pheomelanin and eumelanin production is determined by MC1R protein. Hypomorphic single nucleotide polymorphisms in this gene result in a higher production of pheomelanin than eumelanin resulting in lighter skin pigmentation and red hair. The skin type of individuals is one of the biggest risk factors for skin cancer (Hennessy et al, 2005; Premi et al, 2015).

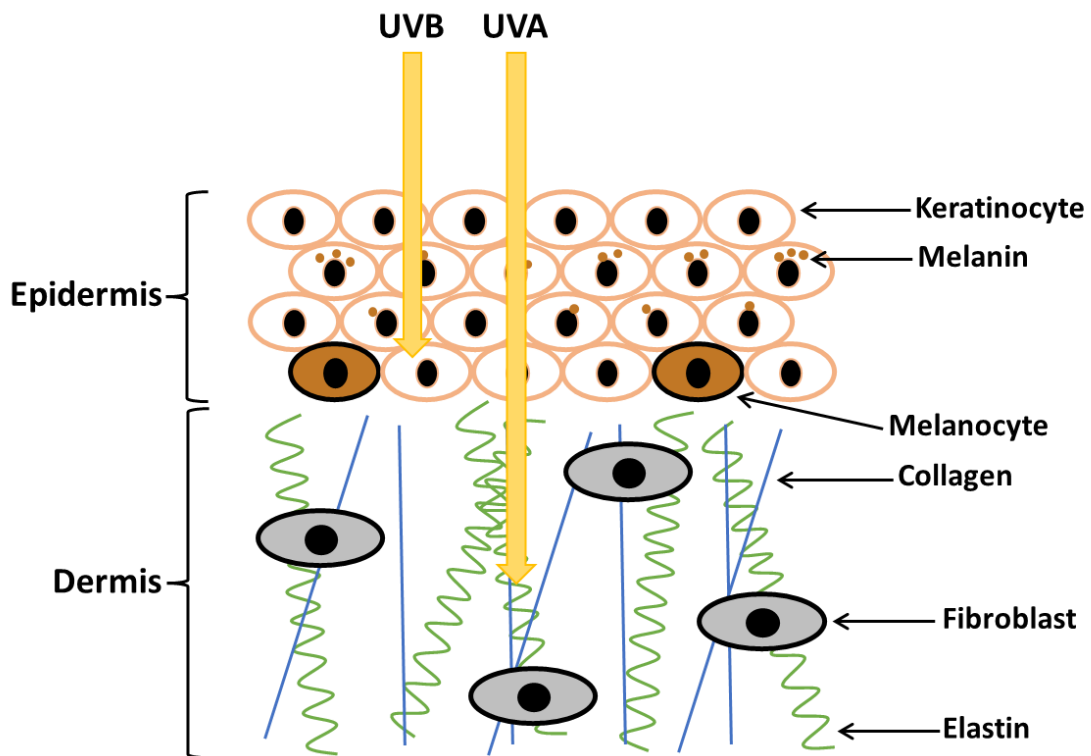


Figure 1.2: Skin anatomy

This schematic displays the various structures and the penetrating abilities of different components of the UV spectrum. UVA is able to penetrate deeper into the skin reaching the dermis whilst UVB only penetrates through the epidermis.

1.2.2. What is skin cancer?

Skin cancer is one of the most prevalent types of cancer globally with one third of new cancer diagnoses each year being a type of skin cancer (Laikova et al, 2019). The incidence has increased over the last few decades now reaching approximately 1.3 million new cases globally in 2018 (Bray et al, 2018; Ferlay et al, 2019). There are two main types of skin cancer: cutaneous malignant melanoma (CMM) and non-melanoma skin cancer (NMSC) and both have many factors influencing the risk of an individual suffering from the disease which will be discussed in the following sections (Khazaei et al, 2019; Seraji et al, 2020).

NMSC was accountable for approximately 80% of skin cancer diagnoses with over one million new cases globally in 2018 (Bray et al, 2018; Ferlay et al, 2019). This type of skin cancer originates from the keratinocytes in the epidermis and falls into two main categories: basal cell carcinomas (BCC) responsible for 80% of NMSC and squamous cell

carcinomas (SCC) which causes 20% of NMSC cases (Khazaei et al, 2019). Although the incidence is high, the long-term prognosis is good, with the majority of patients surviving the disease and only a 6% mortality rate (Bray et al, 2018; Ferlay et al, 2019).

CMM, originating in melanocytes, is responsible for approximately 20% of skin cancer cases however, it caused 48% of skin cancer related deaths globally in 2018 (Bray et al, 2018; Ferlay et al, 2019). This form of skin cancer can be highly metastatic with the added complications of being resistant to many drugs, making it difficult to treat (D’Orazio et al, 2013; Laikova et al, 2019).

1.2.3. Risk factors for skin cancer

Genetic factors are important when determining risk of skin cancer development. The odds of developing skin cancer for an individual with green or blue eyes are increased by 61-68% for BCC and 50-100% for CMM when compared to people with dark coloured eyes (Clough-Gorr et al, 2017; Khalesi et al, 2013). Similar results were observed for hair colour where red hair increased the odds by two-fold for BCC (Khalesi et al, 2013). Meanwhile, red, or blonde hair increases risk for melanoma four-five times compared to dark hair colour (Clough-Gorr et al, 2017). This is due to pigmentation which also applies to the skin in which lighter skin-coloured individuals are twice as likely get skin cancer than those with darker skin tones (Gandini et al, 2005iii; Khalesi et al, 2013). For this reason, it is often found that countries with larger white populations have a higher incidence of skin cancer. For example, Australia where skin cancer accounts for 45% of all new cancer diagnoses each year (Khazaei et al, 2019; Seraji et al, 2020). Furthermore, more than fifteen nevi on a person’s body are associated with an increased relative risk of skin cancer, especially melanoma where the risk can be up to seven times higher for people with one hundred nevi on their body (Gandini et al, 2005i).

1.2.4 Association between skin cancer and UV exposure

Approximately 90% of CMM and up to 85% of NMSC are caused by UV radiation, the source of which can either be solar or artificial such as from tanning beds (An et al, 2021). The main source of UV that individuals are exposed to is solar, but 35% of the adult population and 19.3% of adolescents in Europe have used tanning beds (Wehner et al, 2014). Whilst modern tanning beds emit mostly UVA (>98%) (Zhang et al, 2012), the

dose intensity emitted can be up to three times that of the sun and UVB emissions close to that of bright sun exposure making them a dangerous source of UV (Clough-Gorr et al, 2017).

CMM is more strongly related to short term, high intensity sun exposure such as sunbathing and sunburns, as opposed to chronic sun exposure. It was demonstrated that intermittent sun exposure such as recreational activities of sunbathing or water sports carried an odds ratio of 1.2-1.35 (Clough-Gorr et al, 2017; Seraji et al, 2020) whilst individuals who have experienced sunburn could be twice as likely to develop CMM (Clough-Gorr et al, 2017; Gandini et al, 2005ii). Furthermore, the use of tanning beds can also influence melanoma risk. Use of these just four times a year is associated with an 11% increased risk of CMM (Zhang et al, 2012) whilst tanning bed use of more than ten times per year or first use at under the age of twenty can increase relative risk by up to 50% (An et al, 2021).

The relationship between BCC and sun exposure patterns is still not fully understood. Some research has indicated that it is more intermittent with regards to sunburn, recreational activities, and holidays (Kricke et al, 1995) whilst the distribution of BCC on the body points towards chronic exposure with most cases occurring on the face (Iannaccone et al, 2012). An individual's risk when using tanning beds more ten times per year is 45% and 85% when first used under the age of 20 (An et al, 2021) meanwhile occupational exposure can increase risk of BCC development by 43% (Khazaei et al, 2019).

SCC on the other hand is more strongly associated with chronic UV exposure resulting in an accumulation of DNA damage over time (Wischer et al, 2008). Tanning bed use as little as four times per year increases NMSC risk by approximately 15% (Zhang et al, 2012) and 77% higher in people who are frequently exposed to UV for long periods of time e.g. outdoor workers (Khazaei et al, 2019).

Combined, these studies demonstrate the large impact UV can impose on an individual whether the source is natural or artificial. This is especially concerning for children. A recent study in children in Ireland aged 10-17 years old showed that many children were not protected from natural sun exposure with 17% never using sunscreen whilst only

one third avoided direct sun between 12-3pm and 3% never using any form of sun protection. Furthermore, 90% of children have experienced sunburn at least once and 3% using tanning beds. This data highlights the importance of studying skin cancer and its prevention. Whilst the risks are known, more needs to be done to protect individuals from UV exposure (Költő et al, 2021).

The ability of UVA to induce tumours was demonstrated in mice in a range of experiments. A daily dose of just 20 kJ/m² was sufficient to induce papillomas (benign tumours) whilst 56 kJ/m² led to the development of SCCs. Since these tumours are linked to chronic UV exposure, it took an average of 473 days for tumours to develop (Kelfkens et al, 1991), but at higher doses of 220 kJ/m² reduced the average to just 265 days (Sternberg and Leun, 1990). Meanwhile UVB is a more potent tumorigenic agent inducing tumours in 208 days in mice where a combination of UVA and UVB treatments caused even shorter induction periods for tumour development (Berg et al, 1993). UVC has also been demonstrated to induce SCC in albino hairless mice following daily doses of irradiation (Sternberg et al, 1988) showing how all ranges of the UV spectrum are tumorigenic.

Skin cancer is one of the most preventable forms of cancer. With such a high fraction of skin cancer cases being related to UV, less exposure reduces an individual's risk. For example, not using tanning beds and covering skin with clothing or sunscreen can reduce an individual's life-time risk of developing the disease (Khazaei et al, 2019; Költő et al, 2021). UV intensity is stronger near the equator, at higher altitudes and in the southern hemisphere and since UV is strongly linked to skin cancer risk, an individual's geographical location also determines the likelihood of getting skin cancer (Khazaei et al, 2019; Seraji et al, 2020).

1.3. UV-induced DNA damage

1.3.1. Pyrimidine dimers

Pyrimidine dimers are premutagenic lesions (Rünger et al, 2012; Schuch and Menck, 2010) occurring as a result of UV damage via either direct absorption by the DNA or indirectly by excitation of chromophores. This creates covalent bonds between adjacent pyrimidines distorting the double helix (Chatterjee and Walker, 2017; Cortat et al, 2013;

Douki et al, 2017; Singh et al, 2018). Due to the stringent active site of replicative polymerases, DNA lesions and distorted DNA cannot be replicated leading to stalling of DNA replication. Instead, they are bypassed by translesion synthesis (TLS) polymerases (Hedglin and Benkovic, 2017; Walmacq et al, 2013; Waters et al, 2009). TLS polymerases have a more flexible active site enabling nucleotide incorporation at distortions in the DNA allowing the bypass of lesions such as cyclobutane pyrimidine dimers (CPDs) (Hedglin and Benkovic, 2017; Walmacq et al, 2013). However, they lack the 3' to 5' exonuclease proofreading ability that replicative polymerases have reducing the fidelity of replication (Hedglin and Benkovic, 2017; Walmacq et al, 2013; Waters et al, 2009). The error rate of replicative polymerases is one error in every 10^6 - 10^8 bases which increases to an error in every 10^1 - 10^5 for TLS polymerases (Walmacq et al, 2013; Waters et al, 2009). Some types of TLS polymerases do not use Watson-Crick base pairing contributing to the high error rate (Waters et al, 2009). Some TLS polymerases are optimised to overcome certain types of damage. For example, the TLS polymerase η is used to overcome thymine-thymine dimers with a high degree of accuracy making it important for tolerating UV damage and preventing skin cancer (Hedglin and Benkovic, 2017; Walmacq et al, 2013; Waters et al, 2009). Alternatively, DNA lesions can be repaired via nucleotide excision repair (NER) in which incisions either side of the lesion are created to remove the damage which is resynthesised and ligated. This can occur across the genome (global genome repair) or during transcription to remove obstructing damage (transcription coupled repair) (Cortat et al, 2013; Rastogi et al, 2010).

There are two types of pyrimidine dimers: cyclobutane pyrimidine dimers (CPDs) and 6-4 photoproducts (6-4PP). CPDs occur more frequently making up approximately 90% of this type of DNA damage. These dimers have double covalent bonds between C5 and C6 of 2 adjacent pyrimidines (Figure 1.3) (Cortat et al, 2013; Douki et al, 2017; Singh et al, 2018). Thymine dimers are the most common pyrimidine dimer (Courdavault et al, 2005) and are recognised as being a hallmark of UV-induced DNA damage, but TC, CT and CC dimers can also occur (Douki et al, 2017). Those containing cytosine are more mutagenic due to the ability of cytosine to be spontaneously deaminated to uracil which would pair with adenine upon replication. In the following replication cycle this would result in a C>T transversion mutation or CC>TT tandem mutation which are known as UV signature

mutations (Douki et al, 2017; Kim et al, 2013; Mouret et al, 2006; Rochette et al, 2003; Singh et al, 2018) which are frequently found in tumours associated with UV damage (Courdavault et al, 2005; Douki et al, 2017). Due to the longer time required to repair CPDs, they are more mutagenic than 6-4PPs (Kim et al, 2013). Whilst UVB generally shows a more even spread of CPD type, UVA predominantly shows TT-CPDs (Mouret et al, 2006; Rochette et al, 2003).

CPDs generated during the irradiation period are known as light-CPDs but CPD generation can occur post irradiation and these are called dark-CPDs which make up half of total CPD induction and can be found resulting from both UVA and UVB. It is believed melanin is responsible for this due to an increase in CPD generation for three hours post irradiation in melanin containing melanocytes compared to albino melanocytes with the damage increasing three-fold two hours following irradiation in mice. Furthermore, tyrosinase inhibitors (targeting an enzyme involved in melanin production) reduces dark CPD generation by 85% (Premi et al, 2015). Whilst previous analysis on the level of light CPDs containing thymine and cytosine in response to UVA irradiation has typically shown more thymine-thymine dimers (Mouret et al, 2006; Rochette et al, 2003), dark CPDs contain four times more cytosine containing dimers than TT dimers demonstrating a different mechanism of induction (Premi et al, 2015). This raises further concerns for tumorigenesis since cytosine-containing CPDs are more mutagenic (Douki et al, 2017; Kim et al, 2013). Dark CPDs are made from triplet energy carbonyls formed from dioxetane which transfer their energy to DNA leading to CPD production. UV induced superoxide and nitric oxide are implicated in the formation of these triplet energy carbonyls. The carbonyl moieties have a lifetime of 10 μ s but the oxidative stress in the cell leads to continuous generation, explaining production of dark CPDs as late as three hours post irradiation (Premi et al, 2015).

6-4PP have a covalent bond connecting C6 of the 5' base to C4 of the 3' base (Figure 1.3) (Chatterjee and Walker, 2017; Cortat et al, 2013; Douki et al, 2017; Zhao et al, 2011). This type of lesion has an absorbance of 320 nm falling into the range of UVA which means upon further UVA exposure, it can be converted into a Dewar valent isomer. As UVA is not believed to cause 6-4PPs, it is a combination of UVB generating the 6-4PPs and UVA forming their isomers which leads to the generation of this kind of DNA damage

(Chatterjee and Walker, 2017; Courdavault et al, 2005; Douki et al, 2017; Schuch and Menck, 2010; Yagura et al, 2017). Both 6-4PP and Dewar valent isomers are repaired as equally quick and more rapidly than CPDs making them less dangerous (Courdavault et al, 2005; Kim et al, 2013).

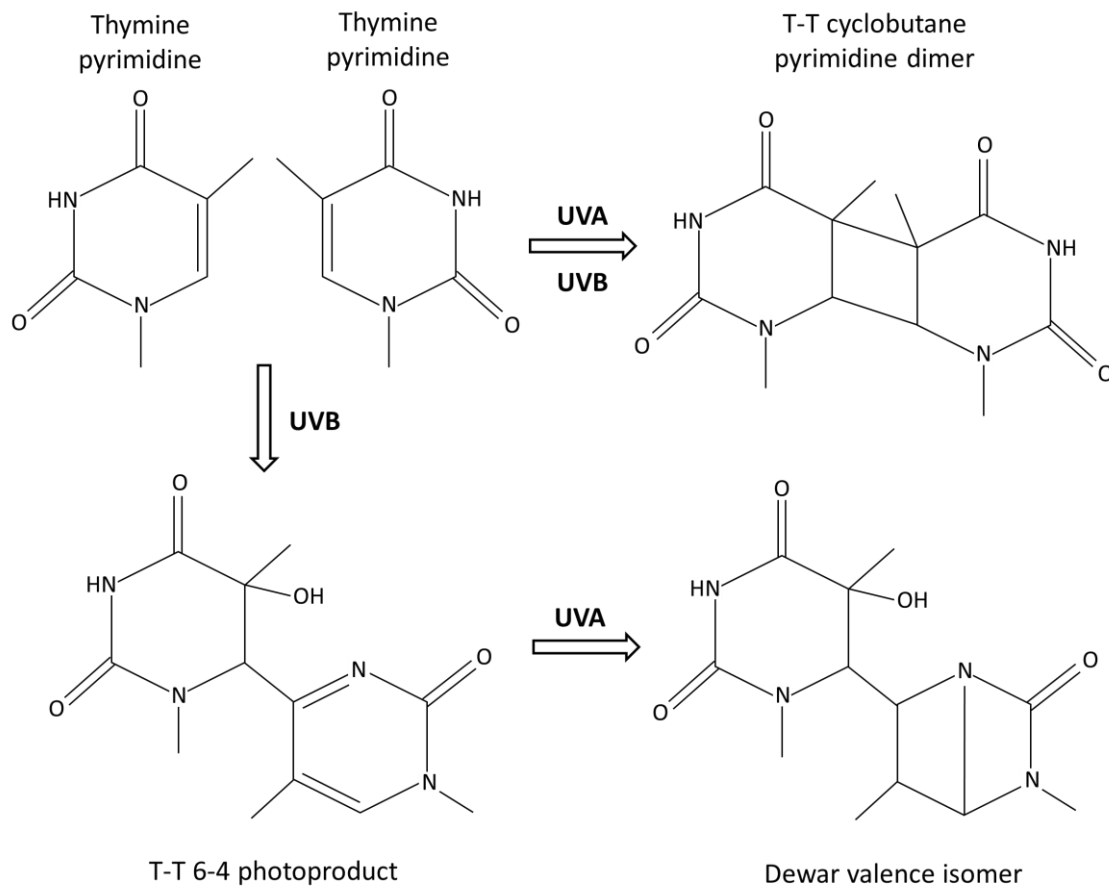


Figure 1.3: Formation of pyrimidine dimers

Formation of different pyrimidine dimers formed from two thymine bases in response to UVA and UVB irradiation. Both UVA and UVB are capable of inducing CPDs whilst UVB forms 6-4 photoproducts which can be converted in Dewar valence isomers using UVA.

These types of DNA lesions are an important focus of research since an estimated 50-100 lesions can occur per second when exposed to UV (Zhao et al, 2011) and can cause apoptosis, mutations, and cancer (Cortat et al, 2013). All regions of the UV spectrum can induce pyrimidine dimers but the efficiency to do so reduces as the wavelength gets

longer making UVA the weakest dimer inducing agent and UVC the strongest (Douki et al, 2017; Girard et al, 2008). This was demonstrated in whole skin samples in which lesion induction for UVB was 518 lesions per 10^6 normal bases per J/cm^2 compared to just 0.081 lesions per 10^6 normal bases per J/cm^2 (Mouret et al, 2006). UVB has the ability to directly induce pyrimidines dimers since the absorbance of DNA falls into the range of UVB. UVA, however, must induce its damage indirectly via triplet energy transfer via a photosensitiser. Due to this, fewer CPDs and no 6-4PPs are produced as a result of UVA compared to UVB (Chatterjee and Walker, 2017; Courdavault et al, 2005; Girard et al, 2008; Mouret et al, 2006; Runger et al, 2012; Schuch and Menck, 2010; Wischermann et al, 2008; Yagura et al, 2017). Yagura et al, 2017, identified the formation of 6-4PP in response to $500 \text{ kJ}/\text{m}^2$ of UVA in a cell free system experimenting only on the DNA from the cells. This meant there was no confounding photosensitisers in the system to indirectly cause DNA lesions. This suggested that with larger doses of UVA exposure, it may have a direct impact on DNA inducing 6-4PP. However, using a cell free system is not physiologically relevant as the UVA rays must penetrate through the cell membrane and nucleus before reaching the DNA. This study also used a larger dose of $500 \text{ kJ}/\text{m}^2$ UVA compared to other research ($0\text{-}120 \text{ kJ}/\text{m}^2$) which could explain the discrepancies between the studies in terms of the types of damage directly or indirectly created by UVA (Yagura et al, 2017).

1.3.2. Oxidative stress

UVA is not of a high enough energy to directly break the covalent bonds in DNA to cause damage. Instead, it induces DNA damage indirectly via the generation of reactive oxygen species such as hydrogen peroxide, hydroxyl radicals, superoxide, and singlet oxygen (Cadet and Douki, 2011; Graindorge et al, 2015; Greinert et al, 2012; Runger et al, 2012). UVA is absorbed by photosensitisers both inside and outside of the cell such as porphyrins, quinones and flavins leading to the production of ROS (Cadet and Douki, 2011; Cortat et al, 2013; Graindorge et al, 2015; Greinert et al, 2012). It is believed the photosensitisers responsible for generating ROS must be in close proximity with the DNA. Although radicals are highly reactive, they have short life spans and diffusion ranges from 2 nm for hydroxyl radicals up to 100 nm for singlet oxygen. Therefore, to

induce DNA damage the photosensitisers must be localised or potentially bound to the chromatin (Greinert et al, 2012; Cannan and Pederson, 2016).

ROS generation can occur via two types of reaction displayed in Figure 1.4. Type I photosensitisation occurs when the excited photosensitiser abstracts an electron and transfers it to another molecule forming two radicals (Cadet and Douki, 2011; Cadet et al, 2015; Cortat et al, 2013; Graindorge et al, 2015). The photosensitiser anion is oxidised back to its original state via oxygen and forms superoxide in the process. Meanwhile, the target cation undergoes hydration or deprotonation forming neutral radicals which can undergo further reactions with oxygen or superoxide and oxidise the DNA (Cadet et al, 2015). Through further reactions this can form hydrogen peroxide and then hydroxyl radicals by the Fenton reaction (Chatterjee and Walker, 2017; Graindorge et al, 2015; Schuch and Menck, 2010). The hydroxyl radical is highly reactive with DNA as it can abstract hydrogen atoms from deoxyribose sugars leading to single strand breaks (Balasubramanian et al, 1998; Cadet et al, 2015; Cannan and Pederson, 2016). The type II photosensitisation reaction converts oxygen from its ground state to its excited state forming singlet oxygen (Graindorge et al, 2015) which reacts with electron rich double bonds such as in guanine (Cadet et al, 2015). This is the main form of ROS by which UVA exerts its damaging effects with 80% of oxidised bases being caused by singlet oxygen and 20% by hydroxyl radicals (Cadet and Douki, 2011). Using enhancers and suppressors of singlet oxygen, Yagura et al, 2017 was able to demonstrate the involvement of UVA in producing singlet oxygen which led to corresponding changes in DNA damage generation represented by fpg sites (formamidopyrimidine DNA glycosylase enzyme – a repair enzyme for oxidative damage) (Yagura et al, 2017).

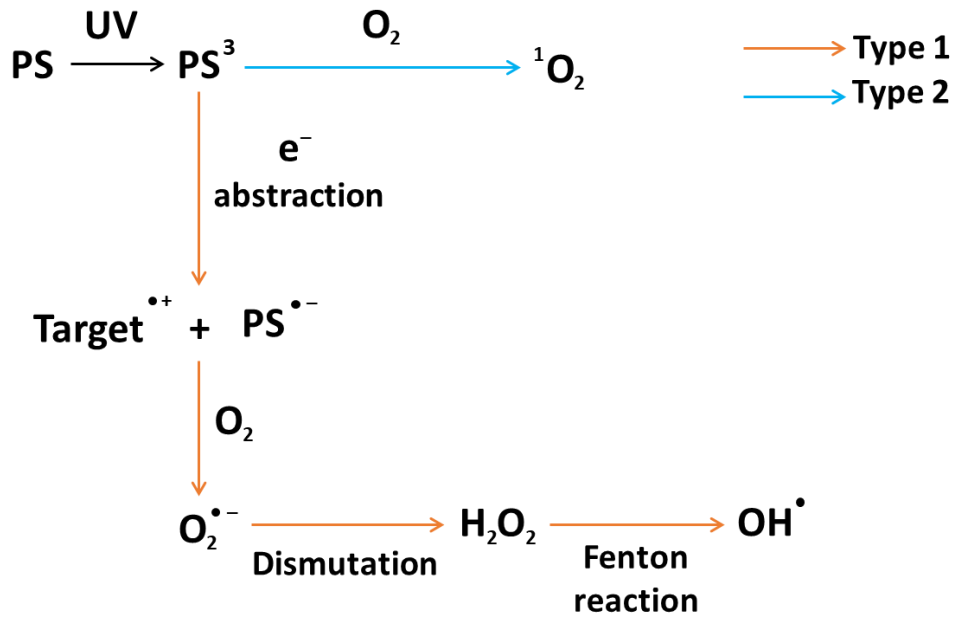


Figure 1.4: Type I and type II photosensitisation reactions

Formation of different ROS from photosensitisation reactions. The photosensitiser (PS) is energised to a triplet state which is then converted into singlet oxygen in the type II via reactions with oxygen or forms radicals due to electron abstraction in the type I pathway. Superoxide is then formed from the radicals reacting with oxygen which is converted into hydrogen peroxide via spontaneous or enzymatic dismutation. This then forms the highly reactive hydroxyl radical via the Fenton reaction with ferrous ion (Cadet et al, 2015).

The ROS generated by UVA can go on to damage macromolecules in the cell such as oxidising proteins impairing their structure and function (Cadet and Douki, 2011; Girard et al, 2008; Montaner et al, 2007), form single strand breaks (SSB) and oxidise the DNA bases. Guanine is the most oxidisable base in DNA; generating 8-oxo-7,8-dihydroguanine (8oxoG) (Cadet and Douki, 2011; Chatterjee and Walker, 2017; Greinert et al, 2012; Wischermann et al, 2008; Yagura et al, 2017) which is now seen as a biomarker for oxidative stress (Cadet and Douki, 2011). 8oxoG pairs with adenine (Figure 1.5) leading to G>T mutations in following rounds of replication potentially causing cancer (Chatterjee and Walker, 2017; Wischermann et al, 2008). Whilst UV irradiation does cause oxidative stress, few G>T mutations occur. The signature mutation of UV damage is C>T mutations generated from pyrimidine dimers. UVB generates two times more CPDs compared to 8oxoG whilst for UVA CPD damage is nine times higher (Mouret et al, 2006). Base excision repair (BER) is a process in which DNA damage is removed, targeting lesions which induce little distortion to the DNA helix such as oxidative damage. The damaged base is removed by DNA glycosylases and the abasic site is repaired by either short- or long-patch repair (Krokan and Bjørås, 2013).

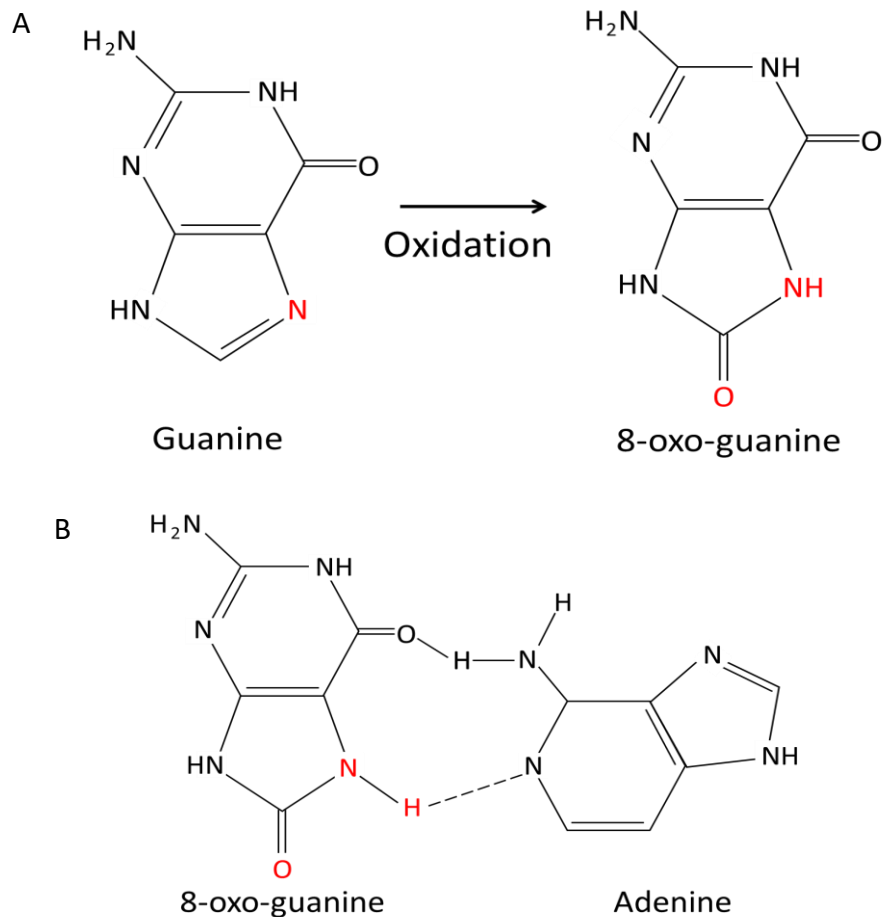


Figure 1.5: Oxidation of guanine

Oxidation of the base guanine into 8-oxo-guanine (A) and how it incorrectly bonds with adenine (B).

1.4. The cell cycle

1.4.1. The cell cycle

The cell cycle is a highly regulated pathway controlled by a complex array of proteins. The cycle can be broken down into four main stages: G1, S, G2 and M. The transitions between each phase are regulated by cyclin-CDK complexes where each complex is specific to a certain region of the cell cycle (see figure 1.6). The cyclin activity increases throughout the duration of the cycle and the complexes are degraded by the ubiquitin mediated proteasome system when they are no longer required in order to ensure forward progression throughout the cycle. Mitogenic signalling is required to stimulate cell growth until it reaches the restriction point in G1 in which the cell is committed to completing the cycle. The mitogens activate transcription factors which upregulates

cyclin D. When this binds to CDK4/6, the retinoblastoma protein becomes phosphorylated and releases its inhibition on E2F transcription factors leading to the production of proteins required for S phase such as cyclin E and DNA replication proteins. The DNA damage checkpoint ensures that no DNA damage is replicated, pausing the cycle for any repairs, or inducing apoptosis if the damage cannot be fixed. There are two further checkpoints in G2 and M phase to ensure DNA damage is not passed on to daughter cells and the genomic integrity is maintained. The APC complex initiates the exit of mitosis and resets the cell ready for the next cycle to begin (Bower et al, 2017; Gookin et al, 2017).

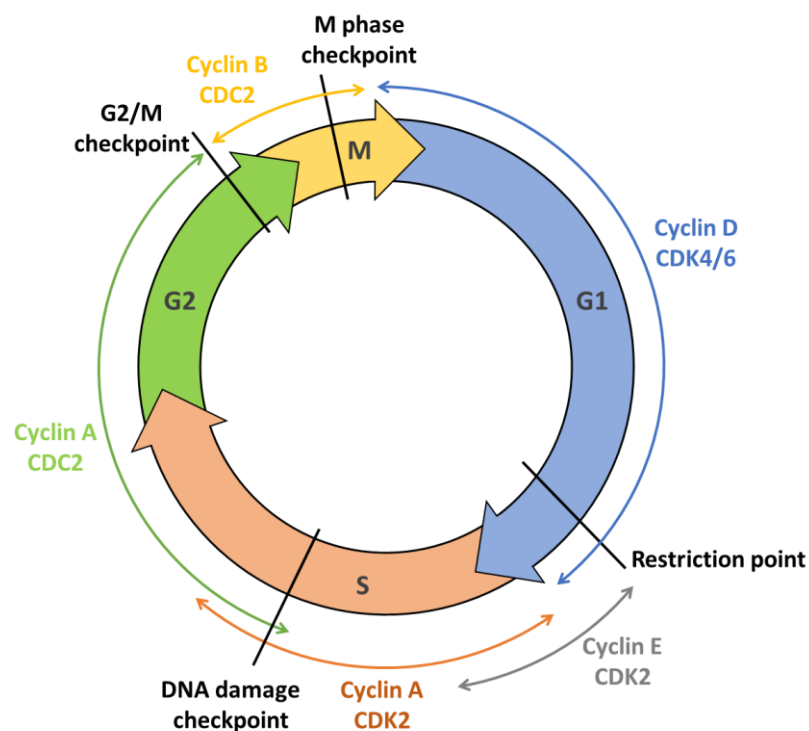


Figure 1.6: The cell cycle.

The cell cycle is composed of four main stages: G1, S, G2 and M each tightly regulated by cyclin-CDK complexes. Increasing cyclin activity throughout the cell cycle along with CDK inhibitors and ubiquitin mediated proteasomal degradation ensure forward progression. The different checkpoints safeguard against DNA damage being replicated and passed on to daughter cells making sure that genomic stability is maintained (Bower et al, 2017; Gookin et al, 2017).

1.4.2. Impact of UV on the cell cycle

Previous research has demonstrated UVA irradiation can cause immediate inhibition of DNA replication, S phase delay and an increased number of cells in S phase (Girard et al, 2008; Graindorge et al, 2015; Runger et al, 2012; Steel, 2016). UVA induced pyrimidine dimers and 8oxoG can hinder the replication process by stalling the replication forks due to distortion of the DNA helix. However, DNA damage can be bypassed or repaired so it does not fully explain the replication stress that occurs (Chatterjee and Walker, 2017; Cortat et al, 2013; Girard et al, 2008; Runger et al, 2012). In addition, replication inhibition also occurs independently of ATM and ATR activation, but DNA damage should activate the checkpoint (Girard et al, 2008). Furthermore, monoubiquitination of PCNA is identified as being a marker of stalled replication forks occurring as a result of DNA damage. This is absent in response to UVA irradiation but is present with equally mutagenic levels of UVC suggesting the mechanism inhibiting replication in response to UVA is different to that of other types of UV irradiation. It is more likely that oxidative damage is causing the UVA induced replication stress as incubation with antioxidants leads to less replication inhibition following UVA irradiation (Girard et al, 2008).

Oxidative damage to proteins can affect their structure and function inactivating them, if this occurs to replication proteins, it may cause the replication forks to stall (Cadet and Douki, 2011; Girard et al, 2008; Montaner et al, 2007). Montaner et al, 2007, identified oxidative modifications to replication protein PCNA whereby the subunits had become covalently crosslinked together in response to UVA. This effect coincided with replication inhibition, but it could not be concluded that the damaged PCNA was the cause as the impact this has on the protein's function is unknown. This study used the base analogue 6-thioguanine (6-GT) which behaves as a chromophore for UVA producing singlet oxygen which can then cause oxidative damage to proteins such as PCNA and other macromolecules in the cell. This damaged PCNA was also identified in response to other ROS e.g., hydrogen peroxide, and also in conditions without 6-GT with larger UVA doses implying a build-up of ROS can induce oxidative damage to PCNA (Montaner et al, 2007). The presence of covalently modified PCNA was also found using 80 kJ/m² of UVA irradiation demonstrating that direct UVA irradiation can induce oxidative modifications to proteins (Girard et al, 2008). If it is possible for ROS to induce

oxidative damage to PCNA, it may also cause similar damage to other cell cycle and replication proteins in the cell which could impair their function and stall the replication forks (Girard et al, 2008; Montaner et al, 2007).

Singlet oxygen has also been shown to slow fork velocity for up to 5 hours post irradiation (80 kJ/m² and 160 kJ/m² UVA) with similar reductions in BrdU incorporation. Three out of four dNTPs were also found to have a reduced concentration following irradiation. However, it was determined that the slow incorporation of the dNTPs was due to reduced fork velocity rather than dNTP concentration limiting DNA replication. Fork velocity had returned to normal earlier than BrdU incorporation suggesting a delay in origin firing further slowing the release of replication inhibition. The presence of singlet oxygen in this system further supports the theory that oxidative stress is responsible for replication inhibition and that ROS could modify replication proteins such as those required for replication machinery assembly which would hinder protein function and delay origin firing (Graindorge et al, 2015).

The cellular response to UVA differs to other forms of UV. For example, there is a reduction in DNA replication occurring in response to both UVA and UVB, but recovery is much faster in UVA taking up to 2 hours compared to 48 hours with UVB in neonatal human fibroblasts. G2/M arrest is also shorter for UVA lasting up to 8 hours and 48 hours for UVB while G1/S arrest does not occur in response to UVA but is present in synchronised cells exposed to UVB. In addition to this there is reduced p53 activation that is seen in UVA exposed cells (Rünger et al, 2012) and replication inhibition is independent of ATM/ATR activation (Girard et al, 2008). Due to differences in the amount and type of DNA damage induced by UVA and UVB, which may influence the cellular response, the study by Rünger et al (2012) used equimutagenic levels of irradiation to prevent this from being a confounding factor. These combined findings show that a reduced response is seen in UVA-exposed cells which may provide greater opportunity for mutations to arise as it is more likely to be replicated (Rünger et al, 2012). Cortat et al, 2013 also reported that there are two peaks of DNA damage seen in human fibroblasts following 120 kJ/m² of UVA observed via fpg-sensitive sites. This showed peaks at 4 hours and 24 hours where the latter is possibly induced by DNA strand breaks from oxidative stress (Cortat et al, 2013). If the cellular response is lower,

it could mean that not all DNA is being repaired before replication continues and the cell cycle progresses into the next phase (Rünger et al, 2012).

DNA strand breaks are another form of damage induced by UVA irradiation (Cadet and Douki, 2011; Cortat et al, 2013; Greinert et al, 2012; Wischermann et al, 2008) which can lead to the induction of chromosomal aberrations, cell death, mutations, and tumorigenesis (Jaiswal and Lindqvist, 2015; Mah et al, 2010). Multiple research papers have reported the induction of single strand breaks (SSBs) and double strand breaks (DSBs) (breaks in both strands of the DNA helix up to 20 bases apart) as a results of ROS production (Cadet and Douki, 2011; Cortat et al, 2013; Girard et al, 2008; Greinert et al, 2012; Mah et al, 2010; Wischermann et al, 2008). It is believed that the highly reactive radicals, such as the hydroxyl radical, react with the sugar-phosphate backbone leading to single strand breaks in the DNA (Balasubramanian et al, 1998; Cadet et al, 2015; Cannan and Pederson, 2016). This can further lead to replication stress, the formation of DSBs and chromosomal aberrations (Chatterjee and Walker, 2017; Cortat et al, 2013; Wischermann et al, 2008). SSBs, as well as other DNA lesions, can obstruct the replication machinery causing the forks to stall and collapse which can lead to the generation of DSB (Cannan and Pederson, 2016; Zhao et al, 2011). This is known as replication-dependent DSB induction, but it has been demonstrated that UVA can cause DSB formation independently of replication. Since it is probable that the photosensitisers are localised to specific regions in the DNA and the resulting ROS have short diffusion ranges, it is likely that oxidative damage, such as SSB generation, occurs in clusters rather than randomly across the genome. During repair, this clustered damage can form DSBs i.e., cuts in both DNA strands created by repair processes occurring between 1-20 bases apart (Greinert et al, 2012; Cannan and Pederson, 2016). On stretched chromatin fibres, Greinert et al (2012) demonstrated that damage was clustered in response to physiologically relevant UVA doses in HaCaT cells and fibroblast cells supporting the theory that DSB production in response to UVA can be replication independent (Greinert et al, 2012).

1.5. DNA damage response

1.5.1. DNA damage response pathway

The DNA damage response (DDR) is a complex pathway designed to identify DNA damage and either repair it or induce apoptosis if the damage cannot be repaired. The overall aim of the DDR is to maintain genomic integrity ensuring all DNA damage is detected and repaired and not passed on to daughter cells as this could lead to cancer. It requires an intricate balance of communication with other cellular processes to halt the cell cycle, enabling repair to take place (Bower et al, 2017; Girard et al, 2008; Jaiswal and Lindqvist, 2015; Zhao et al, 2011). Sensor proteins are responsible for scanning the genome looking for DNA damage and activate transducer proteins which amplify the signal and activate the effector proteins. Following this, either the cell cycle is arrested, and the damage is repaired, or apoptotic proteins are activated inducing cell death (Maréchal and Zou, 2013; Srinivas et al, 2019). A diagram in Figure 1.7 highlights the communication between the discussed proteins in the DDR in this section.

The MRN complex, consisting of Mre11, Rad50 and Nbs1, is an example of a sensor protein which scans the DNA looking for DSBs. It identifies ssDNA-dsDNA junctions and dsDNA ends which it binds to and recruits the transducing protein ataxia telangiectasia mutated (ATM) to the site of damage (Maréchal and Zou, 2013; Tsao et al, 2004; Williams and Zhang, 2021). Breaks in the DNA are also detected by the Ku70/Ku80 complex which activates DNA-PKs (Mah et al, 2010; Rother et al, 2020). ATR on the other hand responds to a broad range of DNA damage including DSB as well as replication stress (Maréchal and Zou, 2013; Shiotani et al, 2013). RPA coats ssDNA to protect it from forming secondary structures and degradation by nucleases (Ma and Dai, 2018; Williams and Zhang, 2021). When replication forks are stalled or breaks occur in the DNA, long stretches of RPA-ssDNA are formed which are identified by ATR (Maréchal and Zou, 2013; Shiotani et al, 2013; Williams and Zhang, 2021). It is this characteristic that allows ATR to identify a broader range of DNA damage compared to ATM (Maréchal and Zou, 2013; Shiotani et al, 2013). However, since SSBs and DSBs can occur from replication stress such as stalled forks, the ATM response can also be activated in these cases (Zhao et al, 2011).

For full ATR activation, multiple factors are required to maintain a high level of regulation in order to prevent inappropriate activation of the DDR as this may lead to activation of repair pathways or induce apoptosis when not required. Large concentrations of ATR and its substrates need to be localised to the site of damage and regulator proteins need to be recruited to activate ATR (Maréchal and Zou, 2013). ATR forms a complex with ATR interacting protein (ATRIP). It is through ATRIP that ATR indirectly binds to RPA-ssDNA localising it to regions of DNA damage. Following this, Rad17 bound to replication factor C (RFC) is recruited and loads the 9-1-1 complex onto the damaged DNA at the ssDNA-dsDNA junctions. TopBP1 is then recruited and binds to a phosphorylation site (Thr1989) on ATR allowing full activation of the ATR kinase activity enabling phosphorylation of effector protein checkpoint protein 1 (Chk1). The activation of ATR is dependent on Rad17-RFC, 9-1-1 and TopBP1 (Maréchal and Zou, 2013; Shiotani et al, 2013; Tsao, et al, 2004; Williams and Zhang, 2021).

Once ATM or ATR are activated, they begin phosphorylating and activating effector proteins which elicit a variety of responses. Chk1 (activated by ATR) and Chk2 (activated by ATM) are effector proteins involved in multiple pathways and can phosphorylate a range of proteins with activating or inhibitory effects. For example, they can phosphorylate and inactivate members of the Cdc25 family (Girard et al, 2008; Jaiswal and Lindqvist, 2015; Williams and Zhang, 2021). Cyclin B-Cdk1 is the complex controlling mitotic entry. When phosphorylated by Wee1 kinase, the complex is inhibited preventing mitosis. Cdc25 phosphatase removes those inhibitory phosphates from cyclin B-Cdk1 inducing mitosis (Lu et al, 2012; Rother et al, 2007; Wang et al, 2007). When Chk1 and Chk2 phosphorylate Cdc25A and Cdc25C it leads to polyubiquitylation and degradation of these phosphatases, preventing the dephosphorylation of cyclin B-Cdk1. This maintains its inhibited phosphorylated state causing G2/M arrest allowing DNA repair to occur. The checkpoint protein responsible for initiating this pathway is determined by the type of type of damage. ATM is usually responsible for responding to DSBs activating Chk2, but replication stress will activate the ATR-Chk1 pathway (Girard et al, 2008; Jaiswal and Lindqvist, 2015; Wang et al, 2007; Williams and Zhang, 2021). In addition to controlling the G2/M transitions, Chk1 can also influence the G1/S transition. Upon activation, Chk1 prevents the phosphorylation of RIF1 via Cdk1 allowing RIF1 to

form a complex with PP1. This complex inhibits the functions of Cdc7 and CDK2 which are involved in replication initiation. Therefore, Chk1 is able to inhibit the activation of origin firing allowing time for DNA repair before it is replicated (Williams and Zhang, 2021).

p53 can also influence the cell cycle. p53 is a tumour suppressor protein activated in response to cell stress such as DNA damage. Known as the guardian of the genome, p53 can either cause cell cycle arrest to allow the DNA damage to be repaired or induce apoptosis, preventing damaged cells from replicating thereby maintaining genomic stability and preventing cancer (Ali et al, 2017; Valente et al, 2020). These outcomes are controlled by p53's ability to activate and repress the expression of different genes (McKay et al, 2000). When inducing cell cycle arrest, p53 causes upregulation of the Cdk inhibitor p21, whilst also repressing Cdc25 and cyclin genes, reducing cyclin-Cdk activity and inhibiting progression into the next phase (Latonen et al, 2001; Rother et al, 2007). p53 regulates the induction of apoptosis by regulating apoptotic genes such as *Bcl-2* and *bax* (Latonen et al, 2001; Valente et al, 2020).

The timing of p53 stabilisation can influence the decision between cell cycle arrest or apoptosis. Following UV irradiation, p53 expression increases along with apoptosis rates. However, p53 expression prior to UV irradiation results in less UV-induced apoptosis. This is possibly due to the changes in transcription induced by p53 before the cells are irradiated protecting them (McKay et al, 2000). The level of ROS present will also determine which pathway p53 takes. When ROS levels are low, p53 targets antioxidant genes for activation in order to scavenge and neutralise ROS reducing oxidative stress. However, when ROS levels are high, antioxidant genes are downregulated and pro-oxidant genes are upregulated tipping the scales to apoptosis (Srinivas et al, 2019).

p53 is tightly regulated and continuously degraded to prevent inappropriate apoptosis or cell cycle arrest. It must therefore be stabilised in the cell before it can carry out its function. Mdm2 is an E3 ubiquitin ligase which ubiquitinates p53 targeting it for degradation via the ubiquitin-proteasome system. p53 itself can regulate Mdm2 at the transcriptional level inducing an autoregulatory loop that maintains low levels of p53. Upon cell stress, ATM is activated which phosphorylates Mdm2 preventing further

ubiquitination of p53 leading to stabilisation and accumulation (Latonen et al, 2001; Williams and Zhang, 2021). p53 is also stabilised by phosphorylation. There are many sites of phosphorylation on p53 induced by different types of damage and kinases. In the region of Ser15 and Ser20 is the binding site of Mdm2. ATR and ATM phosphorylate Ser15 meanwhile Chk1 and Chk2 phosphorylate Ser20 in response to DNA damage. This phosphorylation interferes with the binding of Mdm2 with p53 preventing ubiquitination and degradation therefore stabilising p53 allowing its accumulation (Hirao et al, 2002; Ou et al, 2005).

The importance of p53 was demonstrated by Valente et al, 2020 where they studied the impact of p53 loss in mice. Results showed an increase in aneuploid and polyploid cells, reduced apoptosis and delayed DDR activation and repair of DNA damage. All of these lead to an accumulation of DNA damage and mutations, increasing the likelihood of tumour formation. This clearly highlights the impact p53 has on genomic integrity and its role in preventing cancer (Valente et al, 2020).

Another important protein in the DDR is H2AX, a histone variant of H2A which undergoes post-translational modifications to activate it following DSB detection (Luczak and Zhitkovich, 2018; Mah et al, 2010; Pan et al, 2011; Zhao et al, 2011). It accumulates on DNA flanking the DSB sites forming foci in the nucleus (Mah et al, 2010; Pan et al, 2011; Zhao et al, 2011) which can be used as a biomarker for DSB generation (Luczak and Zhitkovich, 2018; Zhao et al, 2011). Phosphorylation of H2AX at Ser139 forms γ H2AX which acts as a scaffold for other DDR proteins. It promotes the recruitment of DSB repair proteins which can bind, localising them to the site of damage. Such proteins include the MRN complex, BRCA1, 53BP1, ubiquitinating proteins such as RNF8 and RNF168 and cohesin which holds the damaged DNA ends together and holds sister chromatids together during repair (Dickey et al, 2009; Luczak and Zhitkovich, 2018; Mah et al, 2010; Pan et al, 2011; Ström et al, 2004). γ H2AX generation results from ATM activation as expected since this pathway is mostly responsible for DSB detection, but ATR can also lead to the generation of γ H2AX as a result of replication stress and fork collapse leading to DSB generation (Luczak and Zhitkovich, 2018; Pan et al, 2011; Tsao et al, 2004; Zhao et al, 2011).

Following γ H2AX activation there is a ubiquitination cascade initiated by MDC1. MDC1 binds to the phosphorylated C terminus of γ H2AX and recruits the E3 ligase RNF8 which ubiquitinates molecules such as H1 forming Lys63-linked chains. This ubiquitination leads to the recruitment of RNF168 which monoubiquitinates H2A and H2AX at Lys13 and Lys15. For this event to take place, the histones must first be acetylated at Lys5 by TIP60-UBC13. RNF8 then extends the ubiquitination at Lys13+15 forming Lys63-linked chains which are identified by RAP80. RAP80 along with the other listed post-translational modifications, causes the recruitment of BRCA1 and 53BP1 which are important factors in DNA repair pathways (Akagawa et al, 2020; Chatterjee and Walker, 2017; Ikura et al, 2007; Mattioli et al, 2012; Pan et al, 2011; Luczak and Zhitkovich, 2018; Sekiguchi and Matsushita, 2022; Williams and Zhang, 2021). MDC1 also amplifies the response and aids in maintaining MRN. Via associations with the Nbs1 component of MRN, it keeps the complex localised to the DSB. MDC1 also has a positive feedback effect on ATM increasing its activation and γ H2AX generation amplifying the DDR response (Williams and Zhang, 2021).

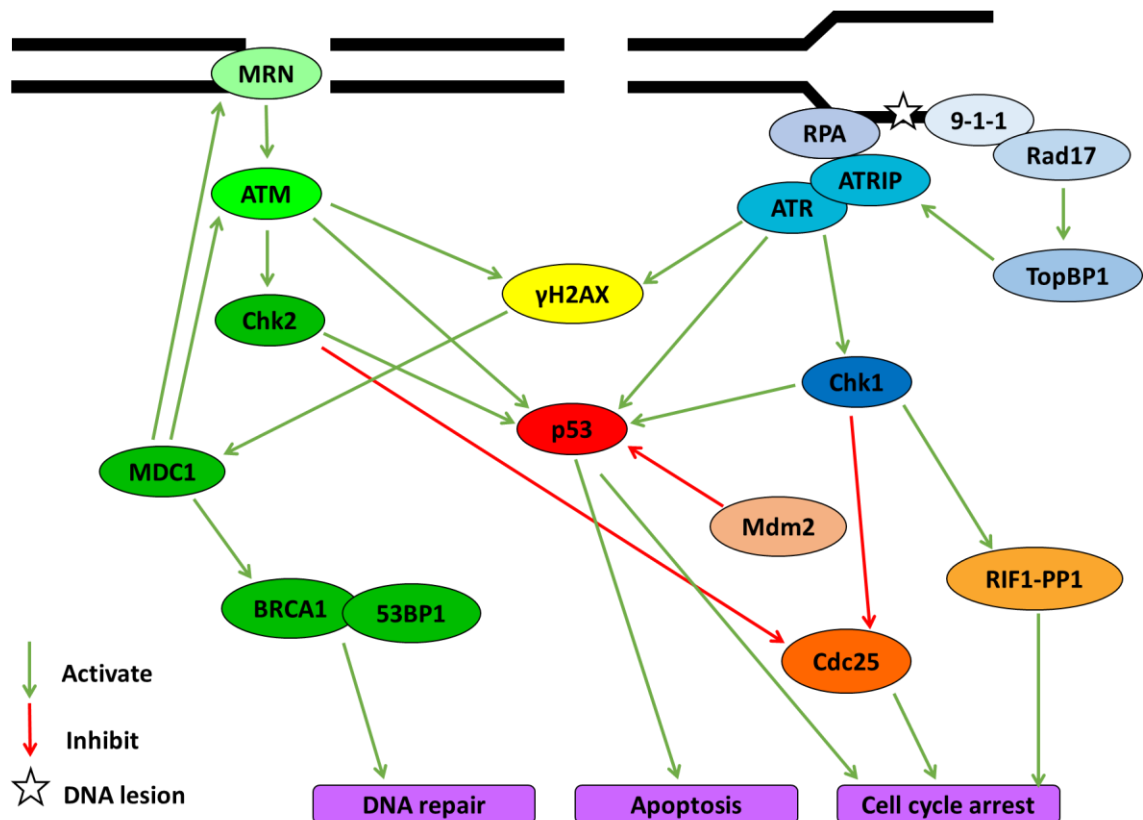


Figure 1.7: DNA damage response

Activation of the ATM response follows detection of the DSB via MRN which leads to the activation of ATM and Chk2 via phosphorylation. DNA lesions on the other hand recruit RPA, 9-1-1, Rad17 and TopBP1 which together localise ATR-ATRIP and activate it along with Chk1. These kinases (ATM, ATR, Chk1 and Chk2) phosphorylate p53 stabilising it leading to cell cycle arrest or apoptosis. Cell cycle arrest also follows an inhibitory phosphorylation of Cdc25 by Chk1 and Chk2 or formation of the RIF-PP1 complex via Chk1. γ H2AX production results from ATM and ATR activation which phosphorylates MDC1 and recruits DNA repair proteins for DSB repair.

1.5.2. Repair of DSBs

Non-homologous end joining (NHEJ) is used to quickly repair DSBs during G1 when there is no homologous DNA to use as a template (Ma and Dai, 2018). The Ku70-Ku80 heterodimer identifies and binds broken ends to protect them and recruits the repair proteins. The ends are bridged together by the Ku complex with XRCC4 and XLF (Cannan and Pederson, 2016; Mah et al, 2010; Rother et al, 2020) and processed by the Artemis nuclease before the gap is filled using DNA polymerases μ and λ and then ligated together with the LIG4/XRCC4/XLF complex (Moscardiello et al, 2015; Rother et al, 2020).

However, because it has no template to work from, this process is error prone and can lead to mutations such as short deletions (Figure 1.8) (Cannan and Pederson, 2016). This pathway is triggered by the activation of 53BP1. When phosphorylated during G1 phase by ATM, 53BP1 forms a complex with RIF1 to recruit Shieldin promoting NHEJ and inhibiting end resection which is associated with homologous recombination (HR) (Rother et al, 2020; Williams and Zhang, 2021). Recruitment of 53BP1 depends on the presence of H2A Lys15 ubiquitination via RNF8 and RNF168 however, binding requires demethylation of Lys20 on histone 4 (H4K20me2) which plays a role in determining which repair process takes place. In non-replicated DNA, H4K20me2 allows for stable binding of 53BP1 initiating NHEJ. However, in replicated DNA this marker becomes diluted reducing 53BP1 recruitment leading to HR (Rother et al, 2020).

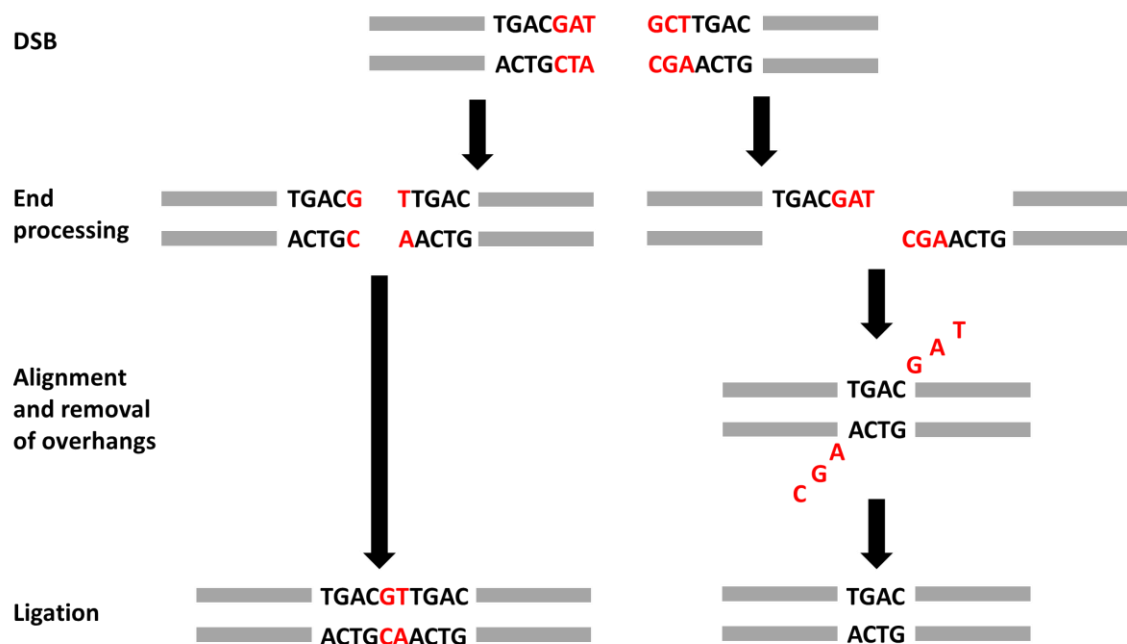


Figure 1.8: Non-homologous end joining

NHEJ to repair DSBs demonstrating the different paths of end processing leading to loss of genetic information.

HR on the other hand occurs during S and G2 phase where it can use the homologous chromosomes as a template to repair the DSB therefore making it error free and ensuring genomic integrity is maintained (Figure 1.9) (Maréchal and Zou, 2013). Following DSB detection and ATM activation, CtIP bridges the broken ends together whilst MRE11 is recruited and begins end resection forming 3' overhangs (Chatterjee

and Walker, 2017; Gnugnoli et al, 2021; Williams and Zhang, 2021). This is enhanced by the recruitment of two more nucleases, Dna2 and Exo1 via CtIP (Gnugnoli et al, 2021; Williams and Zhang, 2021). Furthermore, Ku70/Ku80 complex bound to the end of the break (Mah et al, 2010; Rother et al, 2020) is destabilised and BRCA1 initiates the dephosphorylation 53BP1 via PP4C preventing formation of the 53BP1-RIF1 complex (Williams and Zhang, 2021). As end processing continues, ssDNA becomes longer, switching control from ATM to ATR (Maréchal and Zou, 2013; Williams and Zhang, 2021). Reduced ATM activation decreases 53BP1 phosphorylation and RIF1 recruitment. All of these factors inhibit NHEJ and promote HR (Williams and Zhang, 2021). The RPA coating the ssDNA overhangs is displaced by RAD51 forming a nucleoprotein which invades the homologous chromosome forming the D loop and Holliday junctions. DNA polymerases re-build the DNA strand which pairs with the remaining 3' overhang. The ssDNA is filled in and ligated together (Chatterjee and Walker, 2017; Gnugnoli et al, 2021).

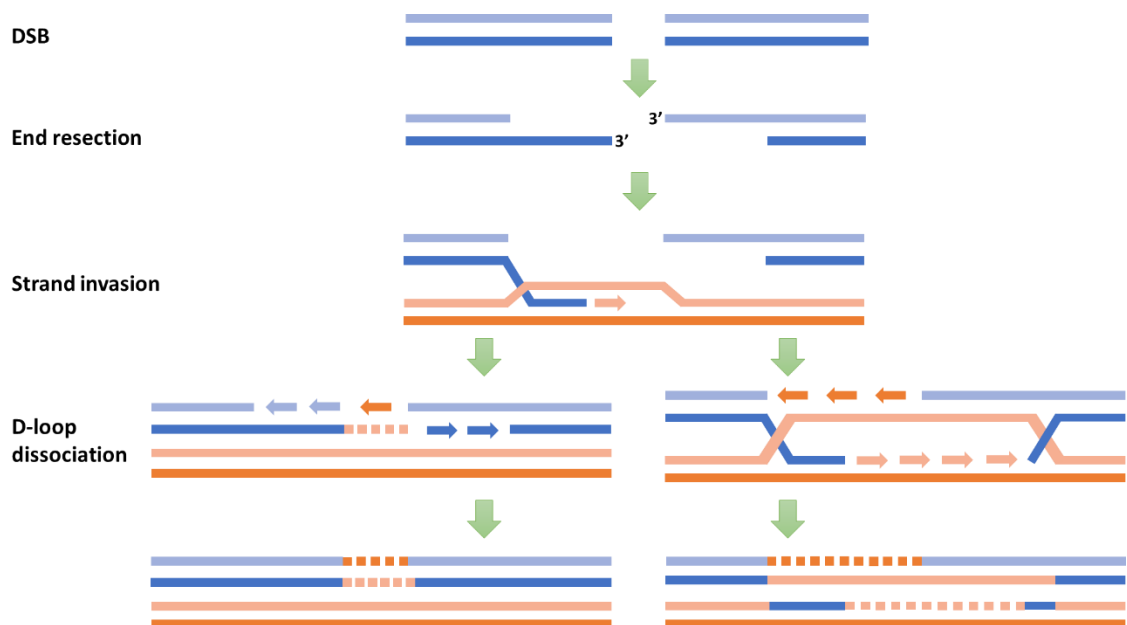


Figure 1.9: homologous recombination

Figure demonstrating homologous recombination to repair DSBs. Initial 3' resection at the DSB allows strand invasion of the sister chromatid using it as a template to ensure error free repair. Depending on how the Holliday junctions are cut, there may be genetic crossover between the sister chromatids.

1.6. The bystander effect

1.6.1. What is the bystander effect?

The bystander effect is when cells experiencing cell stress due to an external factor induce a similar stress like state in the surrounding unexposed healthy cells via signalling molecules (bystander factors). In the case of skin cancer, UV exposure causes cell stress in those directly irradiated leading to DNA damage and oxidative stress. These damaged cells then induce a similar stress like state in the unexposed healthy cells surrounding them. This poses a serious threat to the patient's health as this indirect DNA damage has the potential to lead to skin cancer in the future (Nishiura et al, 2012; Whiteside et al, 2011; Widel, 2012).

The bystander effect is long known to be caused by ionising radiation (reviewed here: Azzam et al, 2013) and has also been linked to causing secondary tumours in patients who have received radiotherapy with genotoxic factors being detected in the patient's blood which have the potential to damage their chromosomes (Lin et al, 2017). It has been demonstrated that other forms of radiation can also cause the bystander effect including UV (Banerjee et al, 2005; Widel et al, 2014). Oxidative stress plays an important role in the IR-induced bystander effect. Since, oxidative stress occurs as a result of UVA exposure, it could be involved in inducing bystander responses leading to skin cancers (Widel, 2012). A number of effects are seen in the bystander effect including mutations, increased apoptosis and reduced cell survival, senescence, micronucleus formation, DNA strand breaks and chromosome aberrations (Krzywon et al, 2018; Nishiura et al, 2012; Widel, 2012; Widel et al, 2014).

1.6.2. Methods for studying bystander effect

There are two types of method that can be used to study UV-induced bystander effects. In the media transfer method, the media that the donor cells are irradiated in is transferred to the bystander cells. The irradiation of the donor cells leads to the production and secretion of bystander factors into the media which can then be transferred to the bystander cell population to induce the bystander effect (Banerjee et al, 2005; Burdak-Rothkamm et al, 2007; Burdak-Rothkamm et al, 2008; Ghosh et al 2013; Nishiura et al, 2012).

The other method is co-incubation of the donor and recipient cells. The donor cells are irradiated in transwell inserts in which the cells are grown on top of a porous membrane which allows for the diffusion of molecules but not the cells. Following irradiation, the transwell inserts are transferred to wells containing the bystander cells. This creates a more physiologically relevant model as there are two layers of cells that are able to communicate with one another (Krzywon et al, 2018; Whiteside et al, 2011; Steel, 2016; Widel et al, 2014).

1.6.3. Bystander communication

It is not yet fully understood what mediates the bystander effect and the mechanism of inducing the effects, but various molecules have been proposed such as ROS. In early research using alpha particle radiation Little et al (2002) demonstrated suppression of the bystander effect with the addition of antioxidants to the system. Catalase (converts hydrogen peroxide into oxygen and water), superoxide dismutase (SOD) (degrades superoxide) and DPI (inhibits the production of superoxide by NADPH oxidase) were all found to suppress the formation of micronuclei in bystander cells, where SOD and DPI had the greatest effect, suggesting superoxide is the main form of ROS contributing to this effect (Little et al, 2002). In other research using microbeam irradiation where γ H2AX foci production was used as an end point, DMSO, a ROS scavenger, was found to reduce foci formation (Burdak-Rothkamm et al, 2007). Furthermore, TGF- β promotes the production of ROS and can suppress the activity of various antioxidants (Liu and Desai, 2015). TGF- β has been found to induce the generation of γ H2AX foci similarly to the bystander response seen with ROS, which again was suppressed by the presence of DMSO (Burdak-Rothkamm et al, 2007) and can enhance the bystander effects seen with x-ray irradiation (Burdak-Rothkamm et al, 2008).

Similar results have been found in the UV-induced bystander effect. Widel et al (2014) identified increased intracellular ROS levels in bystander populations lasting at least 24 hours in response to low doses of 20 kJ/m² of UVA along with increased activity of SOD (Widel et al, 2014). Steel (2016) also used the formation of γ H2AX foci as an end point to study the role of ROS in the UVA induced-bystander effect. As a component of the DNA damage response, γ H2AX production is an indication of DNA damage and therefore the bystander effect. Incubation of bystander cells with catalase post-irradiation

reduced γ H2AX foci production. The same results occurred when cells were incubated with DPI prior to irradiation suggesting an involvement of ROS in inducing the bystander effect (Steel, 2016). Furthermore, shorter wavelengths of UV also imply an involvement of ROS in mediating the bystander effect. Both UVB and UVC create elevations in ROS and SOD activity in bystander cells occurring earlier in UVB compared to UVC (Widel et al, 2014). All together, these experiments provide strong evidence of ROS involvement in mediating the bystander effect.

Other proposed bystander factors are lipid peroxidation by-products (LPB). LPBs such as MDA can form adducts with proteins, phospholipids, and DNA where the latter may induce mutations and have carcinogenic effects (Sander et al, 2003; Widel, 2012). Significant elevations of MDA were found in melanoma biopsies, but MDA was also identified in the surrounding keratinocytes where it may have a mutagenic and carcinogenic effect. Lipid peroxidation can occur during oxidative stress, which is triggered by UVA exposure, but UV can also result in a depletion of the cells antioxidant defences which has been demonstrated in a reduction of SOD activity in non-melanoma tissue biopsies and in the surrounding tissue. Interestingly, elevations of MDA within tumours coincided with a depletion in SOD activity in cells surrounding SCC and an increase of SOD activity in tissue surrounding superficial spreading melanoma. Not only does this demonstrate a bystander effect whereby the antioxidant defences have been affected in association with lipid peroxidation, but this also implies different mechanisms between different types of cancer. Finally, this impairment in antioxidant defences within the surrounding tissue of skin tumours could make cells more susceptible to oxidative damage and lead to cancer (Sander et al, 2003).

Widel et al (2014) also proposed that IL-6 could be acting as a bystander factor as it is found in the medium following irradiation from all three regions of the UV spectrum in co-culture systems and has previously been found in the medium of bystander populations in response to IR. However, it is difficult to determine if IL-6 induces the bystander effect because IL-6 levels in the medium of co-incubated cells was found to be higher than in the medium of irradiated cells suggesting that the bystander cells are also secreting IL-6 as a result of exposure to each of the three UV regions. This means it could be playing a role as a bystander factor since its levels are increased in irradiated

cell medium compared to the control or it could be a result of the bystander effect with levels being further increased when irradiated cells are incubated with bystander cells (Widel et al, 2014).

The bystander factors are not released immediately following irradiation. Whiteside et al (2011) incubated donor cells for up to 3 days post UVA irradiation and then replaced the media and co-incubated them with the recipient cells. They showed that the bystander effect is still induced in the form of reduced cell survival suggesting that the irradiated cells were still producing and secreting bystander factors three days after UVA exposure. They also demonstrated that a minimum of 24 hours is required for bystander factors to accumulate and reach a critical point to induce the effects seen which usually occurs at 48 hours (Whiteside et al, 2011).

The mechanism by which these bystander factors are transported to neighbouring cells is yet to be elucidated but gap junctions have been proposed. Micronuclei were observed in bystander cells upon alpha particle irradiation. However, when lindane – an inhibitor of gap junction communication – was introduced, micronuclei formation was suppressed (Little et al, 2002). A reduced bystander effect was also observed when gap junction communication was inhibited in response to ionising radiation (Dahle et al, 2001). In these methods, a small proportion of cells were irradiated allowing gap junction communication between neighbouring cells (Dahle et al, 2001; Little et al, 2002). However, in co-incubation and media transfer techniques used for UVA, UVB and UVC research, gap junction communication is not possible, but bystander effects are still induced. Bystander factors must be being released from damaged donor cells to be detected by recipient cells. This also supports theories suggesting molecules such as ROS are involved in mediating these bystander responses since, they are soluble factors which can be transferred to neighbouring cells via the media (Steel, 2016; Whiteside et al, 2011; Widel et al, 2014). Therefore, there may not be just one method by which bystander factors communicate between cells, adding to the complexity of the bystander effect.

Lin et al (2017) studied other possible ways in which these bystander factors are transported between neighbouring cells. They proposed that microvesicles containing bystander factors are being secreted by damage cells and release their contents into

non-exposed bystander cells. Microvesicles are a form of communication between cells carrying molecules which elicit different responses in cells so it is possible they could communicate the bystander effect. Using an unspecified type of UV, they observed the bystander effect in non-exposed cells treated with microvesicles from UV irradiated prostate cancer cells as shown by activation of various components of the DDR. This effect was diminished in the presence of annexin V which neutralises microvesicles supporting the theory that microvesicles are involved in communicating this effect (Lin et al, 2017).

Communication of the bystander effect is not limited to the same cell type. It has been shown in multiple studies that the bystander effect can be induced between different cells lines. For example, using an unspecified source of UV to treat A431 cells (epidermoid carcinoma cells) induced activation of the DDR with the increased production of γ H2AX in DU145 cells (prostate cancer) (Lin et al, 2017). It has also been demonstrated that the bystander effect can be transmitted between different skin cell types. Keratinocytes, melanocytes, and fibroblasts were all found to induce the bystander effect as the donor cell population and display bystander responses as the bystander population to one another in response to UVA. This research found that keratinocytes were the most effective donors of the bystander response whilst melanocytes are the most vulnerable to bystander signals (Redmond et al, 2014). The same effect was seen when UVA irradiated HaCaTs (keratinocytes) were co-incubated with MRC5 cells (fibroblasts) which led to the generation of γ H2AX foci representative of bystander induced DNA damage (Steel, 2016). This has important implications as the surface of the skin is formed of keratinocytes and is regularly exposed to UV emitted by the sun. The damaging effect of UVA irradiation could be transmitted via the bystander effect to surrounding cells possibly deeper in the skin. Furthermore, melanocytes were found to be the most vulnerable but are surrounded by dozens of keratinocytes, the most effective donors. This could have implications in DNA damage generation and carcinogenesis such as melanoma (Redmond et al, 2014).

1.6.4. Apoptosis

Irradiating cells with UVA can cause apoptosis seen as early as 3 hours post irradiation lasting up to 12 hours. When these irradiated cells are co-incubated with bystander cells,

similar results are observed with a small delay where apoptosis levels increase 2-fold at 6 hours compared to the control. This bystander effect is also seen when using UVB at an earlier time of 3 hours post incubation with a longer lasting effect of up to 24 hours compared to just 12 hours for UVA (Widel et al, 2014). When UVA and UVB are combined, the increased apoptotic effect can be seen up to 72 hours later when using the media transfer technique with the addition of elevated *fas* and *bax* gene expression in bystander cells (Banerjee et al, 2005). Meanwhile, UVC induced increased apoptosis in bystander cells at just 6 hours post irradiation (Widel et al, 2014). The increase in apoptosis is likely caused by factors released by the directly irradiated cells upon apoptosis which then go on to induce cell death in the bystander population (Banerjee et al, 2005) hence the small delay observed by Widel et al (2014). It is hypothesised this could have a protective function in order to kill any potentially damaged cells surrounding the irradiated area to prevent DNA damage or carcinogenesis (Banerjee et al, 2005).

1.6.5. Impact on the cell cycle and DNA damage response

It has been demonstrated that the bystander effect activates the DDR. Increased expression of Chk1, Chk2, DNA-PK and γ H2AX has been observed in response to unspecified UV irradiation (Lin et al, 2017) whilst p53 and p21 were found to be upregulated in response to alpha particle irradiation suggesting cell cycle arrest was occurring (Little et al, 2002).

γ H2AX foci formation occurred in response to microbeam irradiation indicating DSB and DNA damage generation. These foci were found to last up to 48 hours suggesting there may have been a problem with DNA repair or there is a sustained bystander signal continuously inducing DNA damage (Burdak-Rothkamm et al, 2007).

When studying the activation of the DDR, Burdak-Rothkamm et al, (2008), found that ATM and ATR inhibitors suppressed the x-ray induced bystander effect whilst DNA-PK inhibitors had no effect (Burdak-Rothkamm et al, 2008). In contrast, bystander effects induced by alpha particle irradiation demonstrated that only ATR activated the DDR, as ATM inhibitors had no effect on γ H2AX foci formation. This could suggest that different types of radiations induce different bystander effects and therefore responses (Burdak-

Rothkamm et al, 2007). In the latter study where ATR mutated bystander cells showed no γ H2AX foci formation, directly irradiated ATR mutated cells did, further demonstrating the different responses seen in bystander effects (Burdak-Rothkamm et al, 2007)

The cell cycle has an impact on which cells are more vulnerable to bystander effects. Not all cells in a population display the bystander effect, some cells are more susceptible to this effect than others. Upon further investigation it has been found that only S phase cells exhibit γ H2AX foci which has been shown in different types of radiation, including UVA and microbeam irradiation (Burdak-Rothkamm et al, 2007; Steel, 2016). This was demonstrated following UVA irradiation using EdU (5'ethynyl-2'-deoxyuridine) labelling which can only be incorporated into the DNA of actively replicating cells where only EdU positive cells displayed γ H2AX foci. It was also demonstrated that bystander populations contained a larger proportion of S phase cells but a lower EdU intensity. This implies that the cells experience replication stress possibly caused by stalled replication forks rather than DSBs (Steel, 2016) which is further supported by microbeam and x-ray research where activation of ATR was seen in Burdak-Rothkamm et al, 2007 and Burdak-Rothkamm et al, 2008, as ATR activation is responsible for a wider range of DNA damage including replication stress opposed to ATM which predominantly responds to DSBs (Girard et al, 2008; Maréchal and Zou, 2013; Shiotani et al, 2013; Zhao et al, 2011). Chk1, the downstream effector of ATR, is phosphorylated at Ser345 in response to stalled replication forks. The presence of this protein was identified in EdU positive UVA bystander cells confirming the presence of stalled replication forks (Steel, 2016) explaining the activation of ATR pathway seen in previous research (Burdak-Rothkamm et al, 2007; Burdak-Rothkamm et al, 2008).

1.6.6. Differences between bystander responses

The bystander effect has been studied in a variety of cell lines with different types of irradiations and although there are a lot of similarities such as the involvement of ROS and generation of DNA damage and micronuclei (Burdak-Rothkamm et al, 2007; Jaiswal and Lindqvist, 2015; Little et al, 2002; Nishiura et al, 2012; Widel, 2012), there are also some differences in these findings.

DDR pathways are activated in bystander populations but whilst some see activation of both ATM and ATR pathways (Burdak-Rothkamm et al, 2008), others only see activation of ATR (Burdak-Rothkamm et al, 2008). Both of these studies used T98G glioma cells and media transfer techniques however, Burdak-Rothkamm et al, 2007 used microbeam irradiation opposed to x-rays used in Burdak-Rothkamm et al, 2008. This suggests that different types of irradiations may induce various types of damage leading to activation of different DDR pathways. In addition, the type of radiation also influences the time required to induce bystander effects. When using UVA, a minimum of 24 hours is required before bystander responses are displayed (Whiteside et al, 2011) whereas with UVB, this is halved to 12 hours (Banerjee et al, 2005). The effects different regions of the UV spectrum have on bystander cells also differs. In normal human fibroblasts, UVA and UVB both induce apoptosis in bystander cells, where UVA had the largest impact. Meanwhile UVC only induced apoptosis in directly irradiated cells but not in the bystander population (Widel et al, 2014). UVA, UVB and UVC have different mechanisms of causing DNA damage in directly irradiated cells (D'Orazio et al, 2013; Laikova et al, 2019) but they may also have different effects in bystander responses taking different amounts of time to induce bystander effects and also generating variation in the level and type of damage the cells experience (Banerjee et al, 2005; Whiteside et al, 2011; Widel et al, 2014).

When looking at different responses between cells, Burdak-Rothkamm et al, (2007) looked at γ H2AX foci formation as the end point following microbeam irradiation. Here they demonstrated that DMSO was able to suppress γ H2AX foci generation in T98G glioma cells showing the importance of ROS in creating bystander responses. However, DMSO had no impact in normal human astrocytes (NHA) (Burdak-Rothkamm et al, 2007). Furthermore, different kinds of skin cells respond in different ways to UVA irradiation. Keratinocytes, melanocytes, and fibroblasts each have a different level of vulnerability to the bystander effect and different abilities at inducing it in other cells. Melanocytes have the highest viability and lowest production of hydrogen peroxide but are the most susceptible. Keratinocytes, however, show higher levels of oxidative stress but are least vulnerable to the bystander effect (Redmond et al, 2014). This indicates that the same type of radiation can have different effects between different cell lines

whether it is the type of response seen in the cells, the level of response or how vulnerable they are.

1.6.7. Protective function of the bystander effect

Some research has proposed a protective function for the bystander effect. When studying this effect, bystander cells were incubated with media from UVC irradiated cells. The bystander cells were then irradiated with UVC. Following incubation with the conditioned UVC media, mutation frequency increased, displaying a bystander effect. However, following UVC irradiation of the bystander cells, survival improved. The bystander population had become more resistant to cell death compared to cells which were not incubated with conditioned media. Furthermore, mutation frequency was found to increase in the pre-conditioned cells suggesting error-prone DNA repair had been activated (Ghosh and Bhaumik, 1995). This has been further demonstrated in a different cell line where pre-treatment of cells with UV related release factors improved cell viability upon UVC exposure or treatment with hydrogen peroxide and cells also showed improved antioxidant defence with increased SOD and catalase activity (Ghosh et al, 2012; Ghosh et al, 2013). This implies the bystander effect may have a protective function improving cell viability by activating DNA repair pathways and increasing antioxidant activity (Ghosh and Bhaumik, 1995; Ghosh et al, 2012; Ghosh et al, 2013).

1.7. Aims

1.7.1. The UVA induced DDR in directly irradiated cells

Although the DDR response is well known, the timings of protein activation in response to UVA irradiation are less well known. Therefore, the aim is to address the question: which DDR proteins are activated and when in response to direct UVA exposure? This would create a more in-depth characterisation of the DDR response activated by UVA to get a more detailed account of the process in detecting and responding to UVA-induced DNA damage.

1.7.2. The activation of the DDR in UVA-induced bystander cells

There is a large amount of research studying the communication of the bystander effect, identifying ROS as an important factor not only in signalling but also in inducing damage in bystander cells. Research has also focused on the type of DNA damage bystander cells

exhibit. However, to my knowledge, little is known about the cellular response to this damage in the UVA-induced bystander effect. The research aimed to test if the DNA damage response is activated in bystander cells in response to UVA irradiation addressing which proteins are activated and when.

Chk1 and Chk2 phosphorylation are representative of the two DDR pathways – ATR and ATM – becoming activated in response to the detection of DNA damage (Williams and Zhang, 2021) whilst RPA accumulates on ssDNA in the presence of damage or replication stress (Maréchal and Zou, 2013; Shiotani et al, 2013; Tsao, et al, 2004; Williams and Zhang, 2021). γ H2AX is a marker for DNA damage (Luczak and Zhitkovich, 2018; Zhao et al, 2011) meanwhile p53 is an important factor in determining cell fate in response to damaged DNA (Ali et al, 2017; Valente et al, 2020). Combined, these proteins provide a detailed look into the UV-induced DDR. Studying both directly irradiated cells and bystander cells alongside each other allowed comparisons of the DDR in both conditions to identify any differences. A physiological dose of 108 kJ/m² of UVA irradiation was chosen which equates to approximately 30 minutes of direct sunlight in the Mediterranean at mid-day in summer (Kimlin et al, 2002). Responses were also measured at 72 kJ/m² and 144 kJ/m² to reflect a wider range of UV intensities and periods of time in the sun. I hypothesise that using a higher UVA dosage will lead to increase DNA damage generation and a larger bystander response. Similarly, I aim to test if a lower dose of UVA would lead to less DNA damage and a smaller bystander response.

Chapter 2: Methods

2.1. Buffers and solutions

| | |
|--------------------------|---|
| 4x Loading buffer | 50 mM Tris-HCl pH 6.8, 2% SDS, 10% glycerol, 0.02% bromophenol blue, 100 mM DTT (dithiothreitol) (all from Melford) |
| 10x TBST | 0.5 M Tris, 1.5 M NaCl, 0.5% Tween20, pH 7.4 |
| 10x TGS | 0.25 M Tris, 1.92 M glycine and 1% SDS |
| Milk-TBST | 5% milk powder in 1x TSBT |
| PBS | One tablet of phosphate buffered saline (PBS) (Gibco) added to 500 ml of distilled water. Each tablet contains 10 mM phosphate, 2.68 mM potassium chloride and 140 mM sodium chloride |
| RIPA buffer | 150 mM NaCl, 50 mM Tris, 1% IGEPAL CA-630, 0.5% sodium deoxycholate, 0.1% SDS (all from sigma), pH8.0 with one tablet of PhosStop (Roche), 1 mM EDTA (Lonza), and one tablet of Complete Mini EDTA Free protease inhibitors (Roche) |
| Transfer buffer | 0.26 M Tris base (Fisher Bioreagents), 0.01 M CAPS (Sigma), 10% ethanol (Fisher Chemical), 0.2% SDS |

2.2. Cell culture

2.2.1. Cell culture conditions

1 ml HaCaT cell aliquot was revived from liquid nitrogen into Dulbecco's Modified Eagle Medium (DMEM) (Lonza) and incubated at 37°C and 5% CO₂ in T75 flasks (Nunc). DMEM was supplemented with 10% Foetal Bovine Serum (FBS) (Labtech) and 10 U/ml of penicillin and 10 U/ml of streptomycin (Lonza) was added to the stock solution at 1% concentration. This media was used throughout except for instances where cells were to be irradiated with UVA. In these cases, the medium was changed to a phenol red free and L-glutamine free DMEM (Lonza) supplemented with 10% FBS and 2% L-glutamine (Lonza) prior to irradiation. This was done because phenol red and antibiotics are potentially photosensitising, and this could interfere with the experiment. This form of media will be referred to as PR-free DMEM. Cells were kept below a passage number of

20 and tested for mycoplasma weekly. All cell culture and incubations occurred via these conditions unless stated otherwise.

2.2.2. Trypsinisation and cell counting

HaCaT cells were incubated with 10 ml of 1X Phosphate Buffered Saline (PBS) (Gibco) EDTA (Lonza) solution for 12 minutes. Cells were then incubated in 2 ml of 0.25% trypsin-EDTA (Lonza) for 15 seconds before 1.5 ml of it was removed and cells were subsequently incubated for 3 minutes or until the cells were detached from the flask. 7.5 ml of DMEM was added to stop the action of the trypsin and to resuspend the cells. To maintain the cell line, the cell suspension was passaged 1 in 4 into T75 flasks twice a week or when cell confluency reached 70%. For experimentation, the cells were counted by mixing 10 μ l of cell suspension and 10 μ l Trypan Blue (Sigma) into Luna Cell Counting Slides (Thermo Scientific) and counted in the Luna II Automated Cell Counter before being seeded into 6-well plates (Greiner Bio-One).

2.3. Experimental culture conditions

2.3.1. Direct irradiation cell culture conditions

When studying the direct effects of UVA irradiation, cells were seeded into 6-well plates at a density of 300,000 cells per well 24 hours prior to irradiation in DMEM. Media was replaced with PR-free DMEM for irradiation (section 2.4) and incubated. Samples were collected at 0, 1, 2, 3, 8, and 24 hours post irradiation as in sections 2.5 and 2.6 depending on the experimental procedure.

For the control samples, 300,000 cells were seeded into 6-well plates 24 hours prior to collection. For positive controls of the ATM response, Zeocin (Invivogen) (500 μ g/ml) was added to the well and incubated for 1 hour and for positive controls of the ATR response, cells were incubated with 1 μ M of Camptothecin (CPT) (Selleckchem) for 1 hour before the cell extract was prepared. Nothing was added to the negative control.

2.3.2. Bystander cell culture conditions

The co-incubation method was used for studying the bystander effect. In this technique, Thincerts (Greiner Bio-One) (transwell inserts) were inserted into the wells of 6-well plates allowing two cell populations to be co-incubated. They contained 1 μ m pores which enabled small molecules to pass through for cellular communication. 75,000

donor cells were grown in the Thincerts whilst 150,000 recipient bystander cells were grown in the 6-well plates for 24 hours in DMEM. Prior to irradiation, media was replaced with PR-free DMEM, and donor cells were immediately irradiated (section 2.4). Following irradiation, the Thincerts were transferred to the recipient cells and incubated. Samples were collected 24- and 48- hours post-irradiation as in section 2.5 and 2.6 depending on the experimental procedure.

2.4. UV irradiation

Cells in PR-free DMEM were irradiated using Pro-lite Plus 240V 25W UVA bulbs in 6-well plates. A sheet of mylar film was placed on top of the plate to filter out any UVB radiation. The plates were thermostatically regulated by placing on water-cooled metal plates to avoid heating maintaining the temperature at 25°C. The output of the UVA source was 48 J/m²/s which was used to calculate the time to achieve a certain irradiation dose which is displayed in Table 2.1. 100 kJ/m² is equivalent to 30 minutes in mid-day sun in the South of France during mid-summer (Kimlin et al, 2002).

Table 2.1 Irradiation dose

| Irradiation dose (kJ/m ²) | Irradiation time (minutes) |
|---------------------------------------|----------------------------|
| 72 | 25 |
| 108 | 37.5 |
| 144 | 50 |

2.5. Western blots

2.5.1. Sample collection

Wells were washed with PBS twice before 50 µl of RIPA buffer was added and the surface scraped. The lysate was pipetted into microcentrifuge tubes and centrifuged at 20,000 rcf for 5 minutes at 4°C to remove debris.

2.5.2. Protein concentration quantification via Bradford assay

The protein concentration of each sample was measured prior to electrophoresis to ensure equal loading of samples into the gel. 200 µl of Bradford Ultra (Expedeon) reagent was added to the appropriate number of wells on a 96-well plate (Greiner Bio-

One). 10 µl control samples were added to the Bradford reagent. These were made from a 10 mg/ml solution of BSA (Sigma) diluted to 2, 1, 0.5, 0.25 and 0 mg/ml concentrations using PBS. An equivalent volume of RIPA was added to each control as there was in the cell extracts as it was present in these samples and could interfere with the reaction. For the cell extracts, an appropriate volume of sample was added to the Bradford reagent. Absorbance was then measured at 595 nm. A graph of absorbance versus protein concentration for the control samples was constructed using excel and used to calculate the protein concentration of the cell extracts and the volumes required for loading.

2.5.3. SDS-PAGE

Samples of 20 µg of protein were prepared by diluting the samples with RIPA buffer to an appropriate volume. 5 µl of Loading Buffer was added to each sample and boiled at 95°C for 3 minutes. Novex Wedgewell 10 to 20% Tris-glycine 1.0 mm mini protein gels (ThermoFisher) were used. 5 µl of PageRuler Plus Prestained Protein Ladder (ThermoFisher Scientific) was loaded into the gel along with each sample. The gels were run in 1x TGS running buffer at 225V for 30 minutes or until the samples reached the bottom of the gel using a Mini –PROTEAN® Tetra Vertical Electrophoresis Cell setup.

2.5.4. Gel transfer

Proteins were transferred onto Immobilon-P Transfer membrane (Millipore) which had been pre-soaked in methanol (ThermoFisher) for hydration followed by transfer buffer along with the four pieces of 3 mm chromatography paper (Whatman). The transfer was carried out on a Pierce G2 Fast Blotter at 25V for 11 minutes and 1.3 A per blot.

2.5.5. Protein detection

The nitrocellulose membrane was blocked in milk-TBST for 1 hour at room temperature and then membranes were placed into 50 ml Falcon tubes and incubated on a roller with the appropriate primary antibody (Table 2.2) in milk-TBST overnight at 4°C. The following day, the membranes were washed in 1xTBST and incubated with the appropriate secondary antibody (Table 2.2) in milk-TBST on a roller at room temperature for 1 hour. Membranes were washed in 1x TBST and developed in either SuperSignal West Femto Reagent (Thermo Scientific) or SuperSignal West Pico Reagent (Thermo

Scientific), depending on the antibody. Imaging was carried out on a BioRad Chemidoc XRS+ Imaging System.

Table 2.2: Antibodies for Western blot

| Primary antibody | | | Secondary antibody | | |
|--|----------|-------------------------------|---|----------|----------------------------------|
| Antibody name | Dilution | Supplier | Antibody name | Dilution | Supplier |
| Ms mAb γH2AX 1 mg/ml (ab26350) | 1:2000 | Abcam | Anti-mouse IgG HRP Linked Antibody (70765) | 1:4000 | Cell Signalling Technology |
| Phospho-Chk1 (Ser317) (D12H3) Rabbit IgG (14757) | 1:1000 | Cell Signalling Technology | Anti-rabbit IgG HRP Linked Antibody (7074) | 1:2000 | Cell Signalling Technology |
| Phospho-Chk1 (Ser345) Rabbit IgG | 1:1000 | Cell Signalling Technology | Anti-rabbit IgG HRP Linked Antibody (7074) | 1:2000 | Cell Signalling Technology |
| Phospho-Chk2 (Thr68) Anti- rabbit (96017) | 1:1000 | Cell Signalling Technology | Anti-rabbit IgG HRP Linked Antibody (7074) | 1:2000 | Cell Signalling Technology |
| Phospho- RPA32/RPA2 (Ser8) (E5A2F) Rabbit mAb (P15927) | 1:1000 | Cell Signalling Technology | Anti-rabbit IgG HRP Linked Antibody (7074) | 1:2000 | Cell Signalling Technology |

| | | | | | |
|---|----------|------------------------------|--|--------|----------------------------|
| Purified Mouse Anti-actin Ab-5 | 1:10,000 | BD Transduction Laboratories | Anti-mouse IgG HRP Linked Antibody (70765) | 1:4000 | Cell Signalling Technology |
| Purified mouse anti-human p53 (5267648) | 1:2000 | BD Biosciences | Anti-mouse IgG HRP Linked Antibody (70765) | 1:4000 | Cell Signalling Technology |

2.6. Immunofluorescence

Cells were grown in 6-well plates with the addition of 1-4 glass coverslips (12 mm) in the well. Experimental culture conditions and UVA irradiation was carried out as stated in sections 2.3 and 2.4. At the appropriate time point the coverslips were fixed by washing with PBS twice and incubating with 0.5 ml of 4% paraformaldehyde (ChemCruz) for 15 minutes before being washed again in PBS twice. Fixed cells were permeabilised by incubation in 1 ml 0.5% Triton X-100 (Sigma) for 20 minutes, washed in PBS and transferred to a humidified dish where they were blocked in 3% BSA/PBS (Sigma) for 1 hour. Coverslips were then incubated with 50 µl of the appropriate primary antibody (Table 2.3) in milk-TBST for 1 hour at room temperature, followed by 50 µl of the appropriate secondary antibody (Table 2.3) for 1 hour in the dark at room temperature with 3 wash steps in between. Finally, coverslips were mounted with a small drop of Vectashield Antifade Mounting Medium with DAPI (Vector Laboratories) onto microscope slides and secured in place with clear nail varnish before storage at 4°C in the dark. Cells were imaged using a Zeiss LSM880 confocal microscope using settings displayed in Table 2.4.

Table 2.3 Antibodies for immunofluorescence

| Primary antibody | | | Secondary antibody | | |
|-----------------------------------|----------|--------------------|--|----------|------------|
| Antibody | Dilution | Supplier | Antibody | Dilution | Supplier |
| Ms mAb γ H2AX 1mg/ml | 1:4000 | Abcam (ab26350) | Alexa fluor 633 Goat Anti- mouse IgG (H+L) | 1:1000 | Invitrogen |

Table 2.4: Confocal microscope settings

| Channel | Detection of | Detection wavelength | Excitation wavelength | Excitation source |
|---------|---------------|----------------------|-----------------------|-------------------|
| 1 | γ H2AX | 638-747 | 633 | HeNe633 |
| 2 | DAPI | 410-513 | 405 | ArgonRemote |

2.7. Statistics

IF images were quantified using Fiji Image J software (Schindelin et al, 2012) to measure the fluorescent intensity of individual cells. At least one hundred cells were measured in each condition and overlapping cells were removed from quantitation. Data was then presented in a box and whisker plot where the whiskers represent the 10th and 90th percentile, the box displays the 25th, 50th and 75th percentile, the 'X' represents the mean value, and the circles are the outliers. Statistical analysis was carried out on GraphPad Prism. One-way ANOVAs were used to calculate significance between experimental conditions and the negative controls. A Dunnett's multiple comparisons test was carried out on the direct irradiation experiments described in Chapter 3, as experimental samples were directly compared to the negative control. A Tukey's multiple comparison test was carried out on the bystander experiments described in Chapter 4 as all conditions were compared to each other. Statistical significance is displayed by an asterisk: (*) $p < 0.05$, (**) $p < 0.01$ and (***) $p < 0.001$.

Chapter 3: Characterisation of the DNA damage response in directly UVA-irradiated HaCaT cells

3.1. Introduction

UV is a well-known carcinogen risk factor for skin cancer which is now one of the most prevalent cancers globally (Khazaei et al, 2019). Up to 85% of NMSC and 80% of CMM are believed to be caused by the damaging effects of UV irradiation whether its natural or artificial (tanning beds) (An et al, 2021). The extent of damage induced by UVA can often be underestimated due to its inability to directly cause DNA damage unlike UVB and UVC. Falling outside of the absorbance spectra of DNA, UVA causes its damage indirectly via the generation of ROS created by photosensitisation reactions (D’Orazio et al, 2013; Laikova et al, 2019). ROS can have damaging effects on macromolecules in the cells by oxidising them impairing the structure and function of proteins and lipids (Cadet and Douki, 2011; Chatterjee and Walker, 2017; Girard et al, 2008; Montaner et al, 2007) but more importantly react with DNA: oxidising DNA bases and causing strand breaks (Greinert et al, 2012). 8oxoG is the most common base oxidation product formed from guanine. The modification means this base can pair with adenine causing G>T mutations which can be carcinogenic (Cadet and Douki, 2011; Chatterjee and Walker, 2017; Greinert et al, 2012; Wischermann et al, 2008; Yagura et al, 2017). UVA irradiation can also lead to the generation of pyrimidine dimers which distort the double helix disrupting DNA replication by stalling the replication forks. The consequence is the characteristic C>T and CC>TT mutations (Kim et al, 2013; Mouret et al, 2006; Singh et al, 2018). Furthermore, both SSBs and DSBs have been reported as a result of ROS production (Cadet and Douki, 2011; Cortat et al, 2013; Girard et al, 2008; Greinert et al, 2012; Mah et al, 2010; Wischermann et al, 2008). For example, hydroxyl radicals can react with the sugar-phosphate backbone resulting in SSBs (Balasubramanian et al, 1998; Cadet et al, 2015; Cannan and Pederson, 2016; Wischermann et al, 2008) which along with other forms of DNA damage such as CPDs, can obstruct the replication machinery causing fork collapse and formation of DSBs (Cannan and Pederson, 2016; Wischermann et al, 2008; Zhao et al, 2011). In addition to this, clusters of oxidatively damaged DNA can also form DSBs during their repair (Greinert et al, 2012; Cannan and Pederson, 2016).

The identification of this damage occurs via the ATM and ATR pathways which phosphorylate and activate the effector kinases Chk1 and Chk2 which go on to further

phosphorylate proteins with varying effects (Girard et al, 2008; Jaiswal and Lindqvist, 2015; Williams and Zhang, 2021). For example, phosphorylation of Cdc25 can lead to cell cycle arrest (Wang et al, 2007) whilst phosphorylation of p53 stabilises the protein (Hirao et al, 2002; Ou et al, 2005). Meanwhile, RPA and γ H2AX are sensor proteins which bind to the damaged sites and recruit the necessary proteins depending on the pathway (Mah et al, 2010; Pan et al, 2011; Shiotani et al, 2013). But they also function downstream in which the ubiquitination cascade of γ H2AX recruits repair proteins (Pan et al, 2011) whilst RPA binds to ssDNA until the damage is repaired to protect the DNA from nucleases and secondary structure formation (Gnugnoli et al, 2021; Ma and Dai, 2018; Williams and Zhang, 2021).

3.2. Aims

This UVA-induced DNA damage activates the DDR to maintain genomic stability but the timepoints in which these proteins are activated has not been fully characterised. This study therefore aimed to determine what DDR proteins are activated and when in response to UVA irradiation. Whilst UVA and UVB are known to be carcinogenic, the mechanism of induction by UVA is less clear. This study aims to provide indications into DNA damage generation, its persistence in the genome and how long it takes to repair the damage and develop our understanding of UVA carcinogenesis.

The data in this section demonstrated activation, downregulation and abundance of DDR proteins using a range of UVA exposure periods. It suggested different activation of the DDR branches at alternative UVA doses and late generation of DNA damage.

3.3. Results

Western blot and immunofluorescent (IF) analysis were used to measure DDR proteins p-Chk1 (Ser317 or Ser345), p-Chk2 (Thr68), p-RPA (Ser8), γ H2AX and Ub- γ H2AX. Phosphorylation of Chk1 at Ser317 is required for cell cycle recovery following stalled replication forks (Martin and Ouchi, 2008) whilst phosphorylation at Ser345 localises Chk1 to the nucleus (Jiang et al, 2003). Meanwhile, the phosphorylation of Chk2, RPA and γ H2AX activates these proteins (Girard et al, 2008; Luczak and Zhitkovich, 2018; Maréchal and Zou, 2015; Wang et al, 2007). Whilst Chk2 is an effector protein in the ATM response responsible for activating downstream proteins such as p53 (Hirao et al, 2002; Ou et al, 2005; Williams and Zhang, 2021), RPA binds to ssDNA and recruits ATR to activate the response whilst protecting the DNA from nucleases and secondary structure formation (Ma and Dai, 2018; Shiotani et al, 2013; Williams and Zhang, 2021). γ H2AX and Ub- γ H2AX on the other hand, mark sites of DSB formation to recruit repair proteins (Mah et al, 2010; Pan et al, 2011). HaCaT cells are spontaneously immortalised keratinocytes commonly used in research to model human keratinocyte behaviours. Although this cell line has a defective p53 (Lehman et al, 1993), the measured proteins function independently of p53 and should therefore have no impact on the current research. The HaCaT cells were directly irradiated at physiological doses of 72, 108 and 144 kJ/m² where 100 kJ/m² represents 30 minutes in midday sun in the South of France in summer (Kimlin et al, 2002). This gives a more representative study into UVA induced DDR as different climates and occupations expose individuals to varying levels of UVA irradiation and could therefore provide information about the cellular response at varying doses. Cells were irradiated in phenol red free and antibiotic free media due to the photosensitising abilities of phenol red and antibiotics. Samples were collected at 0, 1, 2, 3, 8 and 24 hours post irradiation to examine how protein levels and post-translational modifications change over time. Zeocin and camptothecin were used as positive controls for activation of the DSB. Whilst zeocin generates DSBs directly via intercalation into the DNA and free-radical mediated cleavage of the phosphodiester backbones (Trastoy et al, 2005), camptothecin is a DNA replication stressor that causes SSBs through inhibition of topoisomerase I (Luczak and Zhitkovich, 2018).

3.3.1. Western blot analysis of DDR protein activation

Asynchronous HaCaT keratinocytes were irradiated with different doses of UVA and cell extracts were prepared at various timepoints post-irradiation, followed by analysis by Western blot to study the kinetics of various DDR proteins.

3.3.1.1. DDR response induced by 72 kJ/m² UVA

Following 72 kJ/m² of UVA irradiation, samples were collected over a 24-hour period and analysed by Western blot with four independent repeats shown in Figure 3.1. HaCaT cells showed phosphorylation of both Chk1 (Ser317) and Chk2 in relation to the positive control (Figure 3.1) suggesting the activation of both ATR and ATM pathways. This indicated the presence of both DSB formation and replication stress in cells, confirmed by the activation of γ H2AX and phospho-RPA. p-Chk1 bands were consistently intense, with bands first appearing at 0 hours, indicative of immediate activation of the DDR response following irradiation (Figure 3.1a and b). Furthermore, p-Chk1 is consistently present at a high abundance between 1-3 hours and low abundance at 24 hours compared to the zeocin control showing a fast and long-lasting response (Figure 3.1a and b). However, the remaining time points show varying results. Although phosphorylation of Chk1 could be detected immediately after irradiation, in some repeats there were high levels of phosphorylation (Figure 3.1a) whilst in others there was low (Figure 3.1b) in relation to the positive control. Similar results were found at 8 hours with one repeat showing no bands (Figure 3.1a) whilst another repeat had high abundance compared to the zeocin control (Figure 3.1b). In addition, in a third repeat (Figure 3.1c), bands were present between 1-8 hours post irradiation, however these bands were as equally intense as the negative control. There was no actin control due to an issue with the blocking reagent in which the milk-TBST had bound to the membrane preventing antibody binding, so it was difficult to determine if p-Chk1 was elevated as there may have been unequal loading of samples.

Levels of phosphorylated Chk2 were also consistently high in relation to the zeocin control between 1-3 hours post-irradiation, peaking at 1 hour (Figure 3.1a, c and d) and lower levels were present at 0 hours demonstrating early activation (Figure 3.1a and d). There was one exception to this however, in which only early phosphorylation occurred at 0-1 hours post irradiation (Figure 3.1b).

RPA was not activated until at least 2 hours following UVA irradiation, with activation lasting up to 24 hours post-irradiation and therefore showing increased activation when both phosphorylated Chk1 and phosphorylated Chk2 were downregulated (Figure 3.1) which indicated DNA repair was taking place due to the binding of RPA to ssDNA generated during the repair process (Gnugnoli et al, 2021). It could have, however, also suggested the persistence or late generation of DNA damage as RPA is a sensor protein for the ATR pathway (Maréchal and Zou, 2013) and its activation was seen as late as 24 hours. RPA and γ H2AX show activation up to 24 hours indicating the presence of DNA damage at least 24 hours post-irradiation (Figure 3.1).

γ H2AX showed consistent activation between 1 and -24 hours post irradiation (Figure 3.1a, b and d) except for Figure 3.1c where no γ H2AX was identified. This suggested DSBs could have been generated activating the ATM response – although stalled replication forks inducing H2AX activation must also be considered – and persisting for the duration of the experiment. The presence of mono-ubiquitinated γ H2AX (Ub- γ H2AX) on the other hand showed inconsistent results. In Figure 3.1a, b and d, either Ub- γ H2AX was not present or its activation was not elevated compared to the negative control. In Figure 3.1c however, bands that occurred at 1, 3 and 8 hours post irradiation appeared to be more intense in comparison to the positive control. The inconsistent findings make this data unreliable and in addition to the absence of an actin control to compare to, conclusions cannot be drawn from Western blot analysis.

Whilst p53 was present, there was no stabilisation due to a mutation in *TP53* in both alleles of HaCaT cells meaning there is no wildtype p53 present. Therefore, it was not measured in subsequent analyses (Figure 3.1).

Figure 3.1a shows two different actin controls, as the same set of samples were run on two separate Western blots, once to measure γ H2AX, Ub- γ H2AX and p53 and the second for p-Chk1, p-Chk2 and RPA. As seen in the first actin, there was no protein present at 24 hours post irradiation explaining the absence or reduction of the above proteins.

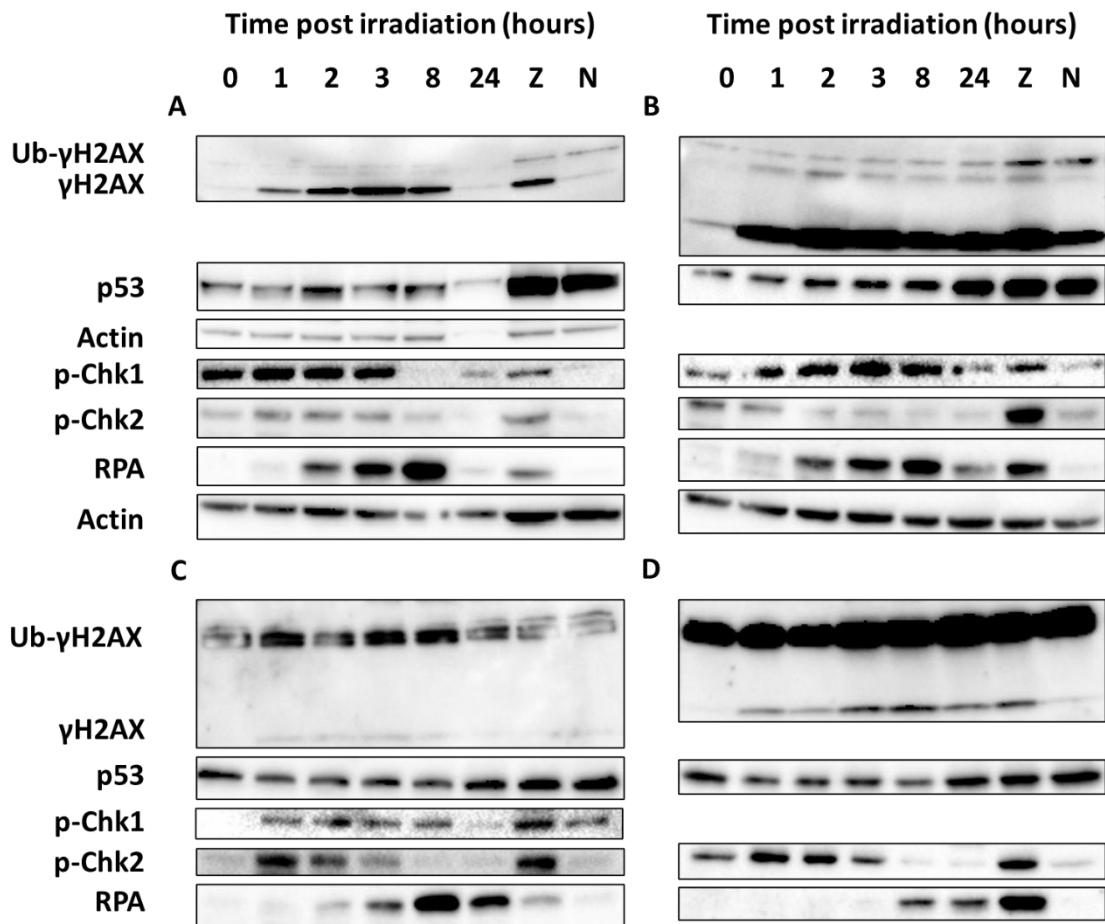


Figure 3.1: DDR protein activation in response to 72 kJ/m² of direct UVA irradiation. Western blot displaying the activation of different components of the DDR. HaCaT cells were directly irradiated with 72 kJ/m² of UVA and samples collected at: 0, 1, 2, 3, 8 and 24 hours post irradiation. The positive control (Z) was prepared by 1 hour incubation with zeocin (500 µg/ml), and the negative control (N) was incubated for 1 hour with no additional reagents. A-D represent four independent repeats of the experiment. n=4.

3.3.1.2. DDR response induced by 108 kJ/m² UVA

HaCaT cells were exposed to a higher dose of 108 kJ/m² UVA and collected over a 24-hour period to be analysed by Western blot. Two independent repeats are displayed in Figure 3.2. Under these conditions, Chk2 was immediately phosphorylated and activated following irradiation, increasing in intensity before peaking at 2 and 3 hours in comparison to the positive control. Levels of phosphorylated Chk2 decreased to basal levels by 8 to 24 hours post-irradiation in relation to the negative control. Levels of Ser345-phosphorylated Chk1 on the other hand were initially low and gradually increased, reaching maximum abundance at 8 hours compared to both positive controls. This suggested an early presence of DNA damage such as DSBs, and replication associated activation of the DNA damage response occurred gradually building at later timepoints (Figure 3.2).

RPA showed a sudden increase in activation at 8 hours with low levels of phosphorylated RPA still present at 24 hours post irradiation compared to the positive controls. The peak activation coincides with the decline of p-Chk1 and p-Chk2 signals which could indicate either late generation of DNA damage or the activation of DNA repair (Figure 3.2).

γH2AX was consistently present at 2- to 24 hours post irradiation, peaking when levels of phosphorylated Chk1 and phosphorylated Chk2 were decreasing in relation to the positive controls. This indicates the presence of DNA damage which may have been caused by oxidative stress based on the activation of p-Chk1. Furthermore, the presence of elevated Ub-γH2AX was observed between 2- and 8 hours post-irradiation (Figure 3.2) and further at 0- and 1-hour post irradiation in Figure 3.2b which implies repair protein recruitment is initiated.

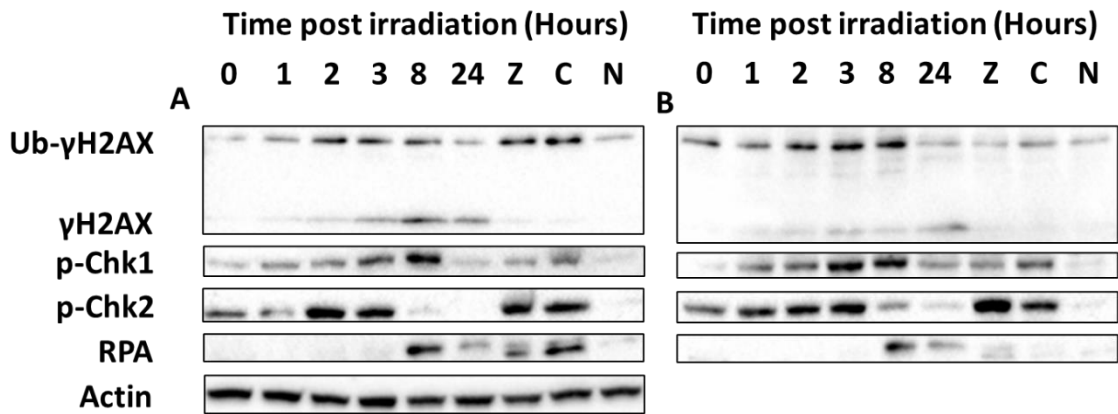


Figure 3.2: DDR protein activation in response to 108 kJ/m² of direct UVA irradiation. Western blot displaying the activation of different components of the DDR. HaCaT cells were directly irradiated at 108 kJ/m² of UVA and samples collected at: 0, 1, 2, 3, 8 and 24 hours post irradiation. The positive controls were prepared by 1 hour incubation with zeocin (Z) (500 μg/ml) or camptothecin (C) (1 μM) and the negative control (N) was incubated for 1 hour with no additional reagents. A and B are two independent repeats of the experiment. n=2.

3.3.1.3. DDR response induced by 144 kJ/m² UVA

A further increase in dose to 144 kJ/m² of UVA was used to irradiate HaCaT cells in two independent repeats for Western blot analysis looking at DDR response proteins (Figure 3.3). At this dose, Ser345-phosphorylated Chk1 showed some inconsistent findings with one repeat only showing activation at 8 hours post irradiation (Figure 3.3a) whilst in Figure 3.3b phosphorylated Chk1 was present at all timepoints showing a small decrease at 24 hours compared to the positive controls. The activation of RPA, however, does coincide with the downregulation of phosphorylated Chk1 at 8 hours post-irradiation maintaining its elevation up to 24 hours post-irradiation compared to the positive controls confirming the presence of DNA damage likely associated with replication stress and persistence in cells for at least 24 hours after UVA irradiation (Figure 3.3).

Chk2 phosphorylation was observed at the earliest timepoint, and levels remained high for at least 2 hours (compared to the positive controls) consistent with rapid activation of the ATM pathway (Figure 3.3). This was followed by the activation of γ H2AX between 2-3 hours post irradiation which lasted up to 24 hours (Figure 3.3) further indicating the generation of DNA damage, such as DSBs, and activation of the ATM pathway.

The detection of formation of Ub- γ H2AX produced inconsistent results. In Figure 3.3a it was immediately activated lasting only 1 hour before reducing and becoming elevated again at 3 hours in relation to the positive controls. Meanwhile in Figure 3.3b Ub- γ H2AX was only elevated at 2 and 3 hours post irradiation. These results must be taken with caution as there is no actin control available due to a problem with the blocking reagent. However, this did imply the early initiation of DNA damage repair (Figure 3.3).

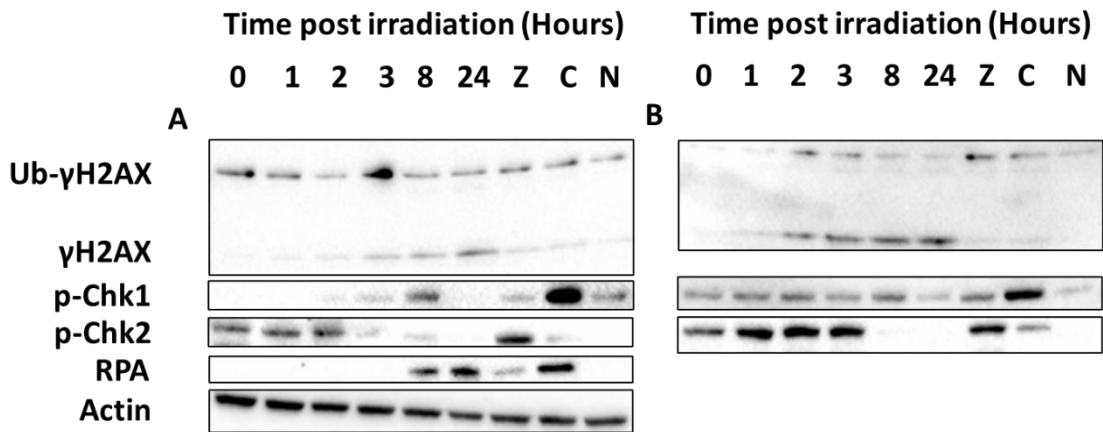


Figure 3.3: DDR protein activation in response to 144 kJ/m² of direct UVA irradiation. Western blot displaying the activation of different components of the DDR. HaCaT cells were directly irradiated with 144 kJ/m² of UVA and samples were collected at: 0, 1, 2, 3, 8 and 24 hours post irradiation. The positive controls were prepared by 1 hour incubation with zeocin (Z) (500 µg/ml) or camptothecin (C) (1 µM) and the negative control (N) was incubated for 1 hour with no additional reagents. A and B are two independent repeats of the experiment. n=2.

3.3.2. Immunofluorescence analysis of γ H2AX

Asynchronous HaCaT keratinocytes were grown on coverslips and irradiated at the same doses of UVA as in Section 3.3.1 for analysis via immunofluorescence confocal microscopy to further study the kinetics of γ H2AX and Ub- γ H2AX at various timepoints post-irradiation.

3.3.2.1. γ H2AX generation induced by 72 kJ/m² UVA

Cells fixed at various timepoints over a 24-hour period following 72 kJ/m² of UVA irradiation showed that mean total γ H2AX (γ H2AX and Ub- γ H2AX based on Western blotting analysis shown in section 3.3.1.) was significantly elevated across all timepoints ($P < 0.001$), except immediately post-irradiation with highest average intensities occurring at 1 and 3 hours (Figure 3.4b). There were small decreases in average intensity, but this did not reduce to the level of the negative control showing sustained activation for 24 hours post irradiation indicating the presence of DNA damage 24 hours later and the initiation of its repair. Later timepoints are required to study trends in its activation and downregulation since total γ H2AX levels were still elevated at the final timepoint of 24 hours (Figure 3.1 and 3.4). Total γ H2AX was activated in most cells at varying levels within each condition suggesting some cells experienced more damage than others or some cells had repaired the damage downregulating the DDR. This was more observable at later timepoints where the interquartile range was larger (Figure 3.4).

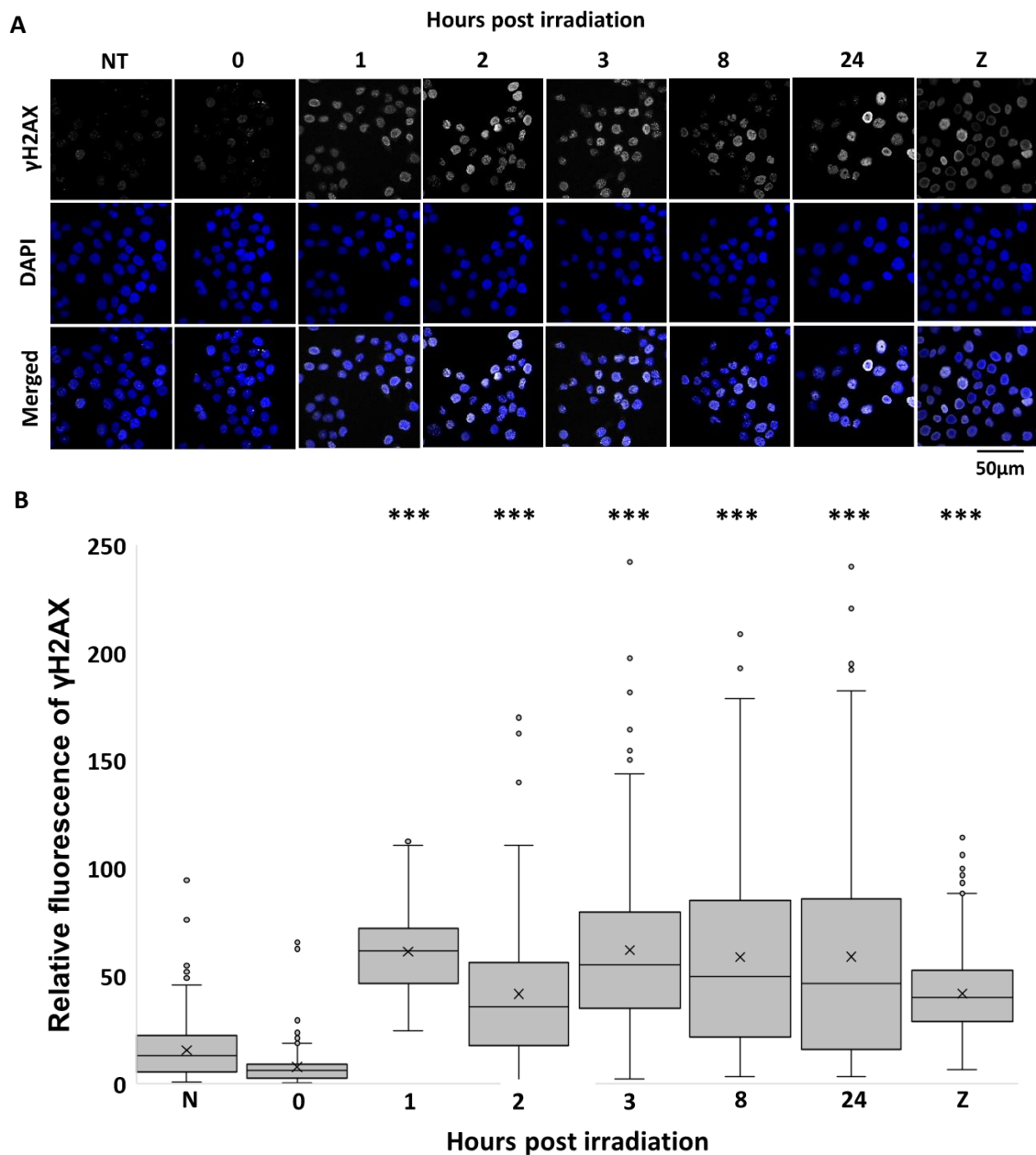


Figure 3.4: γ H2AX protein activation in response to 72 kJ/m² of direct UVA irradiation. (A) Immunofluorescent images of directly irradiated HaCaT at 72 kJ/m² of UVA labelled with γ H2AX. (B) Box and whisker plot showing the spread of γ H2AX relative fluorescence where (***) represents a $p < 0.001$ compared to the negative control carried out by a one-way ANOVA. Timepoints were collected at: 0, 1, 2, 3, 8 and 24 hours post irradiation for (A) and (B). The positive control (Z) was prepared by 1 hour incubation with zeocin (500 μ g/ml), and the negative control (N) was incubated for 1 hour with no additional reagents. A minimum of 100 nuclei were measured for each condition.

3.3.2.2. γ H2AX generation induced by 108 kJ/m² UVA

Using confocal immunofluorescence microscopy following 108 kJ/m² of UVA irradiation, total γ H2AX was observed to be significantly increase from 2- to 24 hours post-irradiation compared to the negative control. Abundance increased and peaked at 3 hours before gradually decreasing but remained elevated at the final timepoint indicating the generation of DNA damage such as DSBs and initiation of their repair as early as 2 hours and continuing beyond the timepoints measured in this experiment. As a result, additional repeats are required with extended timepoints due to inconsistencies between the Western blot and IF data, to get a more accurate representation of γ H2AX and Ub- γ H2AX activation and more importantly its downregulation following 108 kJ/m² of UVA irradiation. As seen with 72 kJ/m², not all cells showed elevated total γ H2AX with the largest variation in the interquartile range (IQR) observed at 3 hours demonstrating how in some cells the damage had been repaired leading to a reduced DDR and increased variation in intensity. A 0-hour sample was collected, but unfortunately the coverslip was damaged and could not be imaged (Figure 3.5).

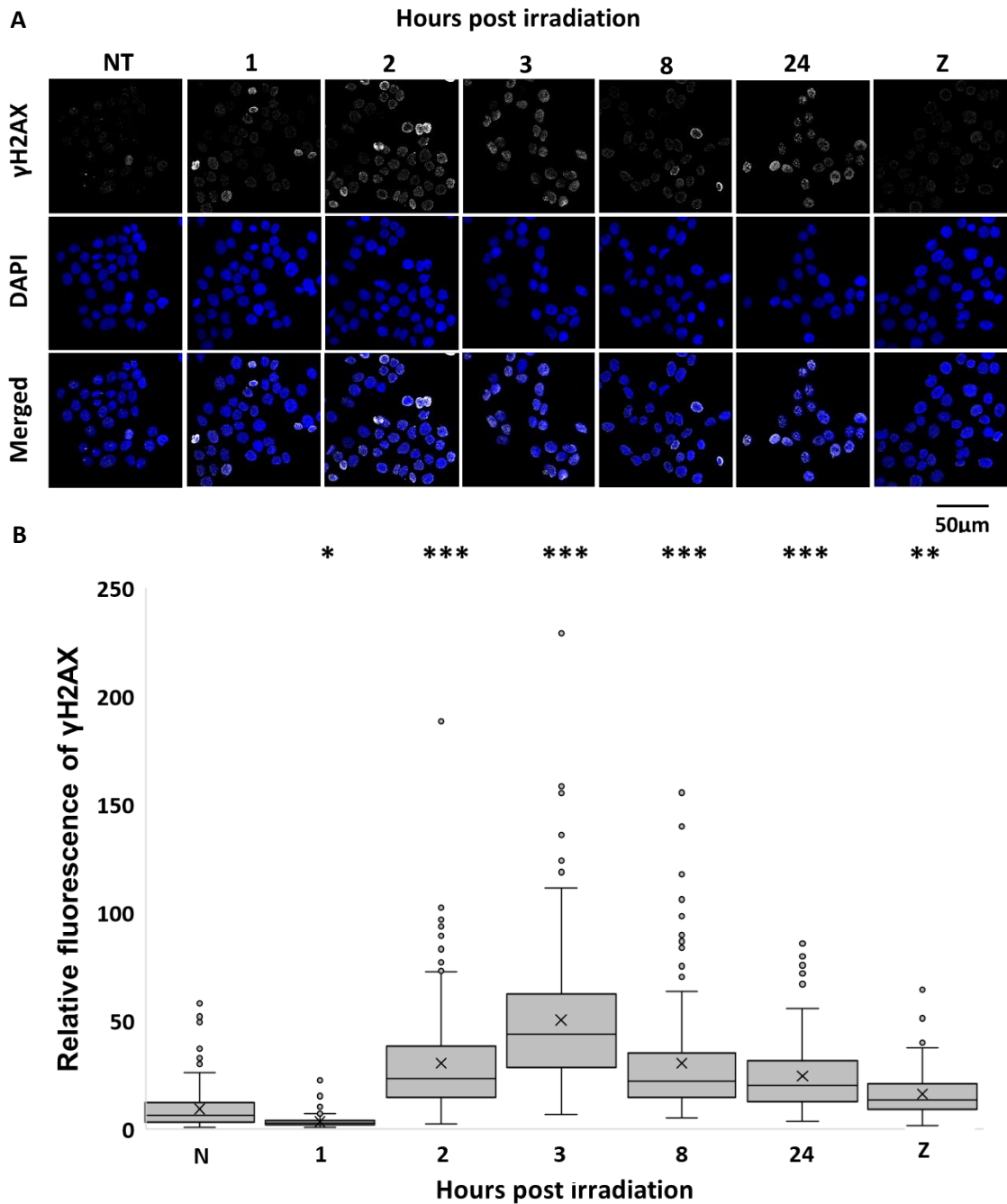


Figure 3.5: γ H2AX activation in response to 108 kJ/m² of direct UVA irradiation. (A) Immunofluorescent images of directly irradiated HaCaTs at 108 kJ/m² of UVA labelled with γ H2AX. (B) Box and whisker plot showing the spread of relative fluorescence of γ H2AX intensity where asterisks signify significant values: (*) $p < 0.05$, (**) $p < 0.01$ and (***) $p < 0.001$ compared to the negative control carried out by a one-way ANOVA. Timepoints were collected at: 0, 1, 2, 3, 8 and 24 hours post irradiation for (A) and (B). The positive control (Z) was prepared by 1 hour incubation with zeocin (500 μ g/ml), and the negative control (N) was incubated for 1 hour with no additional reagents. A minimum of 100 nuclei were measured for each condition.

3.3.2.3. γ H2AX generation induced by 144 kJ/m² UVA

At a higher dose of 144 kJ/m² of UVA using IF analysis shown in Figure 3.6, total γ H2AX demonstrated a significant elevation above the control levels between 3 and 24 hours post-irradiation (Figure 3.6). However, this disagreed with Western blotting data from figure 3.3 in which Ub- γ H2AX showed a higher intensity at earlier timepoints. However, these figures do not show elevation of γ H2AX which may explain why the overall total γ H2AX is not significant. Total γ H2AX peaks at 8 hours post irradiation which coincided with the downregulation of p-Chk2 marking the presence of DNA damage and its repair. It also had the largest range in intensity indicating some cells had repaired their DNA and so were showing decreased activation creating more variation (Figure 3.6). Since total γ H2AX was still elevated at the final timepoint of 24 hours post-irradiation, more repeats are required at later timepoints to study the downregulation of total γ H2AX. A 2-hour sample was collected however, due to a damage on the coverslip it could not be analysed (Figure 3.6).

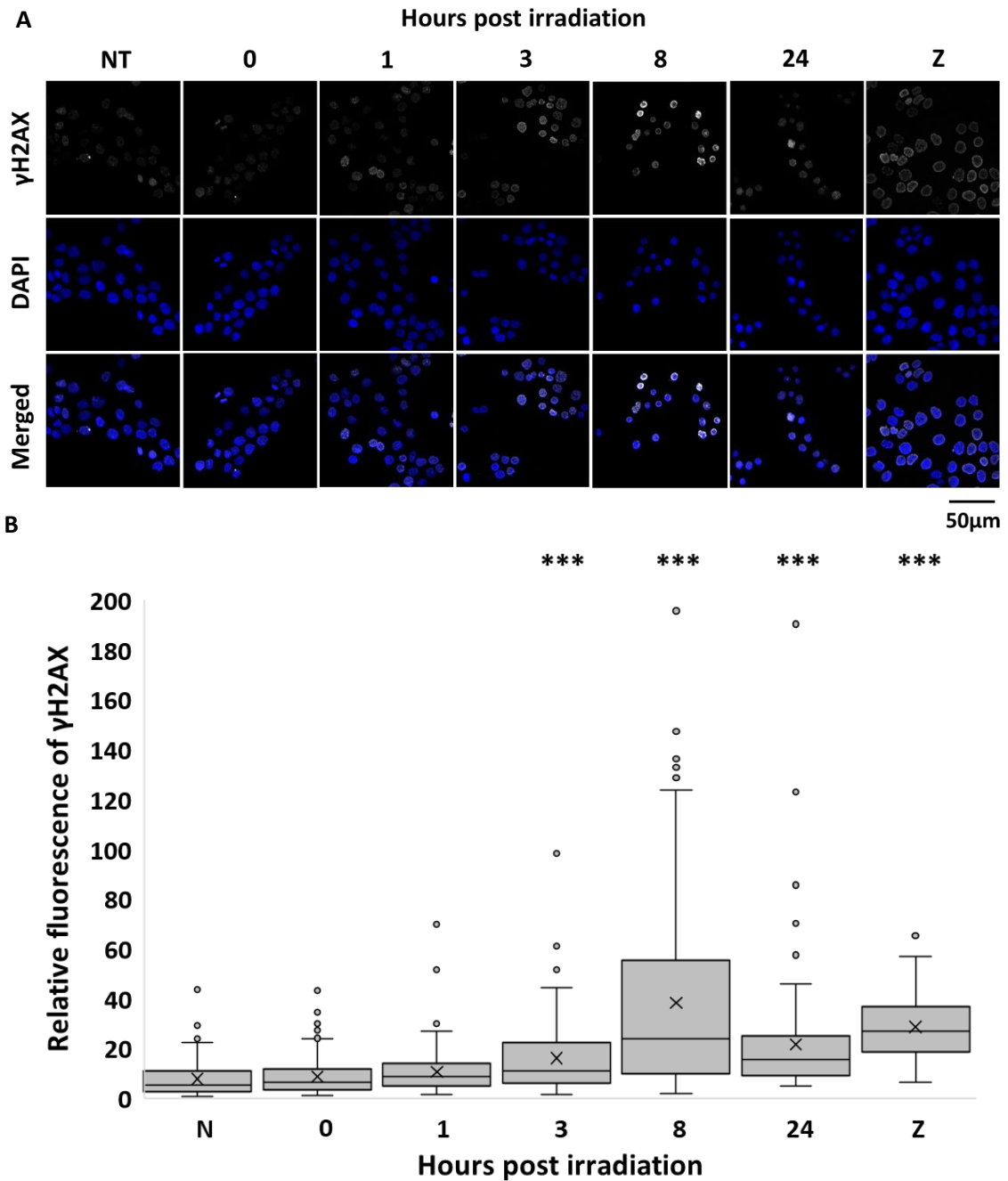


Figure 3.6: γ H2AX activation in response to 144 kJ/m² of direct UVA irradiation. (A) Immunofluorescent images of directly irradiated HaCaTs at 144 kJ/m² of UVA labelled with γ H2AX. (B) Box and whisker plot showing the spread of relative fluorescence of γ H2AX intensity where (***) $p < 0.001$ carried out by a one-way ANOVA compared to the negative control. Timepoints were collected at: 0, 1, 2, 3, 8 and 24 hours post irradiation for (A+B). The positive control (Z) was prepared by 1 hour incubation with zeocin (500 μ g/ml), and the negative control (N) was incubated for 1 hour with no additional reagents. A minimum of 100 nuclei were measured for each condition.

3.3.3. Comparison of doses

Across the three irradiation doses, there were a number of similarities and differences. Chk2 phosphorylation was the most consistent showing immediate activation post irradiation and lasting up to 3 hours at all UVA doses. RPA also showed similarities across the UVA doses becoming activated when p-Chk1 and p-Chk2 were downregulated between 3 and 8 hours post irradiation although it was also occasionally present at other timepoints.

On the other hand, p-Chk1 shows some variation. At 108 kJ/m², Chk1 was phosphorylated between 1 and 8 hours with increasing levels. Although Chk1 phosphorylation was upregulated between 1 and 3 hours post irradiation at 72 kJ/m² similarly to 108 kJ/m², the three repeats were inconsistent showing different ranges of activation making comparisons unreliable (Figure 3.1-3.3). In addition to this, at 144 kJ/m² in Figure 3.3b activation also occurred between 1 and 8 hours post irradiation with the addition of 0-hour timepoint. In contrary to this, in Figure 3.3a p-Chk1 is only present at 8 hours, however this is the only repeat across all irradiation doses which did not follow the pattern of early activation seen with Chk1. Due to variation within experiments, reliable comparisons between UVA doses for p-Chk1 cannot be made.

There was a large amount of variation for Ub- γ H2AX with some repeats showing elevated levels and in others it was not present (Figure 3.1-3.3). This is explained in more detail in Chapter 4.3.4.

For γ H2AX Western blot images consistently showed elevated levels at later timepoints typically between 3 and 24 hours post irradiation which follows p-Chk1 and p-Chk2 downregulation, however some also showed early activation at 1 and 2-hour timepoints (Figure 3.1-3.3). Furthermore, using immunofluorescent microscopy, it was shown that total γ H2AX was significantly elevated at 3-24 hours at all doses and in some cases, it was seen earlier at 1-2 hours post irradiation, but it was not significantly present immediately after irradiation (Figure 3.4-3.6). An interesting observation shown across the three doses showed peak activation was occurring later. At 72 kJ/m² the highest average occurs at 1 and 3 hours (Figure 3.4), at 108 kJ/m² it occurs at 3 hours (figure 3.5) whilst at 144 kJ/m² peak average was at 8 hours post-irradiation (figure 3.6) implying a

longer persistence of DNA damage with increasing UVA dose. Another common feature was variability in total γ H2AX intensity. Across all three doses some timepoints had a wide range in intensity demonstrated by the IQR and the whiskers (Figure 3.4- 3.6). This implied DNA repair had already taken place in some cells and therefore downregulated their responses. Results from Figure 3.1c and d, Figure 3.2b and Figure 3.3b must be studied with caution as they did not contain an actin control due to blocking reagent damaging the membranes. Although an equal volume of protein was calculated and loaded in each well, equal loading could not be confirmed with actin.

3.4. Discussion

UV is a major factor in the induction of skin cancer. The oxidative stress induced by UVA irradiation causes a range of DNA damage which has mutagenic effects on the cells leading to cancer (Cortat et al, 2013; D’Orazio et al, 2013; Schuch and Menck, 2010). The DDR is well established, and activation of different components have been previously studied in response to UVA (Steel, 2016) but to my knowledge, there is no research that gives comprehensive insight that characterises the DDR in response to direct physiological UVA irradiation studying a range of proteins. With UVA making up the majority of the UV individuals are exposed to, this project aimed to study the cellular response to UVA-induced DNA damage by measuring the up- and downregulation of DDR proteins. This provided information as to how quickly the cell responds and how long it lasts giving an indication for the persistence of DNA damage in directly irradiated cells and provide more insights into the damaging effects of UVA.

Each irradiation dose demonstrated activation of all proteins tested indicating the generation of both DSBs and oxidative damage activating both pathways of the DDR. Whilst each condition showed similarities, there were also some differences which could be attributed to the different irradiation doses.

3.4.1. Activation of the DDR branches could be dose dependent

Chk1 and Chk2 are effector proteins in the DDR each activated by a different pathway. Chk1 is phosphorylated by ATR following the formation of RPA bound ssDNA created by a variety of types of DNA damage meanwhile Chk2 is phosphorylated by ATM which is mainly responsible for the identification and repair of DSBs. These proteins can therefore be used to represent the activation of the ATM and ATR pathways (Girard et al, 2008; Jaiswal and Lindqvist, 2015; Maréchal and Zou, 2013; Shiotani et al, 2013; Tsao, et al, 2004; Williams and Zhang, 2021).

p-Chk1 (Ser317 and Ser345) displayed consistent activation between 1-3 hours post irradiation across all doses and returned to normal levels after 24 hours. It was also commonly elevated at 0 and 8 hours however, this did not occur in every instance. It did confirm early (and in most cases immediate) activation of the ATR pathway demonstrating an early occurrence of replication stress induced by oxidative damage.

The level of elevation was where the differences lay with p-Chk1. At 72 kJ/m², the bands were intense from the earliest timepoint and maintained an intensity above that of the positive zeocin control (Figure 3.1a and b) except for 0- and 24 hours in Figure 3.1b. At 144 kJ/m², the experimental bands were equal in intensity but lower compared to the positive control, however there was no actin for this blot so conclusions must be taken with caution (Figure 3.3b). This implied the responses were immediate and maintained but a larger response is implied at 72 kJ/m². At 108 kJ/m² the pattern was different. Rather than the protein abundance being consistently maintained, there was a gradual increase in intensity compared to the zeocin control peaking at the latest timepoint of 8 hours. This could imply there was later generation of replicative damage leading to a slower response suggesting different activation of the DDR branches depending on the dose. As a different phosphorylation site was used for 72 kJ/m² compared to 108 kJ/m² and 144 kJ/m², this could explain the differences. However, the same antibody was used for 108 and 144 kJ/m² which implied the dose was responsible for the differences observed. Changes in p-Chk2 could also help to explain this.

p-Chk2 was consistently elevated between 0-2 hours across all doses, and similarly to p-Chk1, had returned to normal levels by 24 hours post irradiation. This is consistent with immediate activation of the ATM pathway and might suggest the formation of DSBs soon after irradiation. When comparing doses: at 72 kJ/m², p-Chk2 appeared to show a low level of activation with band intensity less than the zeocin control or equal when p-Chk2 peaked, possibly implying a small amount of DNA damage generation and therefore low ATM activation. However, at 108 kJ/m² and 144 kJ/m² the bands were of equal intensity to the zeocin control which suggested more damage had occurred initiating a stronger response with higher levels of activation of p-Chk2.

When comparing the p-Chk1 and p-Chk2 response, p-Chk1 (Ser317) intensity was higher in relation to the zeocin control whilst p-Chk2 had a lower intensity at 72 kJ/m². However, at 108 kJ/m² band intensity is similar for both proteins in relation to the zeocin controls, but p-Chk1 (Ser345) showed a higher intensity at 3 and 8 hours. At 144 kJ/m², the reverse is seen in which p-Chk2 intensity is of an equal or higher intensity compared to zeocin whilst p-Chk1 (Ser345) was as equally intense. This could explain why p-Chk1 changes from remaining at a constant level between 0-8 hours when activated at 72

kJ/m² to a gradual increase between 0-8 hours seen at 108 kJ/m². Ma and Dai, 2018, theorised that when SSBs were in higher abundance than DSBs, SSB repair was prioritised, likely due to more SSBs being created and an accumulation of which leads to DSB formation. However, when SSB levels were lower than DSBs, they were repaired simultaneously (Ma and Dai, 2018). This could explain the changes in p-Chk1 and p-Chk2 abundance in comparison to each other from a low irradiation dose to a higher one. DSBs are highly mutagenic and need to be repaired quickly. But an accumulation of oxidative damage or replication stress can lead to DSB generation (Greinert et al, 2012). A low dose could cause fewer DSBs so the oxidative damage might be prioritised and repaired first forming a lower p-Chk2 response in comparison to p-Chk1. However, at higher doses, more DSBs could be generated and repaired simultaneously with other types of damage which could increase the p-Chk2 response and lead to a more gradual increase in p-Chk1. As both pathways require the same proteins (RPA and γ H2AX), they could be in limited supply during elevated levels of DNA damage and prioritised according to the type of damage and its abundance (Ma and Dai, 2018). Based on Ma and Dai, (2018) research, it may be expected to see similar responses from p-Chk1 and p-Chk2 in relation to the positive control if damage is repaired simultaneously. However, this research only studied SSBs and DSBs. UVA generates a wider range of damage than this including CPDs which Ma and Dai's (2018) research does not consider. This could explain why p-Chk1 changed to a more gradual increase rather than equal levels as this system was host to a wider range of types of DNA damage which could influence the DDR in different ways.

3.4.2. Timings of DNA damage generation and repair

RPA is involved in the activation of the ATR pathway, but this protein's function is to bind to ssDNA which can be generated as a result of DNA damage or can be formed during repair processes when the DNA is resected. RPA can therefore be used as an indicator of both generation of DNA damage and its repair downstream of the DDR (Maréchal and Zou, 2013; Shiotani et al, 2013; Williams and Zhang, 2021). γ H2AX is similar in that it is activated as a result of DNA damage including DSB generation in which it flanks the damaged region (Mah et al, 2010; Pan et al, 2011; Zhao et al, 2011), but it also functions in a feedback loop where it is involved in the amplification of ATM

activation via MDC1 (Williams and Zhang, 2021). Furthermore, it can also be activated by replication stress and the ATR pathway. Therefore, this protein can be used as an indicator of DSB generation and its repair as well as other types of damage (Chatterjee and Walker, 2017; Luczak and Zhitkovich, 2018).

RPA activation occurred late, commonly elevated at 8-24 hours post-irradiation across all doses with earlier occurrences for 72 kJ/m². Its activation coincided with the downregulation of p-Chk1 and p-Chk2 which implied DNA repair was beginning to take place. Furthermore, γ H2AX showed later activation of 2-24 hours post-irradiation. Together, this implied it was taking at least 2 hours before any DNA damage was being detected and repaired. Meanwhile, Ub- γ H2AX generated unreliable data. It showed inconsistent findings across all doses so no conclusions can be drawn. Immunofluorescence analysis of γ H2AX and Ub- γ H2AX (total γ H2AX) was used as an additional measure of its activation. Across the three doses, significant increases of total γ H2AX to $p < 0.001$ occurred from 3-24 hours post irradiation and none showed significant findings at 0 hours. This confirms the generation of DNA damage, such as DSBs, early following UVA irradiation.

Large IQRs from IF data suggested that DNA repair had taken place in some cells. For 108 kJ/m² and 144 kJ/m², the largest IQR coincided with peak total γ H2AX intensity which occurred at 3 and 8 hours. This implied at these timepoints, some cells had already repaired their DNA and begun to downregulate their DDR pathway whilst others still contained DNA damage and elevated DDR proteins. Since this occurred as total γ H2AX intensity peaked, it also suggested that DNA damage was still being generated at this time. As peak intensity and IQR occurred later at 8 hours for 144 kJ/m² compared to 3 hours for 108 kJ/m², this proposed that the higher dose induced more DNA damage therefore taking longer for the DDR proteins to accumulate for cells to repair it. For 72 kJ/m², the IQR continued to increase overtime which suggested a continuous generation of DNA damage and repair. This is explained further in section 3.4.3.

Furthermore, another pattern that emerged from the dose dependent studies demonstrated that activation of total γ H2AX and its peaks activation occurred later in each dose. At the lowest dose, activation occurred at 1 hour and peaked at 1 and 3 hours equally, at 108 kJ/m² activation was seen at 2 hours and peaks at 3 hours whilst at the

highest dose, an elevation was first observed at 3 hours peaking at 8 hours post irradiation. In addition to the IQR data for 108 kJ/m² and 144 kJ/m², this suggested higher doses induce more damage and take longer for the response to achieve its maximum activation in order for repair to take place.

Following 100 kJ/m² of UVA irradiation, Steel (2016) identified significant increases in γ H2AX foci formation at 1 hour post irradiation however, in this research, an increase at 1 hour was only observed at 72 kJ/m² and not at either of the two higher doses (Steel, 2016). Wischermann et al, 2008, demonstrated that following 600 kJ/m² of UVA irradiation in normal human keratinocytes, there was no immediate presence of DSBs. They formed gradually over time where increases in γ H2AX foci generation were still occurring at 6 hours post irradiation. This demonstrated a delay in damage generation but a persistence of DSBs for at least 6 hours post irradiation (Wischermann et al, 2008). This research followed a similar pattern to UV research with no γ H2AX generation occurring immediately after irradiation. Damage was generated gradually with total γ H2AX peaking at 3 hours for 108 kJ/m² and 8 hours for 144 kJ/m². Although this fits the general trend demonstrated by Wischermann et al, 2008, with no immediate damage and a steady increase, data here showed a more delayed response which may be related to a difference in cell type or irradiation dose. Furthermore, more contrasting evidence identified from Steel's (2016) work shows reductions in γ H2AX foci generation at 3 hours whilst this research showed peak γ H2AX intensity at this timepoint using a similar UVA dose. However, reductions were observed after this timepoint implying there could have been a small difference and repeats could not be conducted, therefore it was not possible to identify any anomalies.

3.4.3. Possible late generation of DNA damage

As RPA is a sensor protein for DNA damage activating the ATR response, it would be expected to see its activation early. However, the irradiation periods were long (25-50 minutes), and downstream effector proteins, Chk1 and Chk2, were phosphorylated at 0 hours implying the DDR had already been activated before the first timepoint was taken, so the detection and activation of the DDR could have occurred during the irradiation period. It is therefore more likely that the RPA visualised in the Western blots is indicative of repair processes since ssDNA is generated. However, it has been identified

that CPDs can be generated post irradiation (dark CPDs) (Premi et al, 2015) and late oxidative damage can occur. In NER proficient and deficient cells following 120 kJ/m² of UVA irradiation, oxidative damage was found to be elevated immediately following irradiation and reduced 4 hours later. However, at 24 hours, the oxidative damage had increased again demonstrating that persistent oxidative stress can induce DNA damage long after irradiation (Cortat et al, 2013). Since RPA was identified at 24 hours in this research, it could indicate the later generation of oxidatively induced DNA damage. The initial activation and peak level of RPA at 108 kJ/m² occurred after total γ H2AX intensity peaked implying that DNA damage is being induced after the repair of DNA damage is initiated supporting the theory of late DNA damage generation.

Furthermore, γ H2AX followed a similar pattern. Since it was not identified immediately after irradiation and more commonly found at 2-3 hours (approximately when p-Chk1 and p-Chk2 peak and begin to downregulate), this would imply that the total γ H2AX seen is representative of the damage that initially occurred and is now being repaired. However, it has been identified that clustered oxidative damage can lead to DSB generation. Closely formed SSBs or other forms of damage being repaired can lead to the formation of DSBs (Greinert et al, 2012; Cannan and Pederson, 2016; Ma and Dai, 2018; Wischermann et al, 2008) which could explain the late activation of total γ H2AX at 24 hours post irradiation at all doses and increasing IQR identified at 72 kJ/m² as some cells may continue to generate damage whilst others are repairing it. In addition to this, DSB generation can also result from the collapse of replication forks at DNA damage lesions such as dark CPDs which could cause later generation of DSBs (Cannan and Pederson, 2016; Premi et al, 2015; Zhao et al, 2011) again explaining the late activation of total γ H2AX seen.

3.4.4. UVA may be more mutagenic than first thought

Following this, this research along with other previous studies implied a more concerning result that DNA damage is persisting beyond cell cycle arrest and DNA repair inhibition. These results demonstrated a more prolonged presence of DNA damage compared to Wischermann et al, (2008). Whilst they showed the damage persisted for at least 6 hours, results from this research showed the presence of γ H2AX for at least 24 hours after irradiation where all doses showed significant total γ H2AX increase at 24

hours post irradiation. This was also demonstrated by Steel, 2016, at 24 hours post irradiation and by Mouret et al, 2006, where CPDs were still present after 48 hours implying not all damage is repaired 24 hours later. Wischermann et al, 2008, also showed that damage was repaired in some cells but persisted in other cells for longer leading to increased DNA damage in those cells. Cells with 1-5 γ H2AX foci per nucleus reduced from 68% to 48% whilst simultaneously increasing the number of cells with 6-10 foci from 10% to 20% (Wischermann et al, 2008). This could explain the large IQR range observed in each condition and long activation of γ H2AX as some cells were able to repair their damage much faster whilst others continued to generate it.

This significant increase of total γ H2AX intensity observed at 24 hours post irradiation for each dose creates particular concern for genomic stability. Previous research has identified that UVA irradiation (300 kJ/m^2) leads to S phase arrest and DNA replication inhibition. However, it was identified that this only applied to a small number of cells and lasted for 2 hours before DNA replication and the cell cycle continued (Rünger et al, 2012). Furthermore, Graindorge et al, 2015, identified slightly different results observing a slowing of replication, rather than complete inhibition, in the form of reduced fork velocity lasting up to 5 hours. They used 80 kJ/m^2 and 160 kJ/m^2 of UVA irradiation, but results were similar for both (Graindorge et al, 2015). Although the results differ between the two pieces of research, they still identified slowing or inhibition of DNA replication and S phase arrest lasting no more than 5 hours. Meanwhile data generated in this study along with Steel (2016) and Mouret et al, (2006) showed that DNA damage and repair was still present 24-48 hours post irradiation. This creates concerns that the DNA damage created by UVA has more potential to be replicated and therefore more likely to be mutagenic emphasising the importance of research into UVA induced DNA damage. However, Rünger et al, 2012, and Graindorge et al, 2015, used fibroblasts whilst this research used immortalised keratinocytes – slowing of S phase and DNA replication may be different between the two cell types.

When compared to UVB, the peak activation of γ H2AX is 2 hours and downregulation at 4 hours for UVB irradiation meanwhile, for UVA peak activation varied but was still significantly elevated at 24 hours which implied damage was longer lasting when induced by UVA compared to UVB or a less effective response to repair the damage

(Zhao et al, 2011). In addition, cell cycle data from Runger et al, 2012, demonstrated a faster S phase and DNA replication recovery of 90 minutes for UVA compared to 48 hours for UVB (Runger et al, 2012). Furthermore, whilst equally mutagenic doses of UVA and UVB led to a greater generation of CPDs from UVB irradiation, UVA induced CPDs were more persistent with 72% remaining 48 hours post irradiation compared to 55% for UVB (Mouret et al, 2006). Together, this data along with previous research implied that UVA has more mutagenic potential as the cell cycle is not arrested for as long of a period of time and damage was longer lasting highlighting the importance of research into UVA induced DNA damage and the cell response.

3.4.5. Future research

The DDR is well characterised, but the timings of activation and how prolonged the response is to UVA still requires some research. Whilst this study has provided some more insight in the activation of each branch of the DDR by studying certain proteins, more can be done. Future studies should focus on identifying how long the response occurs for. This research has demonstrated significant elevations of DDR proteins 24 hours following irradiation demonstrating it is still activated at this time but, it is unknown as to when it becomes downregulated to normal conditions. Furthermore, DNA damage and oxidative stress should be measured alongside this to give insight into late generation of DNA damage such as what was identified by Cortat et al, 2013 to determine if this is the reason for a prolonged DDR. By studying proteins involved in DNA repair, it will give a more accurate time for when repair is taking place and how long it takes for all damage to be repaired. Finally, more work needs to be carried in the area of clustered DNA damage to deepen our knowledge and understanding of how UVA induces damage, particularly DSBs.

Chapter 4: Characterisation of the DNA damage response induced by the UVA bystander effect

4.1. Introduction

The bystander effect occurs when a damaging agent indirectly induces cell stress in non-exposed healthy cells via the generation of molecules in the directly affected cells. This can have negative implications such as inducing DNA damage leading to cancer (Nishiura et al, 2012; Whiteside et al, 2011; Widel, 2012). First identified in response to ionising radiation (Nagasawa and Little, 1992), it has since been observed in response to UV radiation with reduced cell survival, apoptosis, micronuclei, and DNA damage being signs the phenomena has occurred (Banerjee et al, 2005; Nishiura et al, 2012; Whiteside et al, 2011; Widel et al, 2014).

The mechanism by which the bystander effect occurs is yet to be completely elucidated however, there are some theories. It was initially believed that these bystander factors were transmitted to neighbouring cells via gap junctions as when this form of communication was inhibited, a reduced bystander effect was observed when using alpha particle or ionising radiation (Dahle et al, 2001; Little et al, 2002). However, this cannot be the only form of bystander communication since when gap junction communication is not possible in certain experimental systems, the bystander effect still occurs. Using transwells or media transfer techniques when using UV irradiation, non-exposed cells still exhibited bystander effects suggesting these factors must be soluble and can diffuse to surrounding cells (Steel, 2016; Whiteside et al, 2011; Widel et al, 2014).

The bystander factors involved in communicating the bystander response are not fully understood but many have been proposed. Using different types of radiation to induce the bystander effect, ROS scavengers including superoxide dismutase (SOD), catalase and DMSO, were all able to reduce the bystander effects observed such as micronuclei formation (Burdak-Rothkamm et al, 2007; Little et al, 2002). Meanwhile, when studying the UVA-induced bystander effect, bystander cells co-incubated with catalase or DPI showed reduced γ H2AX foci formation, indicative of reduced DNA damage (Steel, 2016). Together, this provides strong evidence involving ROS in the bystander effect. Furthermore, it has been identified that the bystander response does not just occur between cells of the same type. Keratinocytes, melanocytes, and fibroblasts are all able to communicate the UVA-induced bystander effect to each other. Keratinocytes were

the most efficient donors and melanocytes were the most sensitive at receiving bystander responses (Redmond et al, 2014). Melanocytes and fibroblasts are found deeper in the skin compared to keratinocytes which are on the surface suggesting the bystander effect could be involved in damaging cells deeper in the skin (D’Orazio et al, 2013; Redmond et al, 2014). This damaging effect has been demonstrated to last three days post irradiation and potentially lead to cancer (Whiteside et al, 2011).

S phase cells have been found to be more vulnerable to the bystander effect than cells in other phases of the cell cycle. Using EdU labelling to identify actively replicating cells, γ H2AX foci were only found in this sub-population. EdU intensity was lower in bystander nuclei, suggesting reduced rates of DNA synthesis, in addition to a larger proportion of cells in S phase and activation of Chk1 (phosphorylation of Ser345), implied the cells were experiencing replication stress (Steel, 2016).

4.2. Aims

Limited work has been carried out on the UVA-induced bystander effect focusing on the activation of the DDR. It is known that elevated γ H2AX and p-Chk1 (Ser345) are observed in actively replicating bystander cells (Steel, 2016), but the underlying mechanisms leading to their activation is not understood. Meanwhile ATM and ATR responses and p53 have been studied for the ionising radiation induced bystander effect (Burdak-Rothkamm et al, 2007; Burdak-Rothkamm et al, 2008; Little et al, 2002).

This study asked the question: What DDR proteins are activated and what are their kinetics in bystander cells induced by UVA irradiation?

4.3. Results

HaCaT cells were used to investigate the activation of DDR proteins – p-Chk1 (Ser345), p-Chk2 (Thr68), p-RPA (Ser8), γ H2AX and Ub- γ H2AX – in the bystander effect using Western blots and immunofluorescence. Phosphorylation of Chk1 at Ser317 recovers the cell cycle after stalled replication forks (Martin and Ouchi, 2008) and phosphorylation at Ser345 localises Chk1 to the nucleus (Jiang et al, 2003). Phosphorylation of Chk2, RPA and γ H2AX activates these proteins (Girard et al, 2008; Luczak and Zhitkovich, 2018; Maréchal and Zou, 2015; Wang et al, 2007). Chk2 is an effector protein in the ATM response which activates downstream proteins such as p53 (Hirao et al, 2002; Ou et al, 2005; Williams and Zhang, 2021), RPA binds to ssDNA and recruits ATR to activate the response whilst protecting the DNA from nucleases and secondary structure formation (Ma and Dai, 2018; Shiotani et al, 2013; Williams and Zhang, 2021). γ H2AX and Ub- γ H2AX, mark sites of DSB formation to recruit repair proteins (Mah et al, 2010; Pan et al, 2011). Research has shown that at least 24 hours is required for bystander factors to accumulate and elicit a response which is usually seen to peak by 48 hours post-irradiation (Whiteside et al, 2011). This research therefore used 24- and 48-hour timepoints to study the bystander effect. Cells were directly irradiated at 72, 108 and 144 kJ/m² of UVA in transwell inserts before being transferred to bystander cells (IR) and incubated for either 24 or 48 hours. Bystander cells were incubated with non-irradiated cells using a transwell (UI) to test if the transwell system has an influence on the results and the negative control consisted of unirradiated cells incubated alone (NT – no transwell) (Figure 4.1).

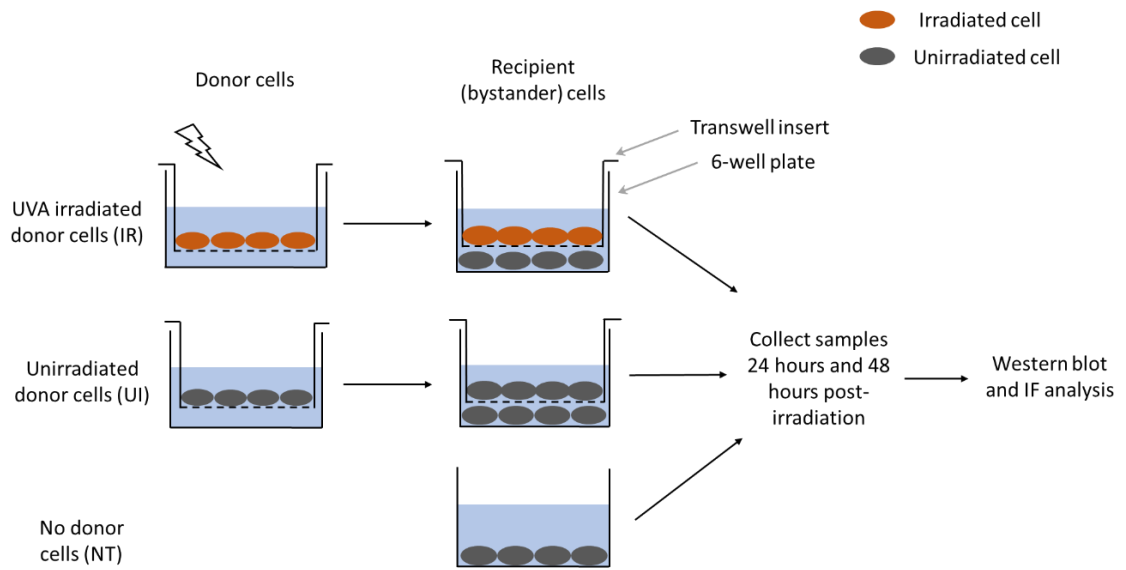


Figure 4.1: Modelling of the bystander effect. Donor cells were grown in transwell inserts in 6-well plates which were transferred to the recipient cells following irradiation or incubation. Samples were collected after 24-48 hours for Western blot and IF analysis of DDR proteins.

4.3.1. Activation of the DDR

Donor asynchronous HaCaT cells were directly irradiated with vary doses of UVA irradiation prior to incubation with non-exposed bystander cells (IR) for 24- and 48-hours. Bystander cells incubated with unirradiated donor cells (UI), and cells prepared from a non-transwell system (NT) were also collected. A range of DDR proteins were measured via Western blot analysis to determine the kinetics of the DDR in the bystander effect.

4.3.1.1. DDR induced by 72 kJ/m² of UVA

HaCaT cells were directly irradiated with 72 kJ/m² of UVA irradiation and co-incubated with bystander cells as well as UI and NT samples being collected to measure DDR proteins 24- and 48-hours post-irradiation. Data for four independent repeats are displayed in Figure 4.2. Under these conditions, small increases in phosphorylated Chk1 (Ser345) and Chk2 are seen in bystander cells. In Figure 4.2a p-Chk2 bands at 24 hours are more intense in the UVA irradiated condition than in the UI or NT controls implying a larger amount of DNA damage had occurred activating the ATM pathway. At 48 hours phosphorylated Chk1 is elevated in respect of the irradiated condition compared to the NT condition however, the IR condition is a similar intensity to that of the UI. It cannot be concluded if a bystander effect is observed here as the irradiated condition is only elevated compared to one negative control.

γ H2AX levels were slightly elevated at 24 hours in UVA bystander cells compared to UI and NT conditions in Figure 4.2a and against the NT condition but not UI in Figure 4.2b. Whereas, Figure 4.2d show a possible bystander effect at 48 hours however, this membrane was of low quality and difficult to determine any differences. In Figure 4.2a, NT sample at 48 hours appeared to be less intense for Ub- γ H2AX than the IR condition but no other evidence of a bystander effect was apparent in the remaining conditions for this protein. Collectively, some repeats implied generation of DNA damage however, the results are inconsistent and require further investigation.

p53 was measured but was not stabilised due to the *TP53* mutation that HaCaT cells contain. For this reason, it was not measured in subsequent experiments.

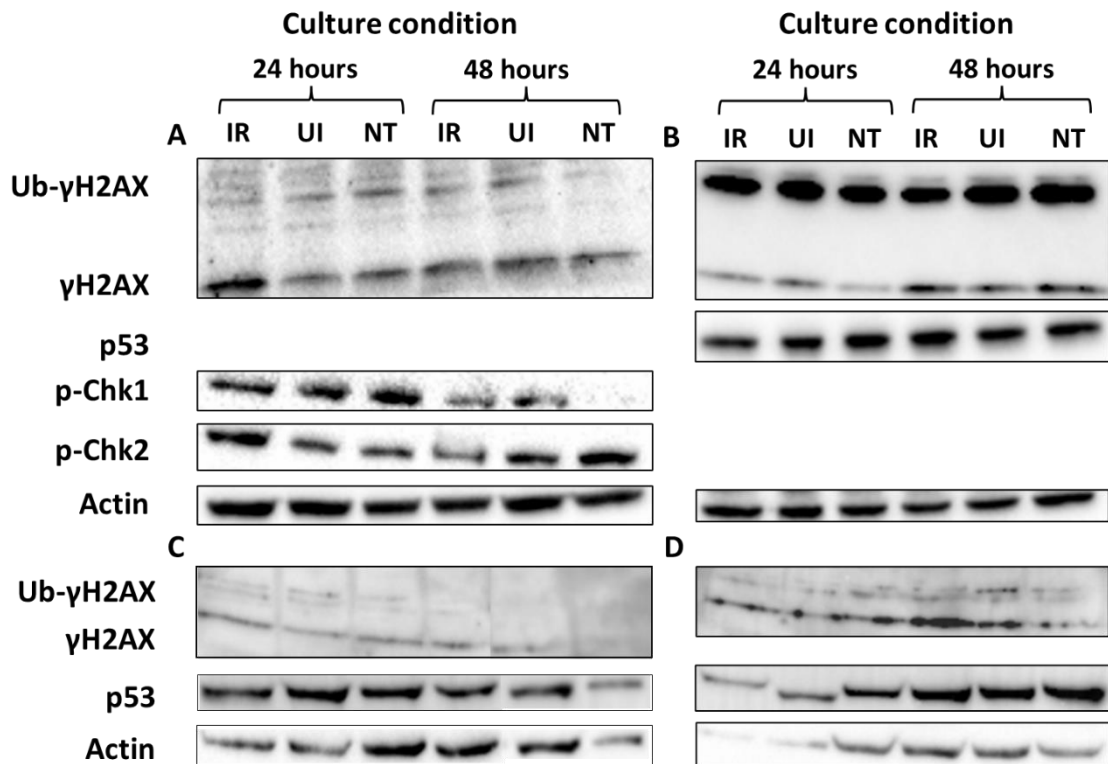


Figure 4.2: Activation of DDR proteins in bystander cells co-incubated with UVA irradiated cells at 72 kJ/m². HaCaT cells were co-incubated with directly irradiated cells using a transwell system at 72 kJ/m² of UVA. Western blot of protein activation of different components of the DDR. IR – bystander cells co-incubated with irradiated cells. UI – bystander cells co-incubated with unirradiated cells. NT – (No transwell) cells incubated alone. All samples were collected following 24 or 48 hours of co-incubation. A-D are four independent repeats of the experiment. n=4.

4.3.1.2. DDR induced by 108 kJ/m² of UVA

The irradiation dose the donor HaCaT cells were exposed to was increased to 108 kJ/m² and then co-incubated with the bystander cells for 24-48 hours. Western blot analysis is displayed in Figure 4.3. Two independent repeats were carried out and displayed in Figure 4.3. At this dose, phosphorylation at Ser345 of Chk1 was only detected in the NT condition at 24 hours. Furthermore, in the 48-hour there was a strong response seen in the UI and NT conditions and a small response in the IR condition (Figure 4.3b). This left uncertainty about activation of Chk1 and the ATR pathway in the bystander effect as no phosphorylation of Chk1 was detected in either IR sample, but it was present in the negative control (NT).

There was increased phosphorylation of Chk2 in the IR condition compared to the NT control at 48 hours (Figure 4.3b) implying the activation of the ATM pathway and generation of DNA damage, but this result was not replicated as no effect was seen in the repeat (Figure 4.3a) and there was no difference in intensity between the UI and IR conditions (Figure 4.3b) questioning whether a bystander effect was observed. At 24 hours, there appeared to be a small elevation of phosphorylated Chk2 in the IR condition in relation to the NT condition (Figure 4.3a) but this only occurred in one out of two repeats (Figure 4.3). The unirradiated 48-hour sample was also elevated in relation to NT (Figure 4.3b). As no actin was present as a control (undissolved milk in the blocking buffer had bound to the membrane preventing the actin antibody from binding) conclusions could not be drawn (Figure 4.3b). The lack of consistency in the results questions the reliability of the data generated and lowers the confidence that a bystander effect was observed.

Only Figure 4.3a displayed any γ H2AX activation, no bands were present in Figure 4.3b. The 48-hour IR condition appears to be more intense than the UI and NT controls suggesting DNA damage was present in this sample as a result of the bystander effect (Figure 4.3a). Ub- γ H2AX showed elevated levels in the IR condition compared to the NT condition demonstrating a bystander effect at 48 hours implying the activation of DNA damage repair (Figure 4.3b) however this did not occur consistently as no response was observed in Figure 4.3a at 48 hours. Additionally, there was an unexpected reduction for 24-hour IR sample in relation to the UI and NT conditions for Ub- γ H2AX (Figure 4.3a).

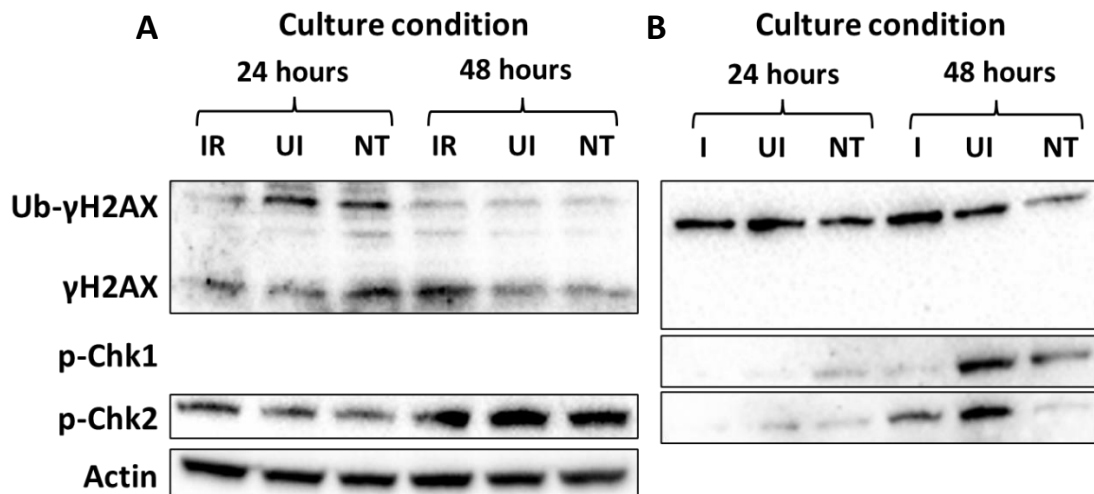


Figure 4.3: Activation of DDR proteins in bystander cells co-incubated with UVA irradiated cells at 108 kJ/m². HaCaT cells were co-incubated with directly irradiated cells using a transwell system at 108 kJ/m² of UVA. Western blot of protein activation of different components of the DDR. IR – bystander cells co-incubated with irradiated cells. UI – bystander cells co-incubated with unirradiated cells. NT – (No transwell) cell incubated alone. All samples were collected following 24 or 48 hours of co-incubation. A and B are independent repeats of the experiment. n=2.

4.3.1.3. DDR induced by 144 kJ/m² of UVA

A further increase to 144 kJ/m² of UVA irradiation was applied to the donor cells before co-incubation with the bystander cells for 24 and 48 hours and analysed by Western blot (Figure 4.4). Chk2 showed an increase in activation at 48-hours for the IR condition compared to the UI and NT conditions, but no difference was seen in the 24-hour condition. No actin control was available due to problems with blocking during the Western blot process, meaning firm conclusions could not be drawn but it was potentially the case that the ATM pathway was activated (leading to phosphorylation of Chk2) by 48 hours post irradiation (Figure 4.4). This was supported by the activation of γ H2AX in the IR sample compared to the UI and NT conditions at 48 hours, but no effect was observed at 24 hours which implied that it took at least 48 hours for a response to be activated to the generation of DNA damage. Furthermore, no change in Ub- γ H2AX was observed (Figure 4.4).

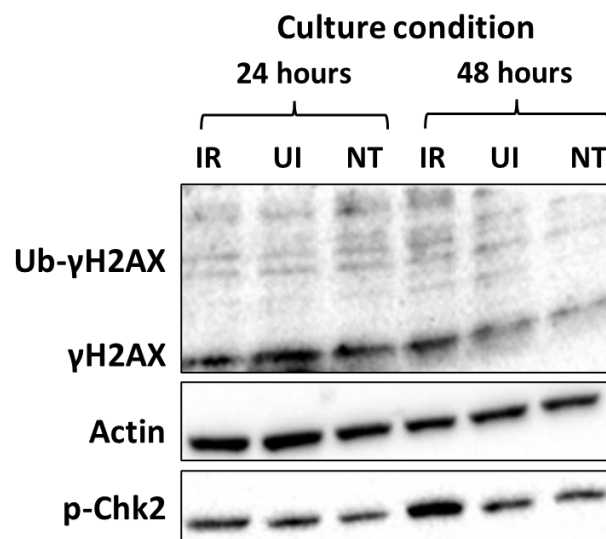


Figure 4.4: Activation of DDR proteins in bystander cells co-incubated with UVA irradiated cells at kJ/m². HaCaT cells were co-incubated with directly irradiated cells using a transwell system at 144 kJ/m² of UVA. Western blot of protein activation of different components of the DDR. IR – bystander cells co-incubated with irradiated cells. UI – bystander cells co-incubated with unirradiated cells. NT – (No transwell) cell incubated alone. All samples were collected following 24 or 48 hours of co-incubation. n=1.

4.3.2. IF analysis of γ H2AX generation

Asynchronous HaCaT cells were irradiated with the same doses of UVA irradiation as used in Chapter 4.3.1. These were then incubated with asynchronous HaCaT cells (IR). Alternatively, non-irradiated donor cells were co-incubated with bystander cells (UI) and a population of cells was incubated alone (NT). Incubation periods lasted 24 and 48 hours. Cells were grown on coverslips to be examined via immunofluorescent confocal microscopy studying γ H2AX kinetics in more detail.

4.3.2.1. γ H2AX generation induced by 72 kJ/m² of UVA in bystander cells

An irradiation dose of 72 kJ/m² of UVA irradiation for the donor cells was used before incubating them with the bystander cells for 24 and 48 hours and analysing them via IF confocal microscopy. Data shown in Figure 4.5 agreed with findings from Figure 4.2 showing a significant increase of total γ H2AX in the IR condition at 24-hours compared to UI and NT conditions and additionally at 48 hours compared to the NT condition. This strengthened the evidence for the generation of DNA damage in bystander cells, with a response occurring as early as 24 hours post-irradiation and lasting at least 48 hours (Figure 4.5). There were inconsistencies between the UI and NT conditions where 24 hours showed no significant difference in levels of γ H2AX intensity but did show a significant increase of UI compared to NT at 48 hours (Figure 4.5b).

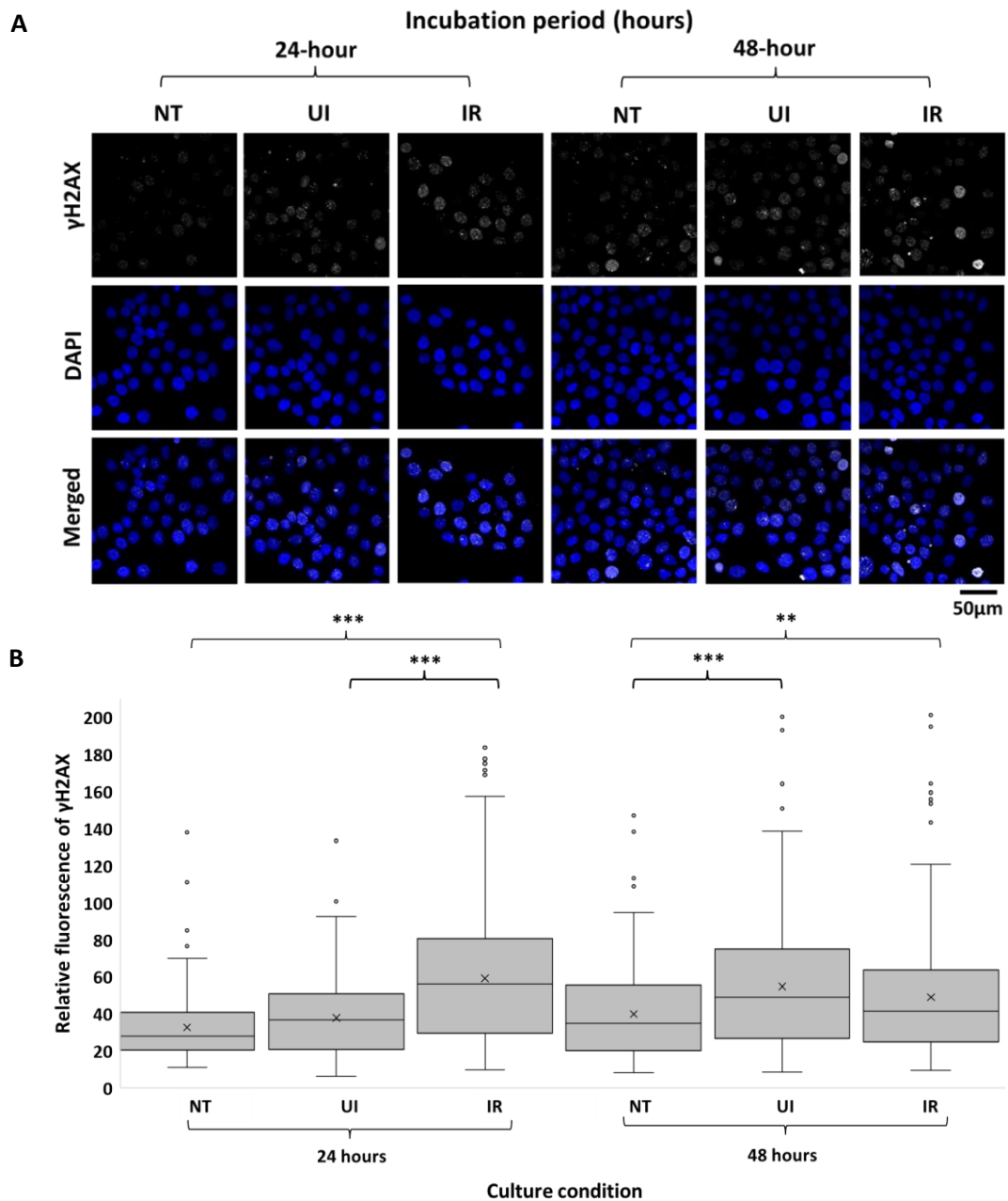


Figure 4.5: Activation of γ H2AX in bystander cells co-incubated with UVA irradiated cells at 72 kJ/m². HaCaT cells were co-incubated with directly irradiated cells using a transwell system at 72 kJ/m² of UVA. (A) Immunofluorescent images of γ H2AX activation. (B) Box and whisker plot displaying the spread of γ H2AX relative fluorescence where (**) $p < 0.01$ and (***) $p < 0.001$. Significance is a measure of irradiated bystander condition (IR) compared to the other conditions carried out by a one-way ANOVA. IR – bystander cells co-incubated with irradiated cells. UI – bystander cells co-incubated with unirradiated cells. NT – (No transwell) cells incubated alone. All samples were collected following 24 or 48 hours of co-incubation. At least one hundred nuclei were measured for each condition.

4.3.2.2. γ H2AX generation induced by 108 kJ/m² of UVA in bystander cells

The pre-incubation UVA dose for the donor cells was increased to 108 kJ/m² with sample collection occurring at 24- and 48-hours post-irradiation. IF quantitation is shown in Figure 4.6. With these conditions, statistically significant reductions of total γ H2AX were identified for the IR condition compared to NT at both 24- and 48- hours and compared to the UI condition at 48 hours (Figure 4.6b) in which minimal staining was observed for the IR condition whilst intense staining occurred in the NT condition (Figure 4.6a). This contradicted findings from Figure 4.3a where a bystander effect was observed at 48 hours in the IR condition compared to UI and NT. It also contradicts IF data presented in Figure 4.5 where a bystander effect was observed at both 24 and 48 hours represented by significant elevations of the IR condition compared to the UI and NT conditions. This conflicting data questioned the activation of total γ H2AX in the UVA bystander effect. Furthermore, there were significant reductions of UI compared NT samples between the 24- and 48- hour conditions (Figure 4.6). The direction of this effect is the reverse of what is observed in Figure 4.5b in which UI is elevated compared to NT. This questions the reliability of the effect observed since the incubation conditions are identical.

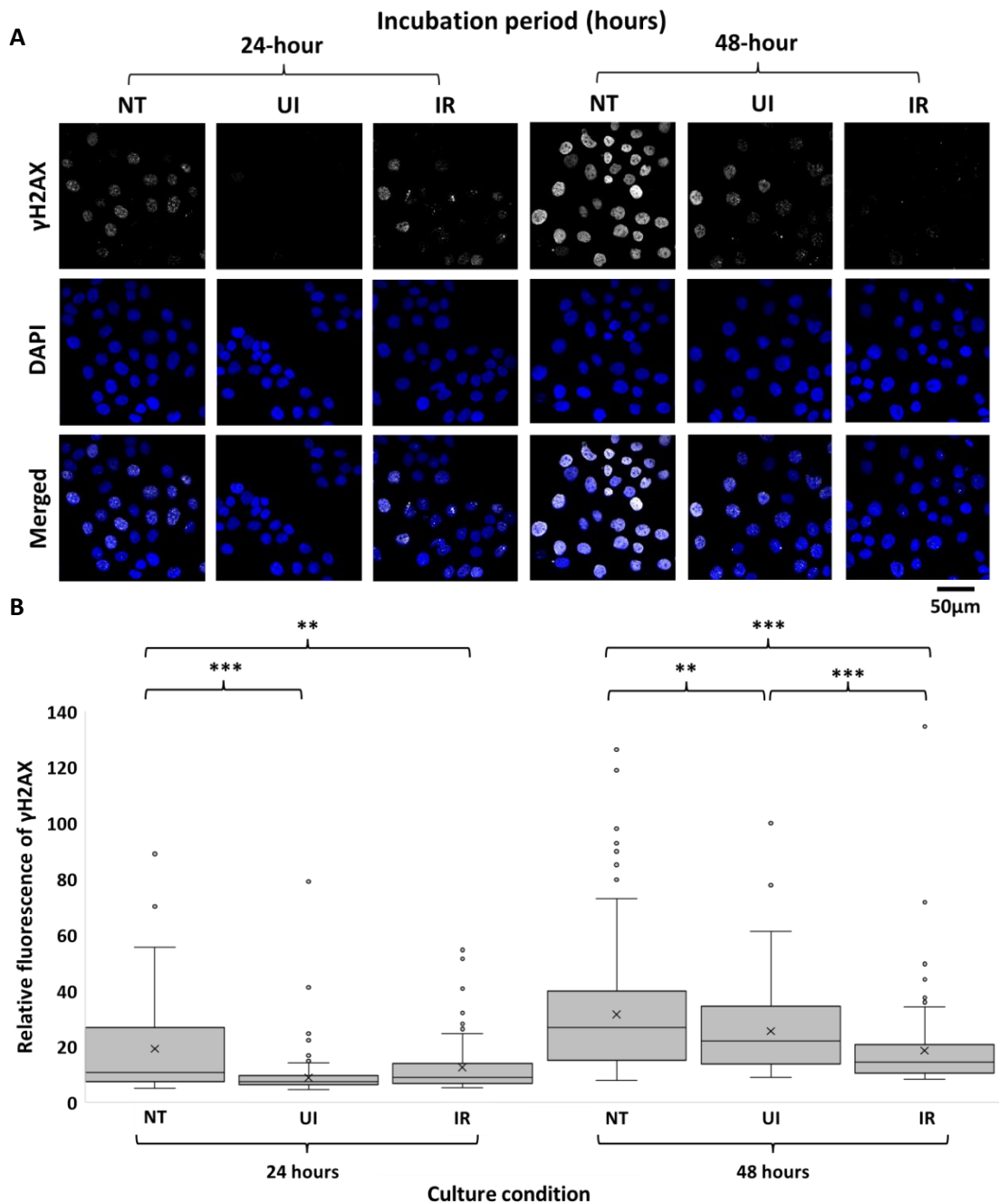


Figure 4.6: Activation of γ H2AX in bystander cells co-incubated with UVA irradiated cells at 108 kJ/m². HaCaT cells were co-incubated with directly irradiated cells using a transwell system at 108 kJ/m² of UVA. (A) Immunofluorescent images of γ H2AX activation. (B) Box and whisker plot displaying the spread of relative fluorescence of γ H2AX where (**) $p < 0.01$ and (***) $p < 0.001$. Significance was measured against the NT sample carried out by a one-way ANOVA. IR – bystander cells co-incubated with irradiated cells. UI – bystander cells co-incubated with unirradiated cells. NT – (No transwell) cells incubated alone. All samples were collected following 24 or 48 hours of co-incubation. At least one hundred nuclei were measured for each condition.

4.3.2.3. γ H2AX generation induced by 144 kJ/m² of UVA

A further increase of UVA dose for the donor cells to 144 kJ/m² led to no significant effect between any condition at 48 hours for total γ H2AX contrary to data in Figure 4.4-4.6. However, a significant decrease of IR compared to NT and UI was observed at 24 hours (Figure 4.7). Significant reductions of total γ H2AX in UI compared to NT was observed at 24 hours (Figure 4.7) similar to what is observed in Figure 4.6 but not at 48 hours. These additional discrepancies further question the reliability of the differences observed between the UI and NT conditions. With many differences in total γ H2AX changes, it was difficult to conclude if DNA damage was generated or if total γ H2AX was upregulated.

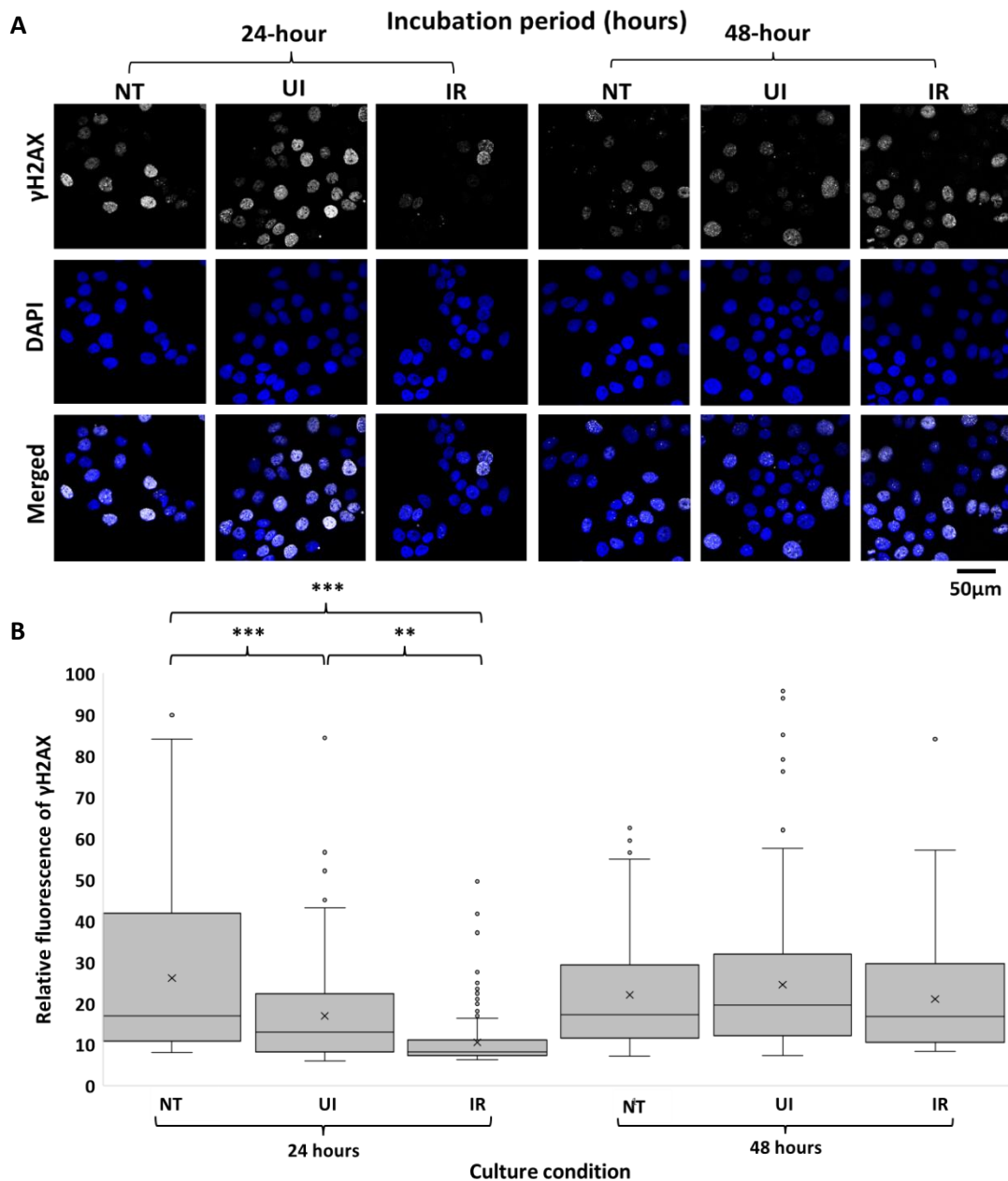


Figure 4.7: Activation of γ H2AX in bystander cells co-incubated with UVA irradiated cells at 144 kJ/m². HaCaT cells were co-incubated with directly irradiated cells using a transwell system at 144 kJ/m² of UVA. (A) Immunofluorescent images of γ H2AX activation. (B) Box and whisker plot displaying the spread of relative fluorescence of γ H2AX where (**) $p < 0.01$ and (***) $p < 0.001$. Significance is a measure of irradiated bystander condition (IR) compared to each UI or NT samples carried out by a one-way ANOVA. IR – bystander cells co-incubated with irradiated cells. UI – bystander cells co-incubated with unirradiated cells. NT – (No transwell) cells incubated alone. All samples were collected following 24 or 48 hours of co-incubation. At least one hundred nuclei were measured for each condition.

4.3.3. Comparison across all doses

Regardless of irradiation dose, findings were inconsistent for all markers of the DDR, demonstrating elevations in UVA bystander cells in some cases and no differences in others. Unexpected increases in protein activation of UI and NT compared to the IR condition and also significant elevations and reductions between the UI and NT conditions were inconsistent. Unfortunately, due to time, further repeats could not be completed so anomalies could not be identified.

4.3.4. Anomalies in γ H2AX activation

During the research discussed in this chapter and the preceding chapter, there were issues with consistency regarding γ H2AX probing in both Western blot and IF analysis. In Western blots, γ H2AX is found at 15 kDa whilst mono- and di- ubiquitinated γ H2AX (Ub- γ H2AX) occurs around the 25 kDa band on the protein ladder of Western blots. Initial blots (Figure 3.1a, 3.1b, 4.2c and 4.2d) showed high levels of activation of γ H2AX and very low levels of Ub- γ H2AX. However, upon further repeats this changed with a large increase in Ub- γ H2AX being detected and less γ H2AX (Figure 3.1d, 3.2, 3.3 and 4.2b) whilst some blots showed no γ H2AX at all (Figure 3.1c, 4.3b). Furthermore, positive control samples using zeocin and camptothecin no longer showed bands for γ H2AX or had low intensity (Figure 3.2 and 3.3 relative to Figure 3.1a and b).

Subsequent troubleshooting took place to identify if there was a problem testing all aspects of the experimental set up including reagents that had been changed between experiments. Media and serum had been replaced and tested against older samples that had previously been shown to generate a stronger γ H2AX response (samples taken from experiment Figure 3.1b), but results demonstrated no difference with Ub- γ H2AX still being highly abundant and no γ H2AX in some cases with both direct and bystander experiments (Figure 4.8 and 4.9). New cells were tested against samples from Figure 3.1d using positive and negative controls only which appeared to solve the problem initially (Figure 4.10), but the strong ubiquitinated γ H2AX returned upon subsequent experimentation with these cells. Antibodies were also tested to ensure they were not contaminated or had stopped working but no differences were observed.

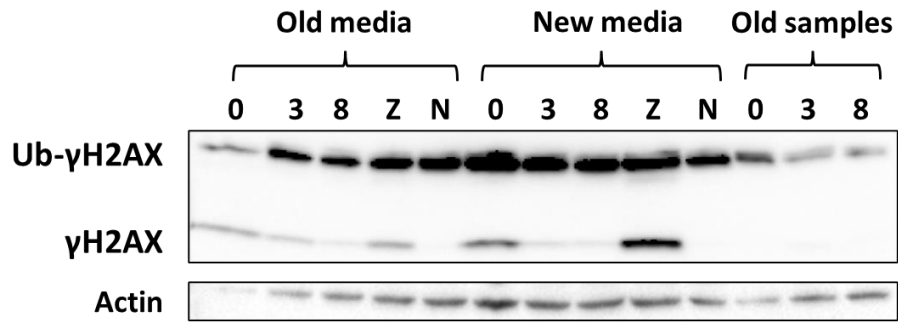


Figure 4.8: γ H2AX troubleshooting with 72 kJ/m² direct UVA irradiation. HaCaT cells were directly irradiated with 72 kJ/m² and samples were collected at either 0, 3 or 8 hours. Positive control (Z) was incubated with zeocin for 1 hour and the negative control (N) was incubated alone for 1 hour. Experiment was repeated with old and new media for troubleshooting purposes. 'Old samples' are samples re-run from Figure 3.1b.

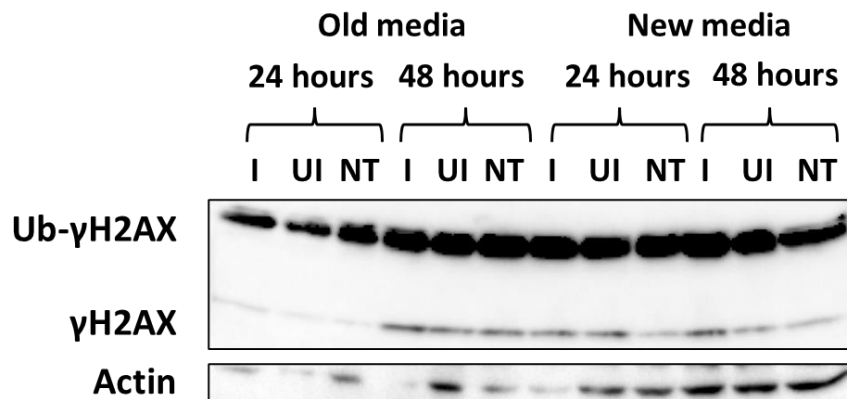


Figure 4.9: γ H2AX troubleshooting with 72 kJ/m² UVA irradiation in bystander cells HaCaT cells were directly irradiated and then co-incubated for either 24 or 48 hours with bystander cells which were then collected. IR – bystander cells incubated with UVA irradiated cells. UI – bystander cells co-incubated with unirradiated cells. NT – cells not irradiated or co-incubated with other cells. Experiment was repeated with old and new media for troubleshooting purposes.

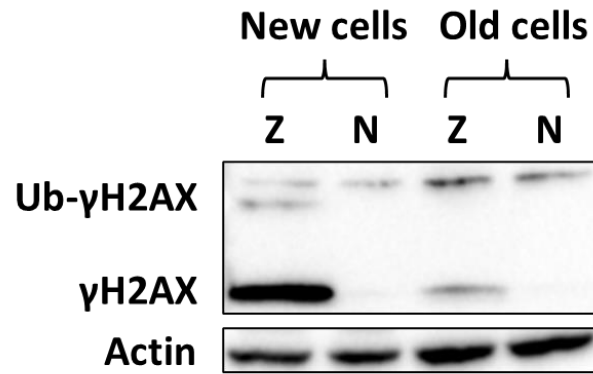


Figure 4.10: γ H2AX troubleshooting with new cells. HaCaT cells were incubated with zeocin (Z) and the negative control (N) was incubated alone for 1 hour. New cells were freshly revived cells whilst old cells refers to samples from Figure 3.1d which were re-run.

4.4. Discussion

The bystander effect is the toxic effect of damaging agents such as UV radiation in which directly irradiated donor cells become damaged and release factors which indirectly induce cellular stress and DNA damage in the surrounding healthy bystander cells (Nishiura et al, 2012; Whiteside et al, 2011; Widel, 2012). It was initially identified as a result of ionising radiation (Nagasawa and Little, 1992) but has now been found to occur as a result of UV irradiation (Widel et al, 2014). Due to its toxic effects, it has implications in cancer as it has been found to induce DNA damage which has the potential to cause mutations (Widel et al, 2012). UVA induces its damage via oxidative stress (Cortat et al, 2013) in which the ROS generated are believed to be bystander factors transmitted to neighbouring cells inducing oxidative stress and DNA damage (Burdak-Rothkamm et al, 2007; Little et al, 2002; Steel, 2016; Widel et al, 2014). This effect is believed to be present in cells for up to three days creating large potential for mutations to occur (Whiteside et al, 2011). Furthermore, melanocytes are very vulnerable to this effect with keratinocytes being the most effective donors (Redmond et al, 2014). Since a single melanocyte is in contact with 9-36 keratinocytes (D’Orazio et al, 2013; Nishiura et al, 2012), and the bystander effect can persist for a few days (Whiteside et al, 2011), it highlights the importance of studying the effect to better understand the causes of skin cancer.

A lot of research is still required to fully understand the bystander effect, in particular for UVA. Some previous work has looked at the damage caused whilst others have tried to determine the mechanism for causing it, but less research has gone into studying the cellular response. γ H2AX foci generation has been used as an end point and p-Chk1 (Ser345) has also been studied (Lin et al, 2017; Steel, 2016), but to my knowledge no-one has completed a more comprehensive review of the DDR in response to the UVA-induced bystander effect. Therefore, the aim was to if DDR proteins are activated and when. This would lead to a better understanding of how long it takes the cells to respond and how long the response lasts for giving an indication of DNA damage persistence.

4.4.1. Dose dependent changes in protein activation

Chk2 showed differences in activation between the lower dose of 72 kJ/m² and the two higher doses of 108 and 144 kJ/m². At 72 kJ/m², p-Chk2 became elevated at 24 hours but reduced at 48 hours below the level of both UI and NT conditions. Meanwhile, no observable difference was identified at 24 hours of incubation at either of the remaining doses. It was elevated however, at 48 hours for 144 kJ/m² and for one repeat at 108 kJ/m². However, the reliability of the data at 108 and 144 kJ/m² was low. Of the two repeats carried out for 108 kJ/m², only one showed Chk2 phosphorylation at 48 hours meaning the results were not reproducible. Meanwhile, neither of the doses had an actin control and therefore it could not be confirmed if the elevations observed were due to increased activation within cells.

For γ H2AX, there also appeared to be a change in activation similar to that of p-Chk2 in which different results were obtained for 72 kJ/m² compared to the other doses. At 72 kJ/m², γ H2AX was elevated at 24 hours in the irradiated bystander condition compared to the UI and NT conditions for two repeats, however a third did demonstrate activation at 48 hours but that blot was of low quality and difficult to interpret. These Western blot data were supported by significant increases in total γ H2AX in the IR condition compared to UI and NT at 24 hours post irradiation. However, at 108 and 144 kJ/m², γ H2AX did not appear to become elevated until 48 hours post irradiation.

In combination with the changes observed for p-Chk2, this implied that 108 and 144 kJ/m² of UVA irradiation led to a later activation of the ATM pathway possibly due to later DNA damage generation such as DSBs or higher levels of other types of damage occurring such as SSBs as has been previously shown that higher levels of SSBs compared to DSBs leads to prioritisation of SSB repair (Ma and Dai, 2018). This would delay the repair of DSBs and could mean that the response takes longer to accumulate.

4.4.2. γ H2AX is possibly activated via ATM and prior to ATR activation

Focussing on the 72 kJ/m² condition (Figure 4.2), it indicated that the ATR pathway was activated later than the ATM pathway. At 24 hours post irradiation, both γ H2AX and p-Chk2 were elevated in the IR condition compared to the UI and NT conditions and returned to normal levels 48 hours later. p-Chk1 on the other hand did not become

elevated until 48 hours post irradiation. Considering p-Chk2 is part of the ATM pathway whilst p-Chk1 is activated by the ATR response, this would imply that the ATM pathway was activated prior to the ATR pathway and that γ H2AX is activated by the ATM response. This may be related to the type of damage being induced. For example, in previous research modelling DSB and SSB repair, the response depended on which type of damage was in higher abundance and one would be preferentially repaired over the other (Ma and Dai, 2018). Using this principle, this could explain why the ATM pathway is activated earlier than the ATR pathway if a certain type of damage, such as DSBs, is in higher abundance and could be prioritised for repair. However, this was only a mathematical model studying only two types of DNA damage (Ma and Dai, 2018) and both ATM and ATR pathways have the ability to respond to a variety of types of damage (Maréchal and Zou, 2013; Zhao et al, 2011). It could also be possible that multiple types of DNA damage are occurring at different times. There may be an immediate generation of one type of damage, such as DSBs, and a later occurrence of other DNA damage types, such as replication stress. This could cause the ATM and ATR pathways to activate one after the other.

Previous work by Burdak-Rothkamm et al, (2007) demonstrated that γ H2AX foci generation was a result of the ATR pathway and independent of ATM. It has been proposed that the likely source of DSB generation in UVA bystander cells results from replication stress since its S phase cells that are affected and p-Chk1 (Ser345) elevations coincide with γ H2AX foci in bystander cells (Steel, 2016). It would therefore be expected during this research that γ H2AX would follow the activation of p-Chk1 however, the opposite was observed with γ H2AX becoming upregulated prior to the phosphorylation of Chk1 and in line or following the activation of Chk2. This would imply that γ H2AX generation was a result of the ATM pathway rather than the ATR pathway and independent of DNA replication. These differences could be attributed to the different sources of irradiation being used. Whilst my research used UVA, Burdak-Rothkamm et al, (2007) used microbeam irradiation (Burdak-Rothkamm et al, 2007). Additionally, whilst my research suggested ATM activation was responsible for γ H2AX foci generation, Steel (2016) showed that neither ATM nor ATR are exclusively responsible for its

induction (Steel, 2016). Therefore, more research is required to fully understand the kinetics of γ H2AX foci formation and its cause.

Unfortunately, p-Chk1 could not be measured at 144 kJ/m² and the p-Chk1 blot for 108 kJ/m² showed an unusual effect of elevated UI and NT conditions compared the irradiated bystander condition at 48 hours whilst no bystander effect of the IR sample compared to either the UI or NT conditions was observed at 24 hours. With no actin control available, no conclusions could be drawn from this data meaning the observed effect seen at 72 kJ/m² could not be tested at other doses.

4.4.3. Bystander effect observed at 24 hours post irradiation

Previous studies have identified that a minimum of 24 hours of exposure is required for the UVA induced bystander effect to be induced but has been suggested that the response was not visible until 48 hours (Whiteside et al, 2011). However, this study found elevations of various DDR proteins at 24 hours post incubation with irradiated cells implying that DNA damage had already been created before this timepoint in order for the pathway to be activated. Furthermore, using neonatal human dermal fibroblasts, a significant increase in intracellular ROS levels was found from as early as 3 hours post irradiation in UVA bystander cells (Widel et al, 2014) implying that the bystander effect may be observed earlier than expected. Whiteside et al, (2011) may not have seen an effect until 48 hours because they used cell survival as an end point. It may have required a build-up of DNA damage and activation of the DDR before cell survival would be reduced. Furthermore, my research demonstrated that although the DDR was activated at 24 hours, it was not always active at 48 hours unlike Whiteside et al (2011). Again, this may be due to the use of cell survival being used as an end point. Some cells may have repaired their damage or induced apoptosis and so downregulation of the DDR would be seen at 48 hours whilst cell survival would reduce.

4.4.4. Unexpected γ H2AX findings

Some unexpected findings were observed for γ H2AX especially for the immunofluorescent data in. When looking at 108 kJ/m² and 144 kJ/m², the IF data does not line up with the Western blot data. At 48 hours at 108 kJ/m², Western blot data showed no difference in Ub- γ H2AX and an elevated IR condition for γ H2AX meanwhile

the IF data showed a significant reduction in total γ H2AX of the IR condition compared to the UI and NT conditions. In addition, at 144 kJ/m² similar results were observed at 24 hours with the Western blot data showing no difference for either γ H2AX or Ub- γ H2AX but IF data implied that the total γ H2AX in the irradiated bystander condition was significantly lower than in both UI and NT conditions. It can be expected that the Western blot data would be different from the IF data as the Western blots show the Ub- γ H2AX and γ H2AX separately whilst the IF cannot distinguish between them so combined it may show a different pattern. However, in the situations explained above, the reverse was seen. Unfortunately, time restrictions meant the experiments could not be troubleshooted or repeated.

As demonstrated in section 4.3.4, other problems arose regarding γ H2AX and Ub- γ H2AX for both direct and indirect irradiations. Literature research has provided some possible explanations. Whilst testing a variety of DSB inducers, it was identified that 80-90% of protein is monoubiquitinated γ H2AX on average, but this depended on the cell type and DSB inducer. Ethanol was found to be an important factor with ethanol-based transfer buffers – as was used in this research – leading to increased binding of monoubiquitinated γ H2AX. Whilst all cell lines identified at least a 1.4 times higher generation of Ub- γ H2AX compared to γ H2AX, this was more pronounced for keratinocytes. Finally, camptothecin was found to mainly lead to monoubiquitinated γ H2AX which was demonstrated in many blots in this research where γ H2AX production in response to this reagent was absent or very low whilst Ub- γ H2AX was pronounced (Luczak and Zhitkovich, 2018). Since this research used an ethanol-based transfer buffer and keratinocytes, it provided some explanation for the higher Ub- γ H2AX that was found in these blots, but these conditions were constant across all repeats and so does not explain why this change occurred or why γ H2AX was initially in higher abundance than Ub- γ H2AX.

4.4.5. Future research

This research provided some new insights into the UVA induced bystander effect, but it also highlighted areas which require further work. Previous research has demonstrated evidence of the bystander effect at 48 hours lasting at least 72 hours (Whiteside et al, 2011) however, this research identified activation of some DDR proteins at just 24 hours

post incubation. More research should be carried out at earlier and later timepoints to study this further enabling better characterisation of DNA damage induction and repair. Future research should also focus on dose dependent studies since differences in DDR protein activation were identified in this research. This would help to highlight risk levels in different climates. Furthermore, it is not fully understood the mechanism in which DNA damage is being generated. Data presented here would imply that γ H2AX induction occurs via ATM, but this is contradicted by previous research (Steel, 2016). Further investigation into this may explain the activation of the ATM response prior to the ATR pathway. Early activation of the ATM response may imply different mechanisms of DNA damage induction between direct and indirect irradiation and requires further investigation.

In other areas, the mechanism which causes the bystander effect is still not understood. More research is required into determining what the bystander factors are and their role in inducing these bystander effects. Finally, most research is in keratinocytes or fibroblasts. However, a previous study identified that melanocytes are the most vulnerable to the bystander effect, so studies need to focus on the level of damage occurring to better understand its implications in inducing melanoma.

Chapter 5: General discussion

5.1. Introduction

Skin cancer is accountable for a third of cancer diagnoses with an increasing incidence every year. NMSC is the most prevalent with over one million new diagnoses per year compared to 290,000 for CMM. However, it is the latter which is responsible for 48% of skin cancer related deaths whilst NMSC generally has a good long-term prognosis (Bray et al, 2018; Ferlay et al, 2019). Whilst factors such as skin pigmentation influence your risk of developing cancer (Gandini et al, 2005iii; Khalesi et al, 2013), UV is responsible for 85% of NMSC and 90% of CMM resulting from solar irradiation or tanning beds (An et al, 2021). Whilst CMM is mostly associated with short-term, high intensity UV exposure such as sun burns, NMSC is linked more to long-term, low intensity exposure such as in individuals who work outdoors (Clough-Gorr et al, 2017; Khazaei et al, 2019; Seraji et al, 2020; Zhang et al, 2012). This also makes it one of the most preventable types of cancer as simply protecting your skin and avoiding tanning beds reduces a person's risk (Khazaei et al, 2019; Költő et al, 2021).

With this in mind, it is becoming increasingly important to understand the basis of skin cancer induction and the cellular response. A vast amount of research has gone into skin cancer over the years determining the mechanism by which UV causes DNA damage and mutations whilst others have looked at the activation of the DNA damage response. The damage induced in UVA irradiated cells is oxidative, demonstrated in a wide variety of experiments using antioxidants to observe changes in DNA damage following irradiation (Greinert et al, 2012; Sander et al, 2003; Steel, 2016; Yagura et al, 2017). The ROS generated induce a wide variety of damage including SSBs and oxidised bases, but pyrimidine dimers can also be induced by UVA – the latter causing C>T or CC>TT transversion mutations characteristic of UV damage (Cadet and Douki, 2011; Chatterjee and Walker, 2017; Douki et al, 2017; Girard et al, 2008; Greinert et al, 2012; Kim et al, 2013; Montaner et al, 2007; Singh et al, 2018; Wischermann et al, 2008; Yagura et al, 2017). These can all have an impact on DNA replication, leading to further DNA damage such as DSB generation and activate the DDR (Chatterjee and Walker, 2017; Cortat et al, 2013; Cannan and Pederson, 2016; Zhao et al, 2011). More recently, studies have investigated the bystander effect to explore other mechanisms of cancer induction. The damage generated in irradiated cells causes the release of factors such as ROS to induce

damage in the surrounding environment for at least 3 days post-irradiation (Nishiura et al, 2012; Whiteside et al, 2011; Widel, 2012). With the penetrative abilities of UVA, the damaging effects could be more widespread than anticipated with different cell types deep in the skin able to transmit and receive this bystander effect (Redmond et al, 2014).

The aims of this research were to provide more details about the DDR in both directly irradiated cells and bystander cells to develop our understanding of the cellular response to UVA induced DNA damage, particularly in bystander cells in which there are fewer details available. Studies have looked at components of the DDR in relation to UV irradiation at various doses usually looking at a few timepoints. However, this research has focussed on creating a more comprehensive review looking at multiple proteins at various timepoints to create a more detailed image of protein activation and downregulation giving indications of DNA damage persistence.

5.2. Characterising the DDR in directly UVA irradiated cells

Chapter 3 focussed on investigating the activation of the DDR in directly irradiated cells between different UVA doses. Findings here conflict some previous studies and provide new insights into dose dependent differences in the DDR.

Previous research has debated the induction of DSBs due to UVA irradiation in a replication independent manner. However, here it was shown that significant increases in γ H2AX more closely follow the downregulation of p-Chk2 compared to p-Chk1 (Ser317 and Ser345) with γ H2AX becoming activated before p-Chk1 in some cases. This would indicate that γ H2AX was becoming activated by ATM rather than the ATR response implying the damage was a marker of direct DSB generation rather than replication stress. However, without cell cycle stage analysis and more specific markers of DSB generation such as 53BP1, it is difficult to confirm the presence of DSBs and if they were independent of S-phase and research has demonstrated it is more likely that γ H2AX activation is in relation to ATR activation and oxidative damage (Moreno et al, 2019).

Another important finding was the time taken for repair to take place and how long damage generation was occurring for. The higher the dose, the longer it took before the IQR for total γ H2AX increased. This wide range in activation implied that some cells had repaired their DNA damage and were downregulating the DDR. This suggested that

larger doses induced more DNA damage and therefore took longer to fully repair their cells. Furthermore, these increases in IQR coincided with peak γ H2AX activation or IQR continued to increase beyond this suggesting that DNA damage was still occurring even at later timepoints of 8-24 hours. This is backed up by the sustained significant increase in total γ H2AX at 24 hours post irradiation marking the late generation of DNA damage possibly due to an accumulation of oxidative damage leading to DSBs and their repair or dark CPD generation which could also induce DSBs via replication stress. This disagrees with previous research which has shown early generation and downregulation of γ H2AX (Steel, 2016) whilst the research presented here implied later activation indicating late generation of DNA damage or a prolonged persistence. However, it was identified that oxidative damage can peak twice at 4 hours and 24 hours at 120 kJ/m² (Cortat et al, 2013) which would explain the presence of RPA and γ H2AX at later timepoints indicating the presence of late DNA damage generation. This is concerning as S phase arrest and DNA replication inhibition is quickly recovered after 90 minutes following irradiation (Rünger et al, 2012) meaning damage could still be produced after the cell cycle continues providing more opportunity for mutations to arise.

The data here implied that Chk1 and Chk2 are activated via phosphorylation within 1 hour of irradiation often showing activation immediately post-irradiation. RPA and γ H2AX were identified as p-Chk1 and p-Chk2 began to reduce as expected indicating the presence of DSBs and oxidative damage and the initiation of their repair. Their sustained activation to the 24-hour mark was also indicative of late DNA damage generation from sustained oxidative damage and dark CPDs. Chk2 was often phosphorylated earlier which implied there was a possibility that some types of damage were occurring earlier and activating the different response pathways at different times. Some DDR proteins were still activated at the latest timepoint of 24 hours which implied the presence of DNA damage for at least this period of time and future research should focus on studying later timepoints to identify the time in which the response becomes downregulated, and protein activation returns to resting levels.

5.3. DDR activation in the UVA-induced bystander effect

Previous research has identified the need for 24 hours of incubation for bystander responses to be observed which were not seen until 48 hours (Whiteside et al, 2011), but this study along with the data from Widel et al, 2014, provided indications that bystander effects could be induced earlier than believed as DDR proteins were activated at the earlier timepoint of 24 hours and increases in intracellular ROS levels have been observed (Widel et al, 2014). However, amongst the three pieces of research, varying doses, cell types and end points were used which could explain the differences. This has prompted the need for more research into the timings of induction of the bystander effect.

The activation of γ H2AX has previously been confirmed (Steel, 2016) but the pathway and cause responsible for its upregulation is still disputed. Whilst a prior study demonstrated γ H2AX foci in S phase cells along with p-Chk1 (Ser345) implying it was stalled replication forks that were responsible for its activation (Steel, 2016), this study demonstrated the presence of γ H2AX before p-Chk1 (Ser317 and Ser345) activation and occurring alongside p-Chk2 which suggested it was the presence of replication independent DSBs or other types of DNA damage that was causing its activation. The exact cause of γ H2AX induction remains unclear and requires further investigation.

5.4. Dose dependent changes in direct and indirectly irradiated cells

Across both the direct and indirect irradiation, a common result was found. The DDR response to 72 kJ/m² of UVA irradiation was usually different to that of the higher doses at 108 kJ/m² and 144 kJ/m². When cells were directly exposed to UVA irradiation at 72 kJ/m², the ATR response – represented by Chk1 activation – appeared to be more intense in relation to the positive controls but changed to a lower and more gradual increase at 108-144 kJ/m². Conversely, p-Chk2 displayed a lower intensity compared to the positive controls at 72 kJ/m² which increased at higher doses. Meanwhile, for bystander cells, p-Chk2 and γ H2AX activation initially occurred following 24 hours at 72 kJ/m² which changed to 48 hours at 108 and 144 kJ/m². The consistent finding of protein activation changes between 72 kJ/m² and 108-144 kJ/m² implied a dose dependent change in DNA damage and the repair mechanism. This could partly be explained by

previous research modelling the activation of the DDR in a system involving SSBs and DSBs whereby different levels of these damage types induced a different response based on a cells apoptotic threshold (Ma and Dai, 2018). The higher doses could create more damage of a certain type switching the cells response.

This could have implications in cancer as people whose jobs are outdoors, spend time on tanning beds or live closer to the equator will experience higher doses of UVA irradiation and may experience different levels of DNA damage which could lead to cancer. Therefore, more research in this field investigating dose dependent changes in DNA damage and repair are required to better understand the causes of skin cancer.

5.5. Final conclusions

This research aimed to investigate the kinetics of the DDR in directly and indirectly UVA irradiated cells. It identified variations in kinetics between different doses of irradiation, such as changes in protein activation patterns, which requires further investigation to fully understand DNA damage and activation of its repair. This research has provided further evidence to question the induction of potential DSBs from both direct and indirect UVA irradiation. They are usually associated with replication stress however, based on the timings of activation of γ H2AX compared to p-Chk1 and p-Chk2, it indicated that DSB generation could be replication independent. Cell cycle stage analysis is required alongside biomarkers of DSBs such as 53BP1 to better understand if DSBs are being generated and how, possibly using DNA combing to study the replication forks in more detail. A broader range of timepoints is required for future research. Significant elevations of total γ H2AX were still identified at 24 hours post irradiation along with the presence of RPA in the direct condition but their downregulation must also be studied to fully understand the kinetics of the DDR. Meanwhile, timepoints earlier than 24 hours and later than 48 hours are needed for investigating the bystander effect to better characterise when the damage is induced and how long it persists for. Research into the bystander effect should focus more on melanocytes due to their increased vulnerability compared to other skin cell types and the mechanism of communication between the irradiated and bystander cells.

| Summary of main findings | |
|--|---|
| Main results | Discussion |
| Direct UVA induction of DSBs | γ H2AX upregulation followed the downregulation of p-Chk2 more closely than p-Chk1 indicating the induction of DSBs rather than replication stress as suggested in previous research. More specific biomarkers of DSB presence eg 53BP1 would be needed to confirm this. |
| Late presence of DNA damage from direct UVA irradiation | Increase in RPA and significant elevations of γ H2AX are present at 24-hours post irradiation marking the presence of DNA damage. This could either result from early damage that hasn't been repaired or the late generation of DNA damage potentially caused by clustered damaged. This late presence indicates a high mutagenic potential for UVA as previous research has demonstrated that DNA replication and cell cycle arrest returns to normal before 24-hours post irradiation. |
| | Future research should study DNA damage abundance eg oxidative stress or CPD and DSB levels, alongside activation of the DNA damage response to understand the cause of this late activation of DDR proteins. |
| Dose-dependent differences for direct and indirect UVA irradiation | 72 kJ/m ² demonstrated a change in DDR in the form of p-Chk1 and p-Chk2 compared to 108 and 144 kJ/m ² . Whilst p-Chk1 was dominant at a lower dose, vice versa was observed at the higher doses. This may be due to a change in damage type and abundance where the response would prioritise the repair of certain damage first. This was also indicated in the indirect UVA irradiations with regard to p-Chk2 and H2AX compared p-Chk1 however, inconsistent results mean more repeats are required before conclusions can be drawn in this area. |
| Indirect UVA induced H2AX | Findings here imply γ H2AX follows the activation of p-Chk2 and therefore the ATM pathway which suggests the generation of |

| | |
|--|--|
| <p>activation may result for DSBs</p> | <p>DSBs. However, previous research has demonstrated p-Chk1/ATR is responsible for γH2AX upregulation indicating replication stress to be the cause. More research is required to investigate the type of damage occurring in the bystander effect.</p> |
| <p>The bystander effect can be observed at 24 hours post irradiation</p> | <p>Findings here in combination with previous research raise questions as to when the bystander effect can occur. This research demonstrated an effect at 24-hours post irradiation whilst previous studies show bystander effects occurring as early as 3-hours and as late as 48-hours post irradiation. However, each piece of research uses a different cell type and end point explaining the inconsistencies. A more detailed analysis is required using a range of end points simultaneously to comprehensively study the kinetics of the bystander effect.</p> |

References

Akagawa, R., Trinh, H., Saha, L., Tsuda, M., Hirota, K., Yamada, S., Shibata, A., Kanemaki, M., Nakada, S., Takeda, S. and Sasanuma, H., (2020) 'UBC13-Mediated Ubiquitin Signaling Promotes Removal of Blocking Adducts from DNA Double-Strand Breaks', *iScience*, 23(4), p. 101027. doi: 10.1016/j.isci.2020.101027.

Ali, A. S., Gronberg, M., Federspiel, B., Scoazec, J., Hjortland, G., Gronbaek, H., Ladekari, M., Langer, S., Welin, S., Vestermark, L., Arola, J., Osterlund, P., Knigge, U., Sorbye, H., Grimelius, L. and Janson, E., (2017) 'Expression of p53 protein in high-grade gastroenteropancreatic neuroendocrine carcinoma', *PLoS ONE*, 12(11), pp. 1–15. doi: 10.1371/journal.pone.0187667.

An, S., Kim, K., Moon, S., Ko, K., Kim, I., Lee, J. and Park, S., (2021) 'Indoor tanning and the risk of overall and early-onset melanoma and non-melanoma skin cancer: Systematic review and meta-analysis', *Cancers*, 13(23). doi: 10.3390/cancers13235940.

Azzam, E., Toledo, S., Harris, A., Ivanov, V., Zhou, H., Amundson, S., Lieberman, H. and Hei, T., (2013) 'The ionising radiation-induced bystander effect: evidence, mechanism, and significance' , *Pathobiology of Cancer Regimen-Related Toxicities*, DOI: 10.1007/978-1-4614-5438-0_3

Balasubramanian, B., Pogozelski, W. K. and Tullius, T. D. (1998) 'DNA strand breaking by the hydroxyl radical is governed by the accessible surface areas of the hydrogen atoms of the DNA backbone', *Proceedings of the National Academy of Sciences of the United States of America*, 95(17), pp. 9738–9743. doi: 10.1073/pnas.95.17.9738.

Banerjee, G., Gupta, G., Kapoor, A. and Raman, G., (2005) 'UV induced bystander signalling leading to apoptosis', *Cancer Letters*, 223(2), pp. 275–284. doi: 10.1016/j.canlet.2004.09.035.

Berg, R. J. W., de Gruijl, F. R. and der Leun, J. C. va. (1993) 'Interaction between Ultraviolet A and Ultraviolet B Radiations in Skin Cancer Induction in Hairless Mice', *Cancer Research*, 53(18), pp. 4212–4217.

Bower, J. J., Vance, L. D., Psioda, M., Smith-Roe, S. L., Simpson, D. A., Ibrahim, J. G., Hoadley, K. A., Perou, C. M. and Kaufmann, W. K., (2017) 'Patterns of cell cycle

checkpoint deregulation associated with intrinsic molecular subtypes of human breast cancer cells', *npj Breast Cancer*, 3(1), pp. 1–9. doi: 10.1038/s41523-017-0009-7.

Bray, F. Ferlay, J., Soerjomataram, I., Siegel, R., Torre, L. and Jemal, A., (2018) 'Global cancer statistics 2018: GLOBOCAN estimates of incidence and mortality worldwide for 36 cancers in 185 countries', *CA: A Cancer Journal for Clinicians*, 68(6), pp. 394–424. doi: 10.3322/caac.21492.

Burdak-Rothkamm, S., Rothkamm, K. and Prise, K. M. (2008) 'ATM acts downstream of ATR in the DNA damage response signaling of bystander cells', *Cancer Research*, 68(17), pp. 7059–7065. doi: 10.1158/0008-5472.CAN-08-0545.

Burdak-Rothkamm, S., Short, S., Folkard, M., Rothkamm, K. and Prise, K., (2007) 'ATR-dependent radiation-induced γ H2AX foci in bystander primary human astrocytes and glioma cells', *Oncogene*, 26(7), pp. 993–1002. doi: 10.1038/sj.onc.1209863.

Cadet, J. and Douki, T., (2011) 'Oxidatively generated damage to DNA by UVA radiation in cells and human skin', *Journal of Investigative Dermatology*, 131(5), pp. 1005–1007. doi: 10.1038/jid.2011.51.

Cadet, J., Douki, T. and Ravanat, J. L. (2015) 'Oxidatively generated damage to cellular DNA by UVB and UVA radiation', *Photochemistry and Photobiology*, 91(1), pp. 140–155. doi: 10.1111/php.12368.

Cannan, W. and Pederson, D., (2016) 'Mechanisms and consequences of double-strand break formation in chromatin', *J Cell Physiol*, 231(1), pp. 3-14. doi:10.1002/jcp.25048

Chatterjee, N. and Walker, G., (2017) 'Mechanisms of DNA damage repair and mutagenesis', *Environmental and Molecular Mutagenesis*, 58, pp. 235-263. doi: 10.1002/em.22087.

Clough-Gorr, K., Titus-Ernstoff, L., Perry, A., Spencer, S. and Ernstoff, M., (2017) 'Exposure to sunlamps, tanning beds, and melanoma risk', *Physiology & behavior*, 176(1), pp. 139–148. doi: 10.1007/s10552-008-9129-6.Exposure.

- Cortat, B., Garcia, C. Quinet, A., Schuch, A., Lima-Bessa, K. and Menck, C., (2013) 'The relative roles of DNA damage induced by UVA irradiation in human cells', *Photochemical and Photobiological Sciences*, 12(8), pp. 1483–1495. doi: 10.1039/c3pp50023c.
- Courdavault, S., Baudouin, C., Charveron, M., Canguilhem, B., Favier, A., Cadet, J. and Douki, T., (2005) 'Repair of the three main types of bipyrimidine DNA photoproducts in human keratinocytes exposed to UVB and UVA radiations', *DNA Repair*, 4(7), pp. 836–844. doi: 10.1016/j.dnarep.2005.05.001.
- D'Orazio, J. Jarrett, S., Amaro-Ortiz, A and Scott, T., (2013). 'UV radiation and the skin', *International Journal of Molecular Sciences*, 14(6), pp. 12222–12248. doi: 10.3390/ijms140612222.
- Dahle, J., Angell-Peterson, E., Steen, H. and Moan, J., (2001) 'Bystander Effects in Cell Death Induced by Photodynamic Treatment, UVA Radiation and Inhibitors of ATP Synthesis', *Photochemistry and Photobiology*, 73(4), p. 378. doi: 10.1562/0031-8655(2001)073<0378:beicdi>2.0.co;2.
- Dickey, J. S. *et al.* (2009) 'H2AX: Functional roles and potential applications', *Chromosoma*, 118(6), pp. 683–692. doi: 10.1007/s00412-009-0234-4.
- Douki, T., von Koschembahr, A. and Cadet, J. (2017) 'Insight in DNA Repair of UV-induced Pyrimidine Dimers by Chromatographic Methods', *Photochemistry and Photobiology*, 93(1), pp. 207–215. doi: 10.1111/php.12685.
- Ferlay, J., Colombet, M., Soerjomataram, I., Mathers, C., Parkin, D., Piñeros, M., Znaor, A. and Bray, F., (2019) 'Estimating the global cancer incidence and mortality in 2018: GLOBOCAN sources and methods', *International Journal of Cancer*, 144(8), pp. 1941–1953. doi: 10.1002/ijc.31937.
- Gandini, S., Sera, F., Cattaruzza, M., Pasquini, P., Abeni, D., Boyle, P and Melchi, C., (2005i) 'Meta-analysis of risk factors for cutaneous melanoma : I . Common and atypical naevi', 41, pp. 28–44. doi: 10.1016/j.ejca.2004.10.015.
- Gandini, S., Sera, F., Cattaruzza, M., Pasquini, P., Zanetti, R., Masini C., Boyle, P. and Melchi, C., (2005ii) 'Meta-analysis of risk factors for cutaneous melanoma: III. Family

history, actinic damage and phenotypic factors', *European Journal of Cancer*, 41(14), pp. 2040–2059. doi: 10.1016/j.ejca.2005.03.034.

Gandini, S., Sera, F., Cattaruzza, M., Pasquini, P., Zanetti, R., Masini C., Boyle, P. and Melchi, C., (2005iii) 'Meta-analysis of risk factors for cutaneous melanoma: III. Family history, actinic damage and phenotypic factors', *European Journal of Cancer*, 41(14), pp. 2040–2059. doi: 10.1016/j.ejca.2005.03.034.

Ghosh, R. and Bhaumik, G. (1995) 'Supernatant medium from UV-irradiated cells influences the cytotoxicity and mutagenicity of V79 cells', *Mutation Research/Environmental Mutagenesis and Related Subjects*, 335(2), pp. 129–135. doi: 10.1016/0165-1161(95)00011-9.

Ghosh, R., Guha, D. and Bhowmik, S. (2012) 'UV released factors induce antioxidant defense in A375 cells', *Photochemistry and Photobiology*, 88(3), pp. 708–716. doi: 10.1111/j.1751-1097.2012.01105.x.

Ghosh, R., Guha, D., Bhowmik, S. and Karmakar, S., (2013) 'Antioxidant enzymes and the mechanism of the bystander effect induced by ultraviolet C irradiation of A375 human melanoma cells', *Mutation Research - Genetic Toxicology and Environmental Mutagenesis*, 757(1), pp. 83–90. doi: 10.1016/j.mrgentox.2013.06.022.

Girard, P. M., Pozzebon, M., Delacote, F., Douki, T., Smirnova, V., and Sage, E., (2008) 'Inhibition of S-phase progression triggered by UVA-induced ROS does not require a functional DNA damage checkpoint response in mammalian cells', *DNA Repair*, 7(9), pp. 1500–1516. doi: 10.1016/j.dnarep.2008.05.004.

Gnugnoli, M., Casari, E. and Longhese, M. P. (2021) 'The chromatin remodeler Chd1 supports MRX and Exo1 functions in resection of DNA double-strand breaks', *PLoS Genetics*, 17(9), pp. 1–20. doi: 10.1371/journal.pgen.1009807.

Gookin, S., Min, M., Phadke, H., Chung, M., Moser, J., Miller, I., Carter, D., Spencer, S. L., (2017) 'A map of protein dynamics during cell-cycle progression and cell-cycle exit', *PLoS Biology*, 15(9), pp. 1–25. doi: 10.1371/journal.pbio.2003268.

Graindorge, D., Martineau, S., Machon, C., Arnoux, P., Guitton, J., Francesconi, S., Frochot, C., Sage, E. and Girard, P., (2015) 'Singlet oxygen-mediated oxidation during

UVA radiation alters the dynamic of genomic DNA replication', *PLoS ONE*, 10(10), pp. 1–26. doi: 10.1371/journal.pone.0140645.

Greinert, R., Volker, B., Henning, S., Breitbart, E., Greulich, K., Cardoso, M. and Rapp, A., (2012) 'UVA-induced DNA double-strand breaks result from the repair of clustered oxidative DNA damages', *Nucleic Acids Research*, 40(20), pp. 10263–10273. doi: 10.1093/nar/gks824.

Hedglin, M. and Benkovic, S. J. (2017) 'Replication Protein A Prohibits Diffusion of the PCNA Sliding Clamp along Single-Stranded DNA', *Biochemistry*, 56(13), pp. 1824–1835. doi: 10.1021/acs.biochem.6b01213.

Hennessy, A., Oh, C., Diffey, B., Wakamatsu, K., Ito, S. and Rees, J., (2005) 'Eumelanin and pheomelanin concentrations in human epidermis before and after UVB irradiation', *Pigment Cell Research*, 18(3), pp. 220–223. doi: 10.1111/j.1600-0749.2005.00233.x.

Hirao, A., Cheung, A., Duncan, G., Girard, P., Elia, A., Wakeham, A., Okada, H., Sarkissian, T., Wong, J., Sakai, T., Stanchina, E., Bristow, R., Suda, T., Lowe, S., Jeggo, P., Elledge, S. and Mak, T., (2002) 'Chk2 Is a Tumor Suppressor That Regulates Apoptosis in both an Ataxia Telangiectasia Mutated (ATM)-Dependent and an ATM-Independent Manner', *Molecular and Cellular Biology*, 22(18), pp. 6521–6532. doi: 10.1128/mcb.22.18.6521-6532.2002.

Iannaccone, M. R., Wang, W., Stockwell, H., O'Rourke, K., Giuliano, A., Sondak, V., Messina, J., Roetzheim, R., Cherpelis, B., Fenske, N. and Rollison, D., (2012) 'Patterns and timing of sunlight exposure and risk of basal cell and squamous cell carcinomas of the skin - a case-control study', *BMC Cancer*, 12. doi: 10.1186/1471-2407-12-417.

Ikura, T., Tashiro, S., Kakino, A., Shima, H., Jacob, N., Amunugama, R., Yoder, K., Izumi, S., Kuraoka, I., Tanaka, K., Kimura, H., Ikura, M., Nishikubo, S., Ito, T., Muto, A., Miyagawa, K., Takeda, S., Fishel, R., Igarashi, K. and Kamiya, K., (2007) 'DNA Damage-Dependent Acetylation and Ubiquitination of H2AX Enhances Chromatin Dynamics', *Molecular and Cellular Biology*, 27(20), pp. 7028–7040. doi: 10.1128/mcb.00579-07.

Jaiswal, H. and Lindqvist, A., (2015) 'Bystander communication and cell cycle decisions after DNA damage', *Frontiers in Genetics*, 5, pp. 1–6. doi: 10.3389/fgene.2015.00063.

- Jiang, K., Pereira, E., Maxfield, M., Russell, B., Gouldelock, D. and Sanchez, Y., (2003) 'Regulation of Chk1 Includes Chromatin Association and 14-3-3 Binding following Phosphorylation on Ser-345', *Journal of Biological Chemistry*, 278(27), pp. 25207–25217. doi: 10.1074/jbc.M300070200.
- Kelfkens, G., De Gruijl, F. R. and Van Der Leun, J. C. (1991) 'Tumorigenesis by short-wave ultraviolet a: Papillomas versus squamous cell carcinomas', *Carcinogenesis*, 12(8), pp. 1377–1382. doi: 10.1093/carcin/12.8.1377.
- Khalesi, M., Whiteman, D., Tran, B., Kimlin, M., Olsen, C. and Neale, R., (2013) 'A meta-analysis of pigmentary characteristics, sun sensitivity, freckling and melanocytic nevi and risk of basal cell carcinoma of the skin', *Cancer Epidemiology*, 37(5), pp. 534–543. doi: 10.1016/j.canep.2013.05.008.
- Khazaei, Z., Ghorat, F., Adineh, H. and Sohrabivafa, M., (2019). 'Incidence and mortality of skin cancer by histological subtype and its relationship with the human development index (HDI)', *World Cancer Research Journal*, e1265
- Kim, S. I., Jin, S. G. and Pfeifer, G. P. (2013) 'Formation of cyclobutane pyrimidine dimers at dipyrimidines containing 5-hydroxymethylcytosine', *Photochemical and Photobiological Sciences*, 12(8), pp. 1409–1415. doi: 10.1039/c3pp50037c.
- Kimlin, M. G., Parisi, A. V., Sabburg, J. and Downs, N. J., (2002) 'Understanding the UVA environment at a sub-tropical site and its consequent impact on human UVA exposure', *Photochemical and Photobiological Sciences*, 1(7), pp. 478–482. doi: 10.1039/b200844k.
- Költő, A., Rodriguez, L., McAvoy, H. and Gabhainn, N., (2021) 'Sunburn, Sun Safety and Indoor Tanning Among Schoolchildren in Ireland', *International Journal of Public Health*, 66(May), pp. 1–10. doi: 10.3389/ijph.2021.1604045.
- Kricker, A., Armstrong, B., English, D. and Heenan, J., (1995), 'Does intermittent sun exposure cause basal cell carcinoma? A case-control study in Western Australia', *Int J Cancer*, 60(4), pp. 489-494. doi: 10.1002/ijc.2910600411.
- Krokan, H. E. and Bjoras, M. (2013) 'Chapter 06: Base Excision Repair', *Cold Spring Harb Perspect Biol.*, 5(4), p. a012583. doi: 10.1101/cshperspect.a012583

Krzywon, A., Widel, M., Fujarewicz, K., Skonieczna, M. and Rzeszowska-Wolny, J., (2018). Modulation by neighbouring cells of the responses and fate of melanoma cells irradiated with UVA. *Journal of Photochemistry and Photobiology*. Vol 178 pp505-511 DOI: <https://doi.org/10.1016/j.jphotobiol.2017.12.012>

Laikova, K., Oberemok, V., Krasnodubets, A., Gal'Chinsky, N., Useinov, R., Novikov, I., Temirova, Z., Gorlov, M., Shved, N., Kumeiko, V., Makalish, T., Bessalova, E., Fomochkina, I., Esin, A., Volkov, M. and Kubyshekin, A., (2019). 'Advances in the understanding of skin cancer: ultraviolet radiation, mutations, and antisense oligonucleotides as anticancer drugs' *Molecules*, 24, doi: 10.3390/molecules24081516

Latonen, L., Taya, Y. and Laiho, M. (2001) 'UV-radiation induces dose-dependent regulation of p53 response and modulates p53-HDM2 interaction in human fibroblasts', *Oncogene*, 20(46), pp. 6784–6793. doi: 10.1038/sj.onc.1204883.

Lehman, T. A., Lehman, T., Modali, R., Boukamp, P., Stanek, J., Bennett, W., Welsh, J., Metcalf, R., Stampfer, M., Fusenig, N., Rogan, E. and Harris, C., (1993) 'p53 Mutations in human immortalized epithelial cell lines', *Carcinogenesis*, 14(5), pp. 833-839

Lin, X., Wei, F., Major, P., Al-Nedawi, K., Saleh, H. and Tang, D., (2017) 'Microvesicles contribute to the bystander effect of DNA damage', *International Journal of Molecular Sciences*, 18(4), pp. 1–13. doi: 10.3390/ijms18040788.

Little, J. B., Azzam, E., Toledo, S. and Nagasawa, H., (2002) 'Bystander effects: Intercellular transmission of radiation damage signals', *Radiation Protection Dosimetry*, 99(1–4), pp. 159–162. doi: 10.1093/oxfordjournals.rpd.a006751.

Liu, R. M. and Desai, L. P. (2015) 'Reciprocal regulation of TGF- β and reactive oxygen species: A perverse cycle for fibrosis', *Redox Biology*, 6, pp. 565–577. doi: 10.1016/j.redox.2015.09.009.

Lu, L. X., Domingo-Sananes, M., Huzarska, M., Novak, B. and Gould, K., (2012) 'Multisite phosphoregulation of Cdc25 activity refines the mitotic entrance and exit switches', *Proceedings of the National Academy of Sciences of the United States of America*, 109(25), pp. 9899–9904. doi: 10.1073/pnas.1201366109.

- Luczak, M. and Zhitkovich, A., (2018) 'Monoubiquitinated γ -H2AX: abundant product and specific biomarker for non-apoptotic DNA double-strand breaks', *Toxicology and Applied Pharmacology*, 355, pp. 238-246. doi: 10.1016/j.taap.2018.07.007.
- Ma, A. and Dai, X. (2018) 'The relationship between DNA single-stranded damage response and double-stranded damage response', *Cell Cycle*, 17(1), pp. 73–79. doi: 10.1080/15384101.2017.1403681.
- Mah, L. J., El-Osta, A. and Karagiannis, T. C., (2010) ' γ H2AX: A sensitive molecular marker of DNA damage and repair', *Leukemia*, 24(4), pp. 679–686. doi: 10.1038/leu.2010.6.
- Maréchal, A. and Zou, L. (2013) 'DNA damage sensing by the ATM and ATR kinases', *Cold Spring Harbor Perspectives in Biology*, 5(9), pp. 1–17. doi: 10.1101/cshperspect.a012716.
- Maréchal, A. and Zou, L. (2015) 'RPA-coated single-stranded DNA as a platform for post-translational modifications in the DNA damage response', *Cell Research*, 25(1), pp. 9–23. doi: 10.1038/cr.2014.147.
- Martin, S. and Ouchi, T., (2008) 'Cellular commitment to reentry into the cell cycle after stalled DNA is determined by site specific phosphorylation of Chk1 and PTEN', *Mol Cancer Ther*, 7(8), pp. 2509-2516. doi: 10.1158/1535-7163.MCT-08-0199
- Mattiroli, F., Vissers, J., Dijk, W., Ikpa, P., Citterio, E., Vermeulen, W., Marteijn, J., Sixma, T., (2012) 'RNF168 ubiquitinates K13-15 on H2A/H2AX to drive DNA damage signaling', *Cell*, 150(6), pp. 1182–1195. doi: 10.1016/j.cell.2012.08.005.
- McKay, B. C., Chen, F., Perumalswami, C., Zhang, F. Ljungman, M., (2000) 'The tumor suppressor p53 can both stimulate and inhibit ultraviolet light-induced apoptosis', *Molecular Biology of the Cell*, 11(8), pp. 2543–2551. doi: 10.1091/mbc.11.8.2543.
- Montaner, B., O'Donovan, P., Reelfs, O., Perrett, C., Zhang, X., Xu, Y., Ren, X., Macpherson, P., Frith, D. and Karran, P., (2007) 'Reactive oxygen-mediated damage to a human DNA replication and repair protein', *EMBO Reports*, 8(11), pp. 1074–1079. doi: 10.1038/sj.embor.7401084.

- Moreno, N. C., Garcia, C., Rocha, C., Munford, V. and Menck, C., (2019) 'ATR/Chk1 Pathway is Activated by Oxidative Stress in Response to UVA Light in Human Xeroderma Pigmentosum Variant Cells', *Photochemistry and Photobiology*, 95(1), pp. 345–354. doi: 10.1111/php.13041.
- Moscariello, M., Wieloch, R., Kurosawa, A., Li, F., Adachi, N., Mladenov, E and Iliakis, G., (2015) 'Role for Artemis nuclease in the repair of radiation-induced DNA double strand breaks by alternative end joining', *DNA Repair*, 31, pp. 29–40. doi: 10.1016/j.dnarep.2015.04.004.
- Mouret, S., Baudouin, C., Charveron, M., Favier, A., Cadet, J. and Douki, T., (2006) 'Cyclobutane pyrimidine dimers are predominant DNA lesions in whole human skin exposed to UVA radiation', *Proceedings of the National Academy of Sciences of the United States of America*, 103(37), pp. 13765–13770. doi: 10.1073/pnas.0604213103.
- Nagasawa, H. and Little, J., (1992) 'Induction of sister chromatid exchanges by extremely low doses of alpha-particles', *Cancer Res*, 52(22), pp. 6394-6396.
- Nishiura, H., Kumagai, J., Kashino, G., Okada, T., Tano, K. and Watanabe, M., (2012) 'The bystander effect is a novel mechanism of UVA-induced melanogenesis', *Photochemistry and Photobiology*, 88(2), pp. 389–397. doi: 10.1111/j.1751-1097.2011.01046.x.
- Ou, Y., Chung, P., Sun, T. and Shieh, S., (2005) 'p53 C-Terminal Phosphorylation by CHK1 and CHK2 Participates in the Regulation of DNA-Damage-induced C-Terminal Acetylation', *Mol Biol Cell*, 16, pp. 1684–1695. doi: 10.1091/mbc.E04.
- Pan, M. R., Peng, G., Hung, W. and Lin, S., (2011) 'Monoubiquitination of H2AX protein regulates DNA damage response signaling', *Journal of Biological Chemistry*, 286(32), pp. 28599–28607. doi: 10.1074/jbc.M111.256297.
- Premi, S., Wallisch, S., Mano, C., Weiner, A., Bacchiocchi, A., Wakamatsu, K., Bechara, E., Halaban, R., Douki, T. and Brash, D., (2015) 'Chemical excitation of melanin derivatives induces DNA photoproducts long after UV exposure', *Science*, 347(6224), pp. 842–847. doi: 10.1126/science.1256022.

- Rastogi, R. P., Richa., Kumar, A., Tyagi, M. B. and Sinha, R. P., (2010) 'Molecular mechanisms of ultraviolet radiation-induced DNA damage and repair', *Journal of Nucleic Acids*, 2010. doi: 10.4061/2010/592980.
- Redmond, R. W., Rajaduri, A., Udayakumar, D., Sviderskaya, E. and Tsao, H., (2014) 'Melanocytes are selectively vulnerable to UVA-mediated bystander oxidative signaling', *Journal of Investigative Dermatology*, 134(4), pp. 1083–1090. doi: 10.1038/jid.2013.479.
- Rochette, P. J., Therrien, J., Drouin, R., Perdiz, D., Bastien, N., Drobetsky, E. and Sage, E., (2003) 'UVA-induced cyclobutane pyrimidine dimers form predominantly at thymine-thymine dipyrimidines and correlate with the mutation spectrum in rodent cells', *Nucleic Acids Research*, 31(11), pp. 2786–2794. doi: 10.1093/nar/gkg402.
- Rother, K., Kirschner, R., Sanger, K., Bohlig, L., Mossner, J. and Engeland, K., (2007) 'p53 downregulates expression of the G1/S cell cycle phosphatase Cdc25A', *Oncogene*, 26(13), pp. 1949–1953. doi: 10.1038/sj.onc.1209989.
- Rother, M. B., Pellegrino, S., Smith, R., Gatti, M., Meisenberg, C., Wiegant, W., Luijsterburg, M., Imhof, R., Downs, J., Vertegaal, A., Huet, S., Altmeyer, M. and Attikum, H., (2020) 'CHD7 and 53BP1 regulate distinct pathways for the re-ligation of DNA double-strand breaks', *Nature Communications*, 11(1). doi: 10.1038/s41467-020-19502-5.
- Rünger, T. M., Farahvash, B., Hatvani, Z., Rees, A., (2012) 'Comparison of DNA damage responses following equimutagenic doses of UVA and UVB: A less effective cell cycle arrest with UVA may render UVA-induced pyrimidine dimers more mutagenic than UVB-induced ones', *Photochemical and Photobiological Sciences*, 11(1), pp. 207–215. doi: 10.1039/c1pp05232b.
- Sander, C. S., Hamm, F., Elsner, P. and Thiele, J. J., (2003) 'Oxidative stress in malignant melanoma and non-melanoma skin cancer', *British Journal of Dermatology*, 148(5), pp. 913–922. doi: 10.1046/j.1365-2133.2003.05303.x.
- Schindelin, J., Arganda-Carreras, I., Frise, E., Kaynig, V., Longair, M., Pietzsch, T., ... Cardona, A. (2012). Fiji: an open-source platform for biological-image analysis. *Nature Methods*, 9(7), 676–682

Schuch, A. P. and Menck, C. F. M. (2010) 'The genotoxic effects of DNA lesions induced by artificial UV-radiation and sunlight', *Journal of Photochemistry and Photobiology B: Biology*, 99(3), pp. 111–116. doi: 10.1016/j.jphotobiol.2010.03.004.

Sekiguchi, M. and Matsushita, N. (2022) 'DNA Damage Response Regulation by Histone Ubiquitination', *International Journal of Molecular Sciences*, 23(15). doi: 10.3390/ijms23158187.

Seraji, M., Khazaei, Z., Momenabadi, V., Beiranvand, R., Naghibzadeh-Tahami, A., NejadSadeghi, E., Zahmatkeshan, M., Moayed, L. and Goodarzi, E., (2020) 'UV-Related Melanoma Cancer and Its Association with the Human Development Index (HDI): GLOBOCAN Sources and Methods', *Iranian Red Crescent Medical Journal*, 22(7), pp. 1–12. doi: 10.5812/ircmj.103605.

Shiotani, B., Nguyen H. D., Hakansson, P., Marechal, A., Tse, A., Tahara, H. and Zou, L., (2013) 'Two Distinct Modes of ATR Activation Orchestrated by Rad17 and Nbs1', *Cell Reports*, 3(5), pp. 1651–1662. doi: 10.1016/j.celrep.2013.04.018.

Singh, S., Singh, M. K. and Das, P. (2018) 'Visual detection of cyclobutane pyrimidine dimer DNA damage lesions by Hg²⁺ and carbon dots', *Analytica Chimica Acta*, 1016, pp. 49–58. doi: 10.1016/j.aca.2018.02.029.

Srinivas, U. S., Tan, B. W. Q., Vellayappan, B. A. and Jeyasekhran, A. D., (2019) 'ROS and the DNA damage response in cancer', *Redox Biology*, 25(December 2018), p. 101084. doi: 10.1016/j.redox.2018.101084.

Steel, H., (2016), 'Characterisation of the cellular response to ultraviolet radiation, with a particular focus on the DNA damage response', *Unpublished data*

Sterenberg, H. and Leun, J., (1990) 'Tumorigenesis by a long wavelength UV-A source', *Photochemistry and Photobiology*, 51(3), pp. 325-330. doi.org/10.1111/j.1751-1097.1990.tb01718.x

Sterenberg, H., Putte, S. and Leun, J., (1988) 'The dose-response relationship of tumorigenesis by ultraviolet radiation of 254nm' *Photochemistry and Photobiology*, 47(2), pp. 245-253. doi: 10.1111/j.1751-1097.1988.tb02722.x

- Ström, L., Lindroos, H., Shirahige, K. and Sjögren, C., (2004) 'Postreplicative recruitment of cohesin to double-strand breaks is required for DNA repair', *Molecular Cell*, 16(6), pp. 1003–1015. doi: 10.1016/j.molcel.2004.11.026.
- Trastoy, M. O., Defais, M. and Larminat, F. (2005) 'Resistance to the antibiotic Zeocin by stable expression of the *Sh ble* gene does not fully suppress Zeocin-induced DNA cleavage in human cells', *Mutagenesis*, 20(2), pp. 111–114. doi: 10.1093/mutage/gei016.
- Tsao, C. C., Geisen, C. and Abraham, R. T. (2004) 'Interaction between human MCM7 and Rad17 proteins is required for replication checkpoint signaling', *EMBO Journal*, 23(23), pp. 4660–4669. doi: 10.1038/sj.emboj.7600463.
- Valente, L. J., Tarangelo, A., Li, A., Naciri, M., Raj, N., Boutelle, A., Li, Y., Mello, S., Biegging-Rolett, K., DeBerardinis, R., Ye, J., Dixon, S. and Attardi, L., (2020) 'P53 Deficiency Triggers Dysregulation of Diverse Cellular Processes in Physiological Oxygen', *The Journal of cell biology*, 219(11). doi: 10.1083/jcb.201908212.
- Walmacq, C., Cheung, A, Kireeva, M., Lubkowska, L., Ye, C., Gotte, D., Strathern, J., Carell, T., Cramer, P. and Kashlev, M., (2013) 'and Its Role in Cellular Resistance to DNA Damage', *Molecular cell*, 46(1), pp. 18–29. doi: 10.1016/j.molcel.2012.02.006.Mechanism.
- Wang, X., Stanbirdge, E., Lao, X., Cai, Q., Fan, S. and Redpath, J., (2007) 'p53-Dependent Chk1 Phosphorylation Is Required for Maintenance of Prolonged G2 Arrest', *Radiation Research Society*, 168(6), pp. 706–715.
- Ward, I. M. and Chen, J. (2001) 'Histone H2AX Is Phosphorylated in an ATR-dependent Manner in Response to Replicational Stress', *Journal of Biological Chemistry*, 276(51), pp. 47759–47762. doi: 10.1074/jbc.C100569200.Article
- Waters, L. S., Minesinger, B., Wiltrout, M., D'Souza, S., Woodruff, R. and Walker, G., (2009) 'Eukaryotic Translesion Polymerases and Their Roles and Regulation in DNA Damage Tolerance', *Microbiology and Molecular Biology Reviews*, 73(1), pp. 134–154. doi: 10.1128/mmbr.00034-08.

Wehner, M., Chren, M., Nameth, D., Choudhry, A., Gaskin, M., Nead, K., Boscardin, J. and Linos, E., (2014) 'International prevalence of indoor tanning a systematic review and meta-analysis', *JAMA Dermatology*, 150(4), pp. 390-400. doi: 10.1001/jamadermatol.2013.6896.

Whiteside, J. R., Allinson, S. L. and McMillan, T. J. (2011) 'Timeframes of UVA-induced bystander effects in human keratinocytes', *Photochemistry and Photobiology*, 87(2), pp. 435-440. doi: 10.1111/j.1751-1097.2010.00881.x.

Widel, M., (2012) 'Bystander effect induced by UV radiation; why should we be interested?', *Postępy higieny i medycyny doświadczalnej (Online)*, 66, pp. 828-837. doi: 10.5604/17322693.1019532.

Widel, M., Krzywon, A., Gajda, K., Skonieczna, M. and Rzeszowska-Wolny, Joanna., (2014) 'Induction of bystander effects by UVA, UVB, and UVC radiation in human fibroblasts and the implication of reactive oxygen species', *Free Radical Biology and Medicine*, 68, pp. 278-287. doi: 10.1016/j.freeradbiomed.2013.12.021.

Williams, R. M. and Zhang, X. (2021) 'Roles of ATM and ATR in DNA double strand breaks and replication stress', *Progress in Biophysics and Molecular Biology*, 161, pp. 27-38. doi: 10.1016/j.pbiomolbio.2020.11.005.

Wischermann, K., Popp, S., Moshir, S., Scharfetter-Kochanek, K., Wlaschek, M., Gruijl, F., Hartschuh, W., Greinert, R., Volkmer, B., Faust, A., Rapp, A., Schmezer, P. and Boukamp, P., (2008) 'UVA radiation causes DNA strand breaks, chromosomal aberrations and tumorigenic transformation in HaCaT skin keratinocytes', *Oncogene*, 27(31), pp. 4269-4280. doi: 10.1038/onc.2008.70.

Yagura, T., Schuch, A., Garcia, C., Rocha, C., Moreno, N., Angeli, J., Mendes, D., Severino, D., Sanchez, A., Mascio, P., Medeiros, M. and Menck, C., (2017) 'Direct participation of DNA in the formation of singlet oxygen and base damage under UVA irradiation', *Free Radical Biology and Medicine*, 108, pp. 86-93. doi: 10.1016/j.freeradbiomed.2017.03.018.

Zhang, M., Qureshi, A., Geller, A., Frazier, L., Hunter, D. and Han, J., (2012) 'Use of tanning beds and incidence of skin cancer', *Journal of Clinical Oncology*, 30(14), pp. 1588–1593. doi: 10.1200/JCO.2011.39.3652.

Zhao, H., Traganos, F. and Darzynkiewicz, Z., (2011) 'Kinetics of UV-induced DNA damage response in relation to cell cycle phase. Correlation with DNA replication', *Cytometry A*, 77(3), pp. 285-293. doi: 10.1002/cyto.a.20839